UNIVERSITY OF CALIFORNIA, SAN DIEGO

SAN DIEGO STATE UNIVERSITY

Mechanisms facilitating engulfment during sporulation in *Bacillus subtilis*.

A dissertation submitted in partial satisfaction of the requirements for the degree Doctor of Philosophy

in

Biology

by

Jennifer Lynn Fredlund Gutierrez

Committee in charge:

University of California, San Diego

Professor Kit Pogliano, Chair
Professor Timothy Baker

San Diego State University

Professor Stanley Maloy
Professor Forest Rohwer
Professor Moselio Schaechter

2010

The Dissertation of Jennifer Lynn Fredlund Gutierrez is approved, and it is acceptable in quality and form for publication on microfilm and electronically:

_____

_____

_____

_____

_____
Chair

University of California, San Diego

San Diego State University

2010

Table of Contents

List of Tables

List of Figures

Chapter I

Chapter II

Chapter III

Chapter IV

Appendix I

Acknowledgements

I would like to sincerely thank my mentor, Kit Pogliano for her support, discussions, and guidance throughout my graduate career. She made it fun. I would also like to thank my family and friends for their continued support and understanding during this time. Lastly, my husband Roberto, for his love and support and really making all of this possible. I have throroughly enjoyed this time with you.

Chapter II, in full, is a reproduction of the material as it appears in Molecular Microbiology 2010. Meyer, Pablo; Gutierrez, Jennifer; Pogliano, Kit; Dworkin, Jonathan. Blackwell Publishing Ltd, 2010. The dissertation author was a significant contributor to the investigation and writing of the manuscript.

Chapter III, in full, is a reproduction of the material as it appears in Jounal of Bacteriology 2010. Gutierrez, Jennifer; Smith, Rachelle; Pogliano, Kit. American Society for Microbiology, 2010. The dissertation author was the primary investigator and author of the manuscript.

Chapter IV, in full, is currently being prepared for submission to Molecular Microbiology. Gutierrez, Jennifer; Broder, Dan; Pogliano, Kit. The dissertation author was the primary investigator and author of the manuscript.

Curriculum Vitae

1999-2003 Bachelor of Science in Microbiology
University of Washington

2004-2005 University of Washington Medical Center
Specimen processing technician

2005 Teaching Assistant, Cell and Molecular Biology Department, San Diego State University

2008 Teaching Assistant, Department of Biological Sciences, University of California, San Diego

2005-2010 Doctor of Philosophy, Joint Doctoral Program in Biology
San Diego State University/University of California, San Diego

Publications

Gutierrez, J., Smith, R., and Pogliano, K. (2010). SpoIID mediated peptidoglycan degradation is required throughout engulfment during Bacillus subtilis sporulation. J Bacteriol, 192(12):3174-3186.

Meyer, P., Gutierrez, J., Pogliano, K., and Dworkin, J. (2010). Cell wall synthesis is necessary for membrane dynamics during sporulation of Bacillus subtilis. Mol Microbiol, 76(4):956-970.

Aung, S., Shum, J., Abanes-De Mello, A., Broder, D.H., Fredlund-Gutierrez, J., Chiba, S. and Pogliano, K. (2007). Dual localization pathways for the engulfment proteins during Bacillus subtilis sporulation. Mol Microbiol, 65:1534-1546.

Moreno-Gonzales, A., Fredlund, J., Regnier, M. (2005). Cardiac troponin C (TnC) and a site I skeletal TnC mutant alter Ca2+ versus crossbridge contribution to force in rabbit skeletal fibres. J Physiol, 562(3):874-884.

ABSTRACT OF THE DISSERTATION

Mechanisms facilitating engulfment during sporulation in *Bacillus subtilis*.

by

Jennifer Lynn Fredlund Gutierrez

Doctor of Philosophy in Biology

San Diego State University, 2010

University of California, San Diego, 2010

Professor Kit Pogliano, Chair

Sporulation in *Bacillus subtilis* begins with asymmetric division, which generates a smaller forespore, which eventually becomes the mature spore, and a larger mother cell, which lyses after spore development. During engulfment, the mother cell membranes move up and around the forespore, fusing at the top and releasing the forespore into the mother cell cytoplasm.

This dramatic cellular reorganization requires two protein machineries. The first, SpoIID, SpoIIM, and SpoIIP, is expressed in the mother cell and is essential for engulfment. They are proposed to act as a motor, pulling the mother cell membranes around the forespore, using peptidoglycan as a track

while they degrade it. The second, SpoIIQ and SpoIIIAH, acts as a ratchet that constitutes a back-up mechanism for membrane migration. SpoIIQ is produced in the forespore and SpoIIIAH in the mother cell, leaving the only possible site of interaction at the asymmetric septum, where they form foci and arcs around the forespore during membrane migration.

I investigated the role of SpoIID by identifying and characterizing *spoIID* mutants unable to support sporulation and using biochemical and cell biological experiments to define the role of SpoIID in engulfment. I utilized timelapse fluorescence microscopy and antibiotics to demonstrate that peptidoglycan synthesis provides a second backup mechanism that facilitates engulfment and is required in the absence of SpoIIQ. I examined interactions between SpoIIQ/SpoIIIAH and SpoIID/SpoIIM/SpoIIP using Fluorescence Recovery After Photobleaching (FRAP) analysis and found that foci characteristic of SpoIIQ localization depend on SpoIID/SpoIIM/SpoIIP, while immobilization of SpoIIQ depends on SpoIIIAH.

These results allow a more complete model for membrane migration and protein localization during engulfment. Specifically, my data suggest that SpoIID cycles in and out of the complex at the leading edge of the engulfing membrane with peptidoglycan degradation activity required for both release from the septum and movement of the complex around the forespore. It also suggests that SpoIID/SpoIIM/SpoIIP interact with SpoIIQ and localize it to arcs at the septum, where it recruits SpoIIIAH. Finally, if SpoIIQ is deleted,

peptidoglycan synthesis becomes required for membrane migration. Thus, engulfment depends on redundant mechanisms for both membrane movement and protein localization.

Chapter I

Introduction

Roles of peptidoglycan in bacterial cellular processes

Being a bacterium isn't easy. While once, not so long ago, scientists believed that these single-celled organisms were simply bags of disorganized DNA and protein, this is not the case. Indeed, bacteria have solved many engineering challenges that have allowed them to thrive on Earth for billions of years. Through the use of cytoskeletal filaments, cell polarity, oscillating protein localization patterns and small molecule based cell-cell communication, bacteria organize their cells and communities in ways that are complicated yet highly elegant. One challenge posed by the simple architecture of their cells is how bacteria, which are under extraordinary turgor pressure, remodel the single macromolecule (peptidoglycan) that resists this pressure to allow for cell growth and development. Although the basics of peptidoglycan structure and biosynthesis were described nearly 50 years ago, many of the details of its organization, growth and three-dimensional structure are still being explored.

My thesis research has focused on engulfment, a process that critically depends on peptidoglycan remodeling and biosynthesis. Thus, I will here discuss the general properties of peptidoglycan in terms of both function and

structure, current models regarding the three dimensional arrangement of peptidoglycan around the cell, recent evidence describing the role of peptidoglycan in cellular processes, and finally, how *Bacillus subtilis* sporulation can be utilized as a model system to learn more about some outstanding peptidoglycan structural questions.

What is peptidoglycan?

One of the most important molecules unique to bacteria is peptidoglycan. Consisting of a large, continuous polymer of variable thickness between species, peptidoglycan is a key element in the bacterial cell envelope, found outside the cytoplasmic membrane and completely surrounding the bacterial cell, forming what is referred to as the sacculus (Fig 1). It is a prominent factor used by scientists to classify bacteria based on their cell envelopes via the Gram stain. Using the method developed by Christian Gram in 1884, Gram negative organisms do not retain a dye and only have a thin layer of peptidoglycan (although two membranes), whereas Gram positive organisms protect the same dye from being washed away and have a thick layer of peptidoglycan (Fig 1A). Over 100 years later, the Gram stain is still used by clinicians to quickly identify infection-causing bacteria and allow for prescription of the most effective antibiotics for the sick patient.

Peptidoglycan has long been studied due to its unusual structure and its presence in nearly all bacteria, with a few exceptions including mycoplasmas and *Chlamidiae* (Chopra *et al.*, 1998, Ghuysen & Goffin, 1999).

Peptidoglycan biogenesis is therefore a terrific target for both naturally occurring and engineered antibacterial compounds, an ever-important focus of research in the infectious disease and public health fields. Peptidoglycan has also been used as a tool to study the evolutionary origins of eukaryotic organelles as many peptidoglycan synthesis genes, and in some cases peptidoglycan itself, persist in plastids and cyanelles in plants (reviewed in (Takano & Takechi, 2010, Hashimoto, 2003)). The presence of peptidoglycan and its precursors in organelles as well as the bacterial nature of organellar rRNA genes (Kuntzel *et al.*, 1981, Gray *et al.*, 1984), together have demonstrated that many critical organelles, including mitochondria and chloroplasts, were once free-living bacteria.

However, being surrounded by a single molecule sacculus presents several complications for the bacterium. First, material must be both broken and added to the cell wall in order to accommodate cell growth without compromising the structural integrity of the wall. Second, septal material must be split without causing cell lysis during division. Third, the cell must be able to import and export the large peptidoglycan precursor molecules through the membrane. Fourth, certain developmental processes, such as sporulation, require remodeling of the peptidoglycan and perhaps a dedicated synthetic apparatus to create new shapes and types of peptidoglycan within the cell. With all these engineering challenges, yet maintenance of peptidoglycan throughout the bacteria, there must also be substantial benefits to having a

peptidoglycan layer, begging the question: what is the purpose of peptidoglycan for an individual bacterium?

Biophysical properties of peptidoglycan

It appears the peptidoglycan serves two primary functions: keeping the bacterium from bursting and maintaining cell shape. It is widely recognized that peptidoglycan exists as a single polymer sac to prevent the bacterium from lysing. Being a single molecule allows peptidoglycan to resist the turgor pressure created by the high concentration of proteins and metabolites inside the bacterium versus the low concentration of solutes outside the cell, a value measured as up to 50 atmospheres in Gram positive organisms (Seltmann, 2002). What is truly amazing about the molecule, however, is that it is not only exceptionally strong and rigid, maintaining its shape when all cell contents have been removed, but that it is also highly elastic and porous. Koch and Woeste (Koch & Woeste, 1992) showed that, in response to osmotic shock, the Gram negative *Escherichia coli* (*E. coli)* sacculus can expand and shrink reversibly up to 3-fold without tearing. This has also been shown for *Bacillus megaterium* (*B. megaterium)* (Marquis, 1968) and *Staphylococcus aureus* (*S. aureus)* (Ou & Marquis, 1970), two Gram positive organisms. Atomic force microscopy (AFM) has been used to verify that the cell envelope is, in fact, elastic and completely recovers its original shape after perturbation (Yao *et al.*, 1999, Vadillo-Rodriguez *et al.*, 2009).

Recent evidence suggests that proteins also contribute to the rigidity of the cell envelope *in vivo*, at least in Gram negative cells. Lpp is a lipoprotein linking the *E. coli* peptidoglycan to the outer membrane, and in *lpp* mutants, immobilized cells recovered their shape more slowly from deformations caused by external stress applied by an AFM tip compared to wild type cells, leading to the determination that *lpp* mutants are 42% less rigid (Vadillo-Rodriguez et al., 2009). Another study examined the influence of the cytoplasmic protein MreB on cell wall stiffness using optical tweezers to bend individual cells with and without an MreB depolymerizing substance (A22). Results suggest that MreB, which forms actin-like cytoskeletal filaments (van den Ent *et al.*, 2001, Jones *et al.*, 2001, Figge *et al.*, 2004), contributes about 30% of cell stiffness to *E. coli* (Wang *et al.*, 2010). As MreB is conserved in many rod shaped Gram positive and Gram negative organisms, it seems probable that a contribution from MreB to rigidity is being made across species. Thus, the biophysical properties of the cell wall likely rely on the chemical nature of the peptidoglycan itself, as well as contributions from both cytoplasmic and extracellular proteins.

Peptidoglycan is also important in cell shape maintenance, as purified sacculi maintain their original shape. However, cell shape itself appears to be determined by how and where new peptidoglycan is added to the already existing sacculus. Cytoskeletal proteins, such as MreB, MreBH, and Mbl, within the cytoplasm have been shown to direct new peptidoglycan insertion in

Caulobacter crescentus (*C. crescentus)* and *Bacillus subtilis* (*B. subtilis)* (Figge et al., 2004, Kawai *et al.*, 2009, Carballido-Lopez, 2006, Carballido-Lopez & Errington, 2003, Daniel & Errington, 2003). Furthermore, in *C. crescentus*, another cytoskeletal element, the intermediate filament related protein CreS, plays a role in mechanically affecting peptidoglycan structure. Cabeen et al (Cabeen *et al.*, 2009) found that CreS is held in the cell in a stretched position, concomitantly exerting a compression force on the section of the cell wall to which it is linked as CreS tries to contract into its 'natural' helical shape. This area of the cell becomes the shorter side of the comma shaped *C. crescentus* cell, indicating that peptidoglycan insertion is slower in the CreS side of the wall than in the opposite side. When CreS was expressed in *E. coli,* the normally rod shaped cells took on bent forms, suggesting that peptidoglycan insertion rates can be mediated simply by local stretch rates, with more stretched peptidoglycan encouraging faster insertion of new peptidoglycan (Cabeen et al., 2009). This also supports an idea that will be discussed later that there is coupling between peptidoglycan synthesis and degradation whereby peptidoglycan degradation by enzymes creates more space in the wall, thereby encouraging faster insertion.

Peptidoglycan structure

There are two main things to consider when speaking of peptidoglycan structure. First, what is the chemical structure of the molecule, the monomers and the polymer? Second, what is the structure of the polymer relative to the

cell and how is new material incorporated? The basic chemical structure of peptidoglycan was largely elucidated in the 1960s and consists of linear glycan strands that are linked together by short peptide side chains, called crosslinks ((Rogers, 1980), reviewed in detail in (Vollmer *et al.*, 2008)) (Fig 1B). While the fine structure of the peptide crosslinks varies considerably, both between species (Schleifer & Kandler, 1972) and within species, depending on growth conditions (Mengin-Lecreulx & van Heijenoort, 1985, Prats & de Pedro, 1989, Holtje, 1998), the gross structure of the peptidoglycan is relatively conserved. The glycan strands themselves are made up of a series of alternating sugar molecules. The first is N-acetylglucosamine (GlcNAc) and the second is N-acetylmuramic acid (MurNAc), with pentapeptides attached to and extending from the MurNAc (Fig 1B). The sugars are linked by a β1-4 bond and the ends of glycan strands are 'capped' with anhydro(1-6) MurNAc. It has long been thought that the peptide side chains extended from the glycan backbone every 90° (Labischinski *et al.*, 1979) due to the pitch of the sugar molecules when linked together. However, recent evidence from crystal structures of synthetic peptidoglycan fragments suggests that the pitch of the strand may be greater, resulting in peptide chains extending at 120°, likely reducing the number of crosslinks possible between adjacent strands (Meroueh *et al.*, 2006).

There is considerable variation in the peptide crosslinks of peptidoglycan, in their density, composition and linkage structure. Peptide

extensions are initially synthesized as five amino acid long chains, most often consisting of: (1) L-Ala (2) D-Glu (3) m-A_2pm (Gm-) or L-Lys (Gm+) (4) D-Ala (5) D-Ala. These side chains are crosslinked from one glycan strand to another as they are inserted into the existing peptidoglycan in a reaction facilitated by the transpeptidase domain of enzymes belonging to the penicillin-binding protein (PBP) family (Sauvage *et al.*, 2008). This cross-linking usually occurs in one of two ways: in a Type A linkage, the 3rd position amino acid of one pentapeptide is linked to the 4th position D-Ala of a second pentapeptide (Schleifer & Kandler, 1972). In Gram negative organisms, this is usually a direct linkage, whereas in Gram positive organisms, a peptide bridge is often involved (Schleifer & Kandler, 1972) (Fig 1B). These bridges are thought to be important in β-lactam resistance (Chambers, 2003) and protein anchoring (Dramsi *et al.*, 2008, Marraffini *et al.*, 2006). In Type B linkages, the 2nd position D-Glu is linked to the 4th position D-Ala of another peptide, however, these linkages are generally only seen in the genus *Corynebacterium*. *Bacillus subtilis,* the most studied Gram positive model organism, has side chains with an identical sequence to *E. coli*: L-Ala-D-Glu-A_2pm-D-Ala-D-Ala and undergoes direct Type A crosslinking (Seltmann, 2002).

Models for 3D peptidoglycan arrangement

The three dimensional arrangement of peptidoglycan around the cell is less obvious, and techniques are still lacking to definitively determine it, but

much research has been done to try and elucidate this next level of structure. It is important to note that the organization of the Gram negative and Gram positive sacculus may be different and that this might affect how these two groups of organisms control peptidoglycan synthesis and degradation. Specifically, Gram negative organisms have a much thinner layer of peptidoglycan, so addition and subtraction of peptidoglycan must be performed carefully in order to avoid cell rupture. A popular model proposed by Holtje (Holtje, 1998), is called the 3-for-1 insertion model. It purports that three glycan strands are crosslinked together before insertion into the sacculus. Then, the two outside strands are linked onto the sacculus surrounding one old strand. Peptidoglycan hydrolases then clip the bonds linking the old strand into the lower layer, releasing it and effectively inserting the trimer in its place. In this way, the sacculus both grows and is recycled without creating any holes in the material. Most models that have been advanced about pepidoglycan 3D structure concern the Gram negative cell wall, largely because it is easier to study due to its thinness, but recent data has also been generated about the suprastructure of *B. subtilis* peptidoglycan (Hayhurst *et al.*, 2008). It is also important to realize that the sacculus of any given bacterium is under constant construction and disassembly due to growth and division, so even if peptidoglycan can be directly viewed, it will be difficult to distinguish newly synthesized peptidoglycan from older peptidoglycan that

might have been remodeled. One can anticipate that most models will only be accurate over small areas of the cell.

Two major models currently exist to explain Gram negative sacculus structure with many variations of each being also been put forth. The classical, and currently best supported, model was originally proposed in 1964 by Weidel and Pelzer (Weidel & Pelzer, 1964), and is referred to as the 'layered' model (reviewed in depth by (Vollmer & Holtje, 2004)). The layered model was largely developed by Koch and Holtje in a series of papers in the 1990s (Koch, 2000, Holtje, 1998, Koch, 1998b, Koch, 1990, Koch, 1998a) and proposes that glycan strands run parallel to each other and parallel to the cell membrane (Fig 1C). The peptide crosslinks between glycan strands also are within the plane of the membrane, creating a sheet-like layer surrounding the cell. In this arrangement, some peptides would also extend above and below the plane, potentially linking multiple layers of peptidoglycan together to form the sacculus. There are many possible arrangements for the glycan strands relative to the cell within this model, including random. However, the most experimentally supported configuration seems to be nearly perpendicular to the long axis (creating hoops around the middle) based on two strong lines of evidence. First, as mentioned earlier, sacculi have been shown to possess elastic properties that allow the cell and sacculus to expand or contract greatly along the long axis, but only minimally in a radial direction (Koch & Woeste, 1992). This elasticity has been reliably attributed to stretch in the peptide

crosslinks (Yao et al., 1999), but in order for this to be true, the peptide crosslinks must be positioned in the plane of the cell and along the long axis. Second, recent cryo electron tomography (cryoET) data has directly visualized peptidoglycan in *E. coli* and *C. crescentus* sacculi as loops around the cell perpendicular to the long axis, although they are not well ordered (Gan *et al.*, 2008). Although this group proposes a 'disorganized' layered model similar to that in (Verwer *et al.*, 1978), it seems reasonable that variation of such a degree could simply be due to variation in growth of the sacculus. The layered model is also supported by evidence from Gram positive bacteria and explains the difference between the two types of organisms as simply variation in the number of layers (Andre *et al.*, 2010, Ou & Marquis, 1970).

A second, less favored, model for the Gram negative cell wall was advanced by Dmitriev et al (Dmitriev *et al.*, 2005, Dmitriev *et al.*, 1999, Dmitriev *et al.*, 2003) and termed the 'scaffold' model. In this scenario, the glycan strands are organized perpendicular to the cell membrane with crosslinks occurring in the plane of the cell membrane (Fig 1D). This model is consistent with sacculus elasticity in the direction of the long axis (Yao et al., 1999) and can explain how certain *E. coli* mutants can adopt vastly different shapes but maintain their peptidoglycan (Young, 2003, Varma & Young, 2004). It is also somewhat easier to reconcile the scaffold model than the layerd model with recent crystal structures of peptidoglycan showing a 120° rather than 90° rotation between peptide chains extending from the MurNAc

(Meroueh et al., 2006). The strongest evidence against this model is the direct cryo-EM visualization of the peptidoglycan structure in sacculi (Gan et al., 2008) and experimental measurements of the dimensions of the cell wall and periplasmic space (Matias *et al.*, 2003, Leduc *et al.*, 1989), which, for this model to explain, require significant cell wall compression to have occurred in all experimental preparations, thus rendering this model unlikely.

B. subtilis cell wall architecture has recently been visualized using AFM, a technique capable of attaining high resolution data on hydrated samples (Hayhurst et al., 2008). Interestingly, the evidence suggests a complicated, elegant, and very different organization than that seen in Gram negative cell walls. First, the authors found *B. subtilis* to harbor very long (up to 5000 disaccharide units, 5 μm) glycan strands, with an average length of 1.3 μm. They also looked directly at the inner and outer sacculus surface and found what they termed a 'cabling' pattern only at the inner surface. This loss of structure towards the outside of the sacculus agrees with evidence that new peptidoglycan is inserted at the inner surface of the wall and is cleaved and moved outwards as it ages (Glauner & Holtje, 1990, Smith *et al.*, 2000). Further examination of partially ripped sacculi reavealed what appeared to be a helix-like rope conformation making up the cables, which are then wrapped radially around cell. The model is explained as small numbers of glycan strands twisted helically into a rope. Ropes are then further helically twisted together to form a cable, which is inserted into the sacculus. This is similar to

the layered model proposed for Gram negative peptidoglycan except that instead of individual glycan strands, cables of already crosslinked glycan strands are used to create the layer, being further crosslinked to each other within the plane. A similar configuration was suggested for *Lactobacillus helveticus*, where 26 nm striations were observed in the cell wall, a spacing similar to what was seen here, and could correspond to cable diameter (Firtel *et al.*, 2004).

Although this arrangement might seem to pose a unique topological challenge for biosynthesis, models have been proposed for how this might be accommodated in the inner wall zone space. For instance, glycan strands have a natural right-handed twist (Leps *et al.*, 1987, Meroueh et al., 2006), so if one glycan strand was synthesized as a template, similar to the 3-for-1 model, other strands could be wrapped around it with subsequent crosslinking causing the observed helical conformation. Having some internal stress in the ropes, as would be created if this were true, would explain the unraveling seen in AFM. Furthermore, the rope like cables described in Hayhurst should be very strong, helping to resist the high turgor pressure of Gram positive bacterial cells.

One important point that must be addressed is that, although there is evidence for this model in *B. subtilis* and some other *Bacilli* (Firtel et al., 2004), other Gram positive organisms, such as *S. aureus*, do not exhibit similar glycan strand lengths (with an average of only 6 nm versus 5 μm (Boneca *et*

al., 2000)) or surface features (Hayhurst et al., 2008). This suggests that there is considerable variation in the Gram positive peptidoglycan architecture and that homologous enzymes involved in the peptidoglycan synthesis process may be organized or regulated differently, such that they perform the same reactions but achieve different architectural results in different organisms. The major differences between the architecture of the Gram positive and Gram negative cell wall seems a bit surprising, as certain lines of evidence argue for similar architecture in both types of organisms. For instance, porosity has been shown to be nearly identical in Gram positive and Gram negative organisms despite the large difference in peptidoglycan thickness, as each allows similar penetration by fluorescent dextrans with an average pore size of approximately 2 nm in *E. coli* and *B. subtilis* (Demchick & Koch, 1996). Although pore size of the meshwork doesn't require similar 3D structure, it is suggestive. One possibility is that Gram negative organisms also utilize peptidoglycan ropes but don't join them into cables, resulting in thinner patterns that can't be directly visualized using available techniques. Gan et al (Gan et al., 2008), observed 4 nm densities rather than the expected 1 nm thickness in flash-frozen *E. coli* sacculi and, although they suggest that the thickness is due to an artifact of processing, small cables would be an alternate explanation. Clearly, additional studies and the development of new techniques will be required before a definitive view of cell wall architecture can be achieved.

Peptidoglycan synthesis and degradation

One obvious conundrum for the bacterial cell no matter how the peptidoglycan is oriented, is how to both grow and divide while encased in a relatively rigid, single molecule, sacculus. In order for these processes to occur, not only does new peptidoglycan have to be added, but existing peptidoglycan also has to be degraded to make space for the new material and accommodate the lengthening cell. These processes are highly regulated and require multiple enzymes for both synthesis and degradation. Furthermore, current evidence indicates that elongation and cell division utilize distinct machineries for both biosynthesis and degradation, in which some proteins are shared and others are unique to one or the other site of biogenesis ((Alaedini & Day, 1999), reviewed in (den Blaauwen *et al.*, 2008)).

Synthesis itself can be broken down into three stages. The first stage is precursor synthesis. All steps of this stage occur in the cytoplasm of the cell and occur quickly, with the result being a Lipid II molecule (reviewed in (de Kruijff *et al.*, 2008)), which consists of an undecaprenyl lipid carrier attached to a GlcNAc-MurNAc-pentapeptide and requires the enzymatic action of both MraY (Brandish *et al.*, 1996, Stachyra *et al.*, 2004)) and MurG (Chen *et al.*, 2002, Ha *et al.*, 2000, Mengin-Lecreulx *et al.*, 1991). Lipid II is thought to be the universal peptidoglycan precursor and is used for both elongation and divisional growth of the sacculus. During the second stage of synthesis, Lipid II must be flipped from the inside of the membrane to the outside. This step

occurs at a rate too fast to rely simply on diffusion and also doesn't occur spontaneously (van Dam *et al.*, 2007), but it remains unclear what protein or proteins facilitate this reaction. RodA or a subcomplex of the localization proteins has been proposed to serve this function (Ishino *et al.*, 1986) although there is no direct evidence for either of these scenarios (Fay & Dworkin, 2009, Real *et al.*, 2008). The third stage of peptidoglycan synthesis occurs outside the cytoplasm, either in the Gram negative periplasm or in the recently identified, inner-wall-zone in Gram positive organisms (Matias & Beveridge, 2005, Matias & Beveridge, 2006, Matias & Beveridge, 2007, Zuber *et al.*, 2006), and encompasses polymerization of the glycan strands, peptide crosslinking, and insertion of the strands into the sacculus.

Two types of enzymes are logically essential for peptidoglycan synthesis outside the cytoplasm: glycosyltransferases that link together the sugar molecules of the monomer to form the glycan strands, and transpeptidases that link together the peptides to form the crosslinks between the glycan strands. It is also logically true then, that the cognate enzymes for breaking these bonds will be required to clip the peptidoglycan to allow growth of the sacculus: endopeptidases, carboxypeptidases, or amidases to cleave the peptide crosslinks, and muramidases, lytic transglycosylases, or glucosaminidases to cleave the glycan strands. It has been proposed that a complex of proteins that exhibits all of these functions, plus possibly the Lipid II synthesis enzymes, exists and would act as a holoenzyme, a unit that would

be capable of creating, degrading, and inserting peptidoglycan into the existing sacculus (Holtje, 1996). There is considerable evidence that higher-order complexes of the peptidoglycan synthetic enzymes occur in a variety of organisms, including *E. coli* (reviewed in (den Blaauwen et al., 2008)), *Hemophilus influenza* (Alaedini & Day, 1999), *Pseudomonas aeruginosa* (Legaree & Clarke, 2008), *Mycobacterium tuberculosis* (Hett *et al.*, 2010) and *B. subtilis* (Fay *et al.*, 2010, Vasudevan *et al.*, 2007), but linking these complexes with a complete set of degradative enzymes has been more challenging and progress has only recently been reported (Uehara *et al.*, 2010, Hett et al., 2010, Legaree & Clarke, 2008, Carballido-Lopez *et al.*, 2006).

Peptidoglycan degradative complexes

Three cellular processes require peptidoglycan degradation (Fig 2): daughter cell separation, septum formation, and elongation. In *B. subtilis,* daughter cell separation occurs by splitting the thick peptidoglycan layer some time after cytokinesis is complete. Splitting the septum depends on several degradative enzymes with overlapping functions: LytC, LytD, LytE (Blackman *et al.*, 1998), LytF (Ohnishi *et al.*, 1999), LytG (Horsburgh *et al.*, 2003) and CwlS (Fukushima *et al.*, 2006). In *E. coli*, three amidases, AmiA, AmiB, and AmiC are required for daughter cell separation (Heidrich *et al.*, 2001, Priyadarshini *et al.*, 2007, Uehara & Park, 2008), and cells lacking these proteins form long chains. However, Uehara and Park (Uehara & Park, 2008)

observed that only 15% of products generated from peptidoglycan degradation during separation result from amidase activity. Indeed the lytic transglycosylase, Slt70 (Heidrich et al., 2001) and endopeptidase PBP4 (Priyadarshini *et al.*, 2006) are also known to be important for cell separation. One difficulty faced by studies of cell separation in both *E. coli* and *B. subtilis* is that typically inactivating more than one enzyme is required before a phenotype is observed (Blackman et al., 1998, Murray *et al.*, 1998).

Interestingly, peptidoglycan degradation is also required for septum formation in *E. coli*. During septation in *E. coli*, peptidoglycan is inserted only at the leading edge of the invaginating membranes in a PBP3 dependent manner (Wientjes & Nanninga, 1989). However, in *amiABC* mutants (Priyadarshini et al., 2007), which lack three amidases, the peptidoglycan layer remains incomplete although the membranes are completely fused. This argues for the presence of architectural constraints on the glycan strands during insertion that might prevent the final closure of septal peptidoglycan and a requirement for coordination between the synthesis and degradative machineries to complete cell division.

Recently, this interaction between these amidases and the divisome has been elucidated. Uehara, et al (Uehara et al., 2010), showed that EnvC, a member of the *E. coli* septal ring (Bernhardt & de Boer, 2004, Hara *et al.*, 2002), activates the amidases AmiB and AmiA *in vitro* to greatly increase the rate at which they degrade peptidoglycan. *In vivo* activity of the separate

domains of EnvC demonstrated that the domain responsible for localizing EnvC to the divisome was also important for regulation of the amidase activation by EnvC. This supports a model where, once EnvC is at the septum, interactions between it and its localization determinant cause release of inhibition of the activating domain and allow for EnvC to interact with AmiB and AmiA to promote peptidoglycan degradation. This interaction is required to allow for outer membrane fusion and cell separation (Heidrich et al., 2001, Priyadarshini et al., 2007). An identical interaction was seen for NlpD, which localizes to the septum, and the amidase AmiC (Uehara et al., 2010). These findings elegantly explain how *E. coli* coordinates the splitting of septal peptidoglycan with the invagination of the outer membrane.

Another example of coupling of peptidoglycan synthesis and degradation during cell division in *E. coli* has been demonstrated *in vitro*. PBP1b, a peptidoglycan synthesis enzyme, is present in the divisome and has been shown to interact with the lytic transglycosylase MltA via the structural protein MipA (Vollmer *et al.*, 1999). This is a key finding not only in that it provides a concrete link between proteins that are involved in peptidoglycan synthesis and degradation, but also in that MltA is anchored in the *E. coli* outer membrane while PBP1b is in the inner membrane, so MipA must be linking the two in the periplasm and forming a contact between the two membranes and possibly facilitating outer membrane constrictions.

Peptidoglycan degradation is also required for elongation of the cell to create space in the sacculus for new peptidoglycan to be inserted. In *B. subtilis*, Carballido-Lopez et al (Carballido-Lopez et al., 2006), showed an interaction between MreBH and the peptidoglycan hydrolase LytE using both yeast two-hybrid and *in vitro* co-immunoprecipitation. MreBH knockouts show a mild shape defect (Soufo & Graumann, 2003) and MreBH colocalizes in helical filments with MreB and Mbl, at least at the resolution achievable using fluorescence microscopy (Carballido-Lopez & Errington, 2003), suggesting it interacts with MreB and Mbl, both important in wall peptidoglycan insertion (Jones et al., 2001, Daniel & Errington, 2003, Carballido-Lopez & Errington, 2003). A GFP-LytE construct also showed cylindrical cell wall localization in an MreBH, but not MreB or Mbl, specific manner, suggesting that there is a direct *in vivo* relationship between the two proteins. MreBH is cytoplasmic where as LytE is secreted into the cell wall, leading the authors to suggest that MreBH targets LytE for secretion. It is possible that the MreBH-LytE interaction couples peptitdoglycan degradation and biosynthesis during elongation.

Division and elongation both require the activity of the low-molecular weight PBPs, which trim peptide side chains on the newly synthesized MurNAc to regulate crosslinking (Popham & Young, 2003), although deletion of these enzymes is rarely lethal (Denome *et al.*, 1999). In *E coli* and *B subtilis*, PBP5 is required for maintenance of cell shape (Young, 2003, Varma

& Young, 2004, Ghosh & Young, 2003, Nelson & Young, 2001, Todd *et al.*, 1986). Interestingly, this family of proteins has not been well studied, but seems to play a more prominent role in cell shape determination than any of the high-molecular weight PBPs, which are responsible for both transpeptidation and transglycoslyation of the new peptidoglycan (Sauvage et al., 2008).

One reason peptidoglycan synthesis and degradation has been challenging to study is that bacterial species contain multiple copies of PBP family proteins and hydrolases, leading to functional redundancy for both biosynthesis and degradation (Murray et al., 1998, Popham & Setlow, 1996, Popham *et al.*, 1999). One system where peptidoglycan synthesis is known to occur but that is not essential is sporulation in *B. subtilis*, making it an attractive model system for asking questions about peptidoglycan holoenzyme activity and organization.

Potential coupling of peptidoglycan biosynthesis and degradation during engulfment in *B. subtilis*

Endospore formation is an evolutionarily conserved process in *B. subtilis* and other related Gram positive bacteria that occurs in response to changes in the environment, such as nutrient depletion. Many dramatic morphological changes occur during sporulation (Fig 3), each requiring a host of specialized proteins (reviewed in (Errington, 2003, Hilbert & Piggot, 2004)).

The first step of sporulation is an asymmetrically positioned cell division event that relies on many of the same enzymes as vegetative cell division (reviewed in (Errington *et al.*, 2003)). This division event allows the onset of cell specific gene expression that mediates subsequent steps in morphogenesis. The second overt morphological change during sporulation is engulfment of the forespore by the mother cell (Fig 3), a process that involves dynamic protein localization and large-scale rearrangements of the cellular membranes, which migrate around the forespore. The completion of engulfment releases the forespore into the mother cell cytoplasm, where it is surrounded by two membranes, one derived from the original outer membrane of the cell and one from the engulfing mother cell membranes. Engulfment also allows activation of late cell specific transcription factors required to produce proteins necessary to direct completion of the spore coat and cortex. Finally, the mother cell lyses to release the mature endospore into the environment where it can persist for thousands of years (Yung *et al.*, 2007).

Peptidoglycan synthesis during sporulation occurs in two distinct stages and results in two discernible peptidoglycan layers in the intermembrane space surrounding the forespore. The first layer of cell wall to be synthesized is the germ cell wall, which is thought to serve as the template for the vegetative cell wall after spore germination (Popham *et al.*, 1996). This layer of peptidoglycan is thinner than normal Gram positive peptidoglycan but has the same chemical structure (Meador-Parton & Popham, 2000). The germ cell

wall is synthesized by enzymes produced in the forespore using precursors generated in the forespore membrane (Tipper & Linnett, 1976, McPherson *et al.*, 2001). The second layer of peptidoglycan is called the cortex. It is thick, accounting for 80% of the spore peptidoglycan (Meador-Parton & Popham, 2000), and has a unique structure with half of the normal MurNAc units converted to muramic lactam, which often lack tetrapeptide side chains (Popham et al., 1996, Gilmore *et al.*, 2004, Atrih *et al.*, 1996). The peptidoglycan in the cortex also shows reduced crosslinking, with just 2% of available peptides crosslinked versus 44% in vegetative *B. subtilis* peptidoglycan (Atrih *et al.*, 1999, Atrih *et al.*, 1998). The spore cortex is synthesized by enzymes produced in the mother cell (Sekiguchi *et al.*, 1995, Vasudevan et al., 2007) using precursors that are made in the mother cell membrane (Tipper & Linnett, 1976). Interestingly, cortex synthesis is temporally regulated by the induction of enzymes that produce peptidoglycan precursors after σ^K is activated in the mother cell (Vasudevan et al., 2007), although the cortex synthesis enzymes SpoVD, SpoVE, SpoVB, and SpoVM are produced much earlier by σ^E (Eichenberger *et al.*, 2003).

Peptidoglycan degradation is critical for engulfment, which commences with the process of septal thinning, whereby peptidoglycan is degraded starting at the center of the sporulation septum. This process is mediated by SpoIID, SpoIIM, and SpoIIP, the only three proteins required for engulfment under all conditions (Smith *et al.*, 1993, Lopez-Diaz *et al.*, 1986, Frandsen &

Stragier, 1995). Peptidoglycan is also degraded at the leading edge of the engulfing membranes by the enzymes SpoIID and SpoIIP (Abanes-De Mello *et al.*, 2002, Chastanet & Losick, 2007, Aung *et al.*, 2007, Morlot *et al.*, 2010, Gutierrez *et al.*, 2010), which are the subject of Chapters 3 and 4 of this thesis. These enzymes have been proposed to use the cell wall as a track to pull the membranes up and around the forespore (Abanes-De Mello et al., 2002), a model that is consistent with, but not directly proven by, results presented in Chapter 3. The SpoIID and SpoIIP degradative enzymes are the primary machinery for engulfment and are essential under all conditions for this process. Prior studies, and those in this thesis, have documented two backup machineries for engulfment. The first is the zipper like interaction between the forespore expressed protein SpoIIQ and the mother cell expressed protein SpoIIIAH, which are necessary for engulfment when SpoIID or SpoIIP activity is reduced (Broder & Pogliano, 2006). The second backup mechanism is peptidoglycan biosynthesis, which I show in Chapter 2 of this dissertation to be involved in engulfment and required for membrane migration when SpoIIQ is deleted.

Thus, deletion of the backup engulfment protein SpoIIQ demonstrates that *B. subtilis* engulfment requires both peptidoglycan synthesis and degradation, which supports a close relationship between these two machineries. Since cortex synthesis isn't started until after engulfment is complete (Vasudevan et al., 2007), it is likely to be germ cell wall synthesis

that is required for membrane migration. My studies show that peptidoglycan synthesis and degradation are both localized at the leading edges throughout engulfment, but resolution is limited and this does not necessarily mean there is a direct interaction between the two complexes. Thus, additional biochemical studies are required to determine if the engulfment machinery interacts directly with the peptidoglycan biosynthetic enzymes, an interaction that would occur in the intermembrane space, similar to that seen by SpoIIQ/SpoIIIAH. Engulfment is less redundant than cell division in that it requires fewer enzymes to degrade and synthesize peptidoglycan (there are more than 30 hydrolytic enzymes in *B. subtilis* alone (Smith et al., 2000), and 12 functional PBPs in *E. coli* (Sauvage et al., 2008, Denome et al., 1999). Engulfment is also dispensable for growth, making it an attractive model system for examining how peptidoglycan synthesis and degradation are coordinated.

Figures

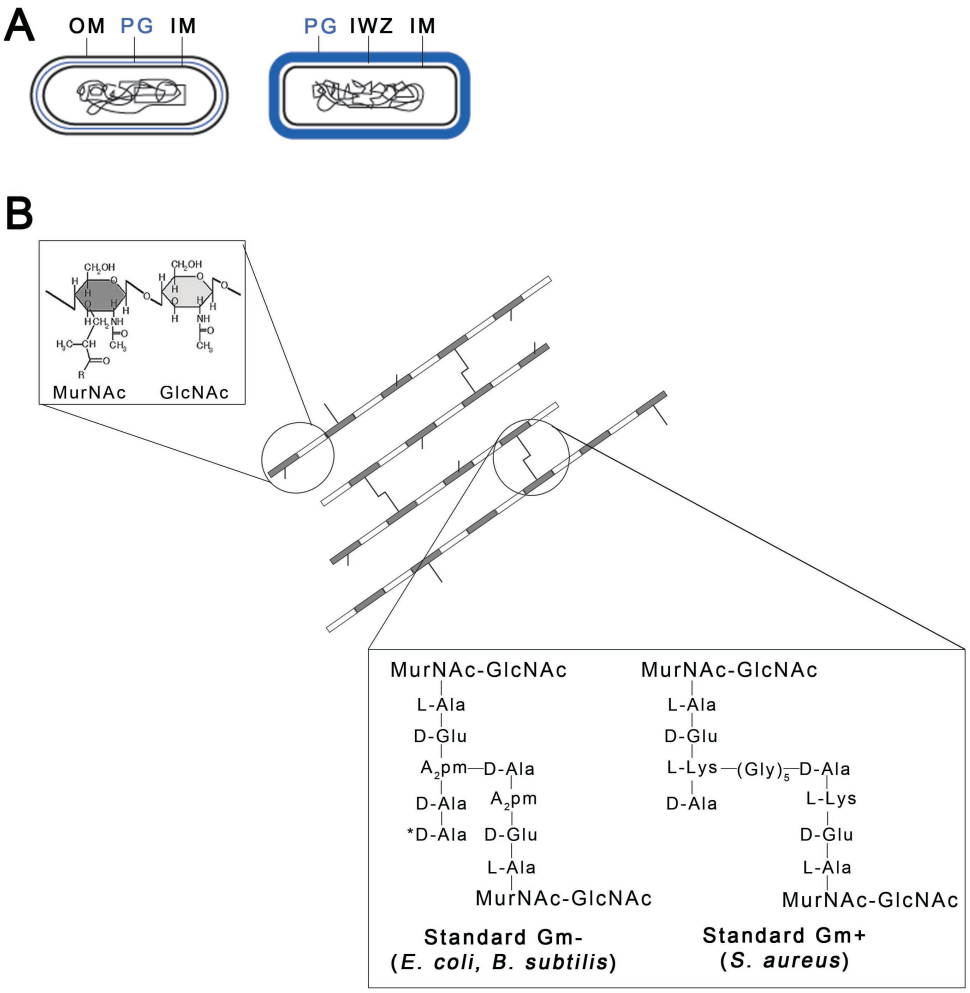

Figure 1. (Part 1) Peptidoglycan basics.
(A) The cell envelope structures of Gram negative (left) and Gram positive (right) bacteria. OM = outer membrane, PG = peptidoglycan, IM = inner membrane, IWZ = inner wall zone. (B) Chemical structure of GlucNAc-MurNAc monomer showing β1-4 linkage as a zoom out from a single sheet of crosslinked of glycan strands. Lower zoom depicts a the peptide chain and crosslink structure of both Gram positive and Gram negative peptidoglycan.

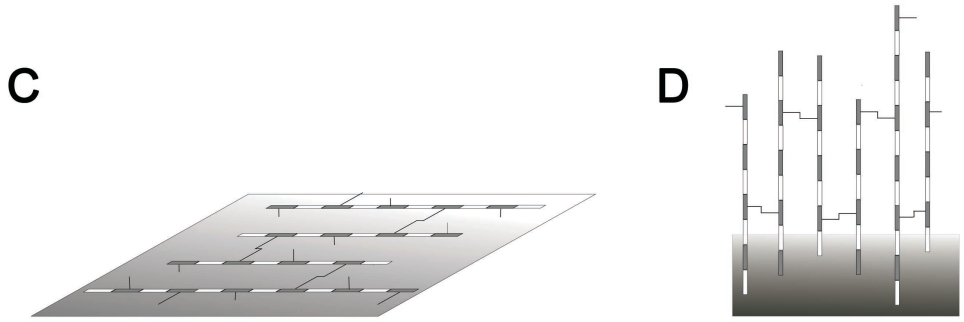

Figure 1. (Con't.)

(C) Layered model of peptidoglycan. Glycan strands and peptide crosslinks are in the plane of the cell membrane forming single layer around the cell. (D) Scaffold model of peptidoglycan. Glycan strands are perpendicular to the cell membrane while peptide crosslinks are in the plane.

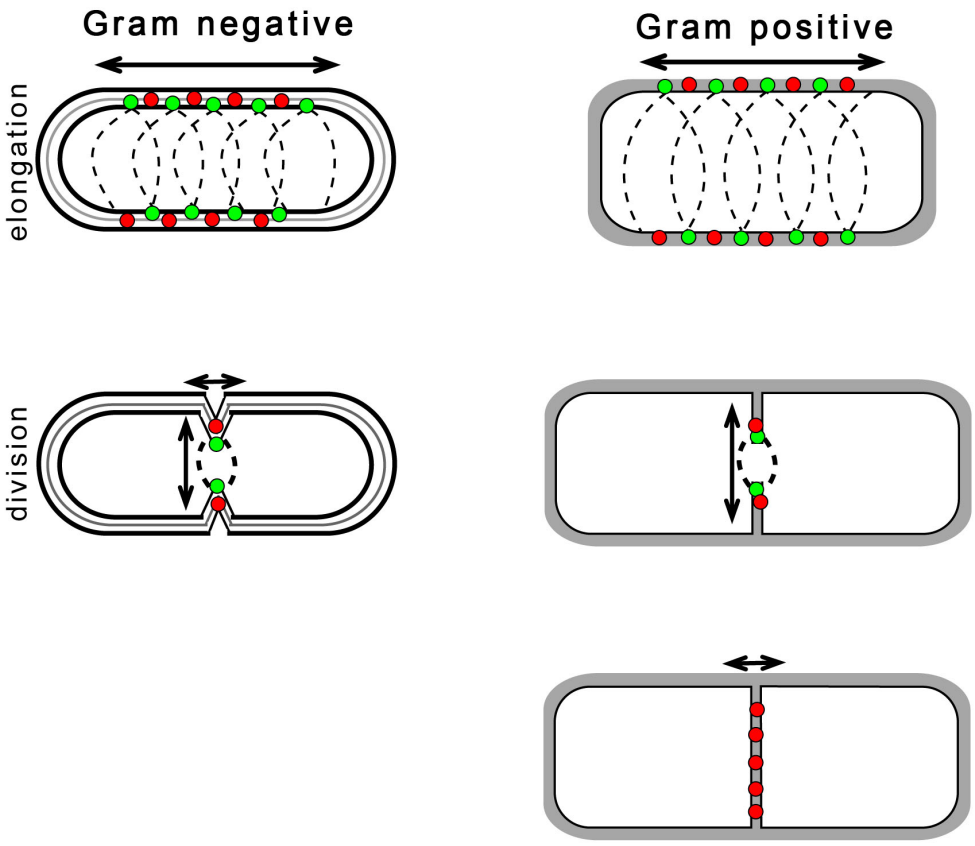

Figure 2. Cellular processes mediated by peptidoglycan dynamics.

Gram negative and Gram positive cells are pictured. Red circles represent peptidoglycan degradation and green circles represent peptidoglycan synthesis. During elongation (top panels), peptidoglycan remodeling is required for lengthening of the cylindrical cell walls. During cell division (middle panels) septum formation and, in Gram negative organisms, daughter cell separation require peptidoglycan synthesis and degradation. Daughter cell separation in Gram positive organisms occurs after cell division and requires only peptidoglycan degradation (lower panel).

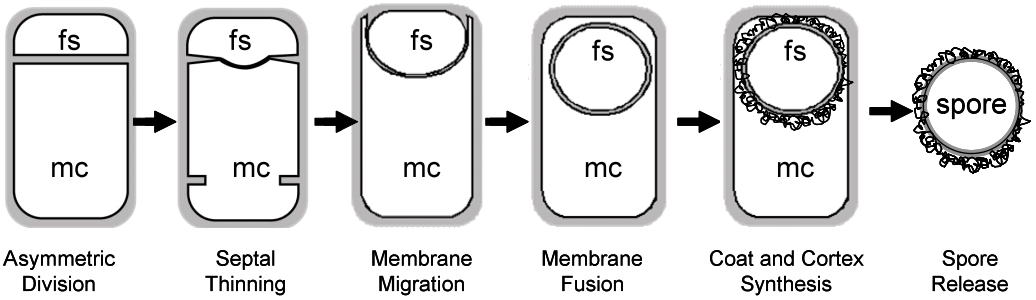

Figure 3. Sporulation in *B. subtilis*.

Sporulation in *B. subtilis* begins with asymmetric division, dividing the cell into the forespore (fs) and mother cell (mc) compartments. The process of engulfment includes septal thinning, membrane migration and membrane fusion. Peptidoglycan is indicated in gray and coat and cortex indicated with black squiggles.

Chapter II

Cell wall synthesis is necessary for membrane dynamics during sporulation of *Bacillus subtilis*.

Molecular Microbiology (2010) 76(4), 956–970 ■
doi:10.1111/j.1365-2958.2010.07155.x
First published online 19 April 2010

Cell wall synthesis is necessary for membrane dynamics during sporulation of *Bacillus subtilis*

Pablo Meyer,[1] Jennifer Gutierrez,[2] Kit Pogliano[2] and Jonathan Dworkin[1]*
[1]*Department of Microbiology and Immunology, College of Physicians and Surgeons, Columbia University, New York, NY 10032, USA.*
[2]*Division of Biological Sciences, University of California at San Diego, La Jolla, CA 92093, USA.*

Summary

During *Bacillus subtilis* sporulation, an endocytic-like process called engulfment results in one cell being entirely encased in the cytoplasm of another cell. The driving force underlying this process of membrane movement has remained unclear, although components of the machinery have been characterized. Here we provide evidence that synthesis of peptidoglycan, the rigid, strength bearing extracellular polymer of bacteria, is a key part of the missing force-generating mechanism for engulfment. We observed that sites of peptidoglycan synthesis initially coincide with the engulfing membrane and later with the site of engulfment membrane fission. Furthermore, compounds that block muropeptide synthesis or polymerization prevented membrane migration in cells lacking a component of the engulfment machinery (SpoIIQ), and blocked the membrane fission event at the completion of engulfment in all cells. In addition, these compounds inhibited bulge and vesicle formation that occur in *spoIID* mutant cells unable to initiate engulfment, as did genetic ablation of a protein that polymerizes muropeptides. This is the first report to our knowledge that peptidoglycan synthesis is necessary for membrane movements in bacterial cells and has implications for the mechanism of force generation during cytokinesis.

Introduction

A central question in cell biology is the nature of the forces driving membrane movement. During endocytosis, the cellular membrane invaginates and ultimately forms a lipid-bounded compartment that is distinct from the membrane. This event rarely occurs spontaneously and is dependent upon enzymes that facilitate this process. Proteins that polymerize into filaments, such as actin and tubulin, convert the chemical energy of polymerization into mechanical work (Theriot, 2000; Phillips *et al.*, 2009). For example, actin polymerization mediates contractile ring formation during cytokinesis in *Schizosaccharomyces pombe* (Pelham and Chang, 2002) and facilitates deformations of the plasma membrane seen during endocytosis (Qualmann *et al.*, 2000) or in protruding lamellipodia (Mitchison and Cramer, 1996). Microtubule polymerization drives the movement of organelles and chromosomes (Inoue and Salmon, 1995). However, while the polymerization of actin (Miyata *et al.*, 1999) or tubulin (Elbaum *et al.*, 1996) can generate a mechanical force that distorts membranes *in vitro*, it remains unclear whether polymerization is sufficient to explain *in vivo* membrane dynamics.

A process of membrane fission is seen in *Bacillus subtilis* that are responding to nutritional limitation. As part of this response, called sporulation, *B. subtilis* divides asymmetrically and undergoes engulfment, an endocytic-like process of membrane fission that results in one cell, the forespore, being entirely encased in the cytoplasm of the larger cell, the mother cell (Fig. 1A, top). Initially, an asymmetric division septum forms generating the two differently sized cells. The subsequent increasing curvature of this septum causes the forespore to assume a rounded shape comprised of a double membrane separated by a thin layer of peptidoglycan. SpoIID and SpoIIP are autolysins that hydrolyse cell wall and they have been proposed to drive this membrane movement by generating a force through a ratchet-like mechanism driven by the hydrolysis of peptidoglycan (Abanes-De Mello *et al.*, 2002; Broder and Pogliano, 2006). Engulfment is also facilitated by the formation of the SpoIIQ–SpoIIIAH protein–protein zipper between the forespore and mother cell, which is required for membrane migration when the activity or levels of SpoIID and SpoIIP are reduced (Broder and Pogliano, 2006). During this movement, the forespore remains attached to the mother cell but in the final step, the forespore pinches off from the mother cell. However, the source of the force responsible for this final step remains unknown.

Accepted 24 March, 2010. *For correspondence. E-mail jonathan.dworkin@columbia.edu; Tel. (+1) 212 342 3731; Fax (+1) 212 305 1468.

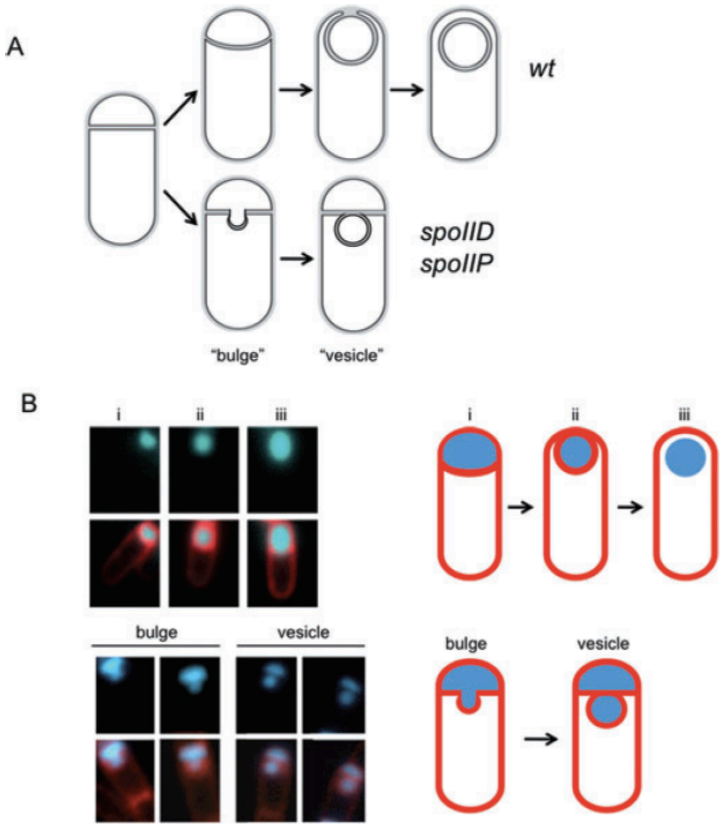

Fig. 1. Membrane bulge and vesicle formation in engulfment mutants.
A. Sporulating wild-type cells undergo engulfment where the smaller forespore compartment becomes a free cell within the larger mother cell (top). Strains carrying *spoIID* or *spoIIP* mutations are blocked at the stage of asymmetric septation and undergo membrane bulging, eventually leading to the formation of membrane bound vesicles (bottom).
B. Wild-type (AES574) and *spoIID* strains (JDB2494) expressing CFP (blue) under control of a forespore-specific promoter (P_{spoIIQ}) as a forespore marker were imaged at T4 in resuspension medium and stained with FM4-64 (red) to visualize membranes. Top, CFP is expressed in: (i) the forespore of wild-type cells undergoing asymmetric septation stained with FM4-64, (ii) engulfing cells stained with FM4-64 and (iii) engulfed cells not stained with FM4-64. Bottom, *spoIID* cells contained either a continuous CFP signal distribution between the forespore and the membrane protrusion ('bulge'), or two distinguishable CFP signals separated by a membrane ('vesicle').

Membrane-bound compartments in other bacteria are thought to result from involutions of the cell membrane. For example, magnetosomes are membrane-associated organelles observed in magnetotactic bacteria composed of crystals of magnetite that are surrounded by a lipid bilayer (Komeili *et al.*, 2006; Scheffel *et al.*, 2006) and *Escherichia coli* carrying mutations in a gene necessary for proper cell shape produce membrane invaginations and cytoplasmic vesicles (Bendezu and de Boer, 2008). Sporulating *B. subtilis* strains carrying *spoIID* or *spoIIP* null mutations form asymmetric septa that fail to proceed with engulfment. Instead, membrane bulges appear gradually at the septa (Fig. 1A, bottom). Electron microscopy (Lopez-Diaz *et al.*, 1986; Illing and Errington, 1991; Smith and Youngman, 1993; Bylund *et al.*, 1994; Frandsen and Stragier, 1995) and staining with the membrane impermeable stain FM4-64 (Abanes-De Mello *et al.*, 2002) indicate that the bulges in *spoIIP* and *spoIID* mutants are continuous with the forespore compartment. The origin of the forces which drive bulge formation are unknown, although by analogy with the roles of actin and tubulin polymerization in eukaryotic membrane fusion and fission, a protein or peptide capable of polymerizing could serve a similar role. Bulge formation in these mutants therefore offers a useful system to examine candidate force-generating mechanisms responsible for membrane movements in bacteria.

Most bacteria contain peptidoglycan, a rigid polymer built from disaccharide peptide monomers that can be up to 5000 units in length (Hayhurst *et al.*, 2008). Peptidoglycan monomers, also known as muropeptides, are synthesized in the bacterial cytoplasm by a series of essential and highly conserved enzymes that convert the sugar UDP-GlcNAc to the lipid-linked UDP-disaccharide pentapeptide (van Heijenoort, 2001) which is flipped across the membrane to the outside of the cell where cross-linking transpeptidation and polymerizing transglycosylation reactions link these muropeptides to mature peptidoglycan (Sauvage *et al.*, 2008). While the glycan polymers of peptidoglycan are generated by transglycosylases, inhibition of the transpeptidation reaction by vancomycin also results in a loss of this polymerization activity in *Staphylococcus aureus* (Kim *et al.*, 2008).

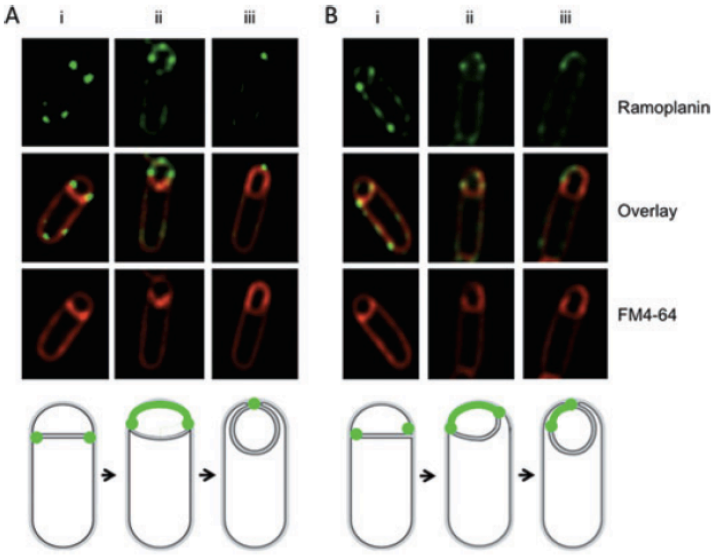

Fig. 2. Peptidoglycan synthesis during engulfment. Engulfing cells contain sites of active peptidoglycan synthesis. Ramoplanin-FL (top) and FM4-64 (bottom) staining of (A) wild-type (PY79) cells and (B) *spoIID(D210A)* cells; centre panel are the overlay of the two images. (i) Ramoplanin-FL staining at septal tips, (ii) ramoplanin-FL staining around the forespore, (iii) ramoplanin-FL staining restricted to the point of contact between the advancing arms. Diagrams shown represent ramoplanin-FL (green) signals at different stages of engulfment corresponding to wild-type (left) and *spoIID(D210A)* (right) images.

Finally, since cell wall peptidoglycan has a Young's modulus of 1.7–25 MPa (Yao *et al*., 1999; Francius *et al*., 2008), it is up to 10^4 times stiffer than actin, so formation of mature peptidoglycan would produce mechanical work.

The requirement for peptidoglycan synthesis during bacterial growth complicates assessment of the hypothesis that it provides a driving force for membrane movement. We have therefore examined the role of peptidoglycan synthesis in three different membrane movements that occur during the non-essential process of *B. subtilis* sporulation. First, during the initial stages of engulfment, the membranes surrounding the forespore undergo a process of migration that results in the formation of curved membranes. We find that inhibition of peptidoglycan synthesis blocks this migration in a strain missing a secondary membrane migration system requiring SpoIIQ and we find that peptidoglycan biosynthesis is localized to the leading edge of the engulfing membrane in wild-type cells and in a mutant in which membrane migration occurs asymmetrically. Second, during the last stage of engulfment, peptidoglycan synthesis is localized to the last site of attachment between the two cells and antibiotics that inhibit peptidoglycan synthesis prevent separation of the two cells and completion of engulfment. Third, peptidoglycan synthesis occurs at sites of bulge formation in *spoIID* and *spoIIP* mutants and compounds that inhibit the synthesis of muropeptides block the initiation of these bulges and their ultimate formation as membrane-bounded, 'vesicle'-like compartments. Consistent with the action of these compounds, a null mutation in a gene encoding a protein necessary for the synthesis of mature cross-linked peptidoglycan suppresses bulge formation. Together these results suggest that during engulfment, membrane migration and membrane fission require peptidoglycan biosynthesis.

Results

Peptidoglycan synthesis during engulfment

During the process of engulfment, the asymmetric septum becomes rounded and eventually pinches off from the mother cell, resulting in the formation of a membrane-bounded compartment (Fig. 1A, top). Sites of active peptidoglycan synthesis in engulfing cells were identified using a fluorescent ramoplanin that binds the reducing end of nascent glycan chains found at the initiation sites of peptidoglycan synthesis (Tiyanont *et al*., 2006). Sporulating cells showed a clear strong fluorescent signal at the sporulation septum during engulfment (Fig. 2A, i). This signal was due to active peptidoglycan synthesis because treatment of sporulating cells before polar septation with fosfomycin, an inhibitor of peptidoglycan synthesis, showed no ramoplanin labelling (Fig. S1, middle) and a derivative of ramoplanin that does not label lipid II (Tiyanont *et al*., 2006) did not produce similar patterns of staining (Fig. S1).

Ramoplanin-FL fluorescence was enriched at the edges of the septal disk at early (Fig. 2A, i) and intermediate stages of engulfment (Fig 2A, ii and Fig. S2A) and eventually localized to the area of membrane fission (Fig. 2A, iii and Fig. S2B). The reduced signal in other

regions of the forespore was likely not the result of reduced accessibility to the space between the two forespore membranes because forespore staining was similar in a *spoIIQ* mutant where the forespore membranes are less tightly associated (Broder and Pogliano, 2006) as compared with the wild type (Fig. S2). Once engulfment completed and the forespore had separated from the mother cell, the ramoplanin signal in the forespore disappeared (data not shown) likely because it is unable to cross the lipid bilayer (Hamburger *et al.*, 2009). Next, we took advantage of a *spoIID(D210A)* mutant (KP1102; Gutierrez *et al.*, 2010) where cells stained with FM4-64 show a clear asymmetry in membrane migration (80% of cells, 53 out of 66 cells) as exemplified by a single cell where one of the tips of the migrating membranes advances further than the other tip (Fig. 2B, cells ii and iii). Sites of peptidoglycan synthesis showed a similar asymmetrical staining pattern (Fig. 2B, top and middle), indicating that the pattern of peptidoglycan synthesis during engulfment reflects the asymmetrical migration of the membrane.

Inhibition of peptidoglycan synthesis blocks membrane migration

During engulfment, the septal membranes migrate around the forespore compartment ultimately resulting in the production of a cell within a cell. The observation that ramoplanin stained the leading edges of the engulfing forespore (Fig. 2A, ii) suggested that active peptidoglycan synthesis was involved in this process. We examined this possibility by performing time-lapse microscopy to follow single sporulating cells with FM4-64-stained membranes (Becker and Pogliano, 2007) and determining the effect of fosfomycin, an antibiotic that specifically inhibits MurAA, the first enzyme in the peptidoglycan biosynthetic pathway (Walsh, 2003). When 5 mM fosfomycin was added to wild-type cells at T1.5 after initiation of sporulation and cells were imaged starting at T2, no significant disruption could be detected in membrane migration (Fig. 3A and B and Fig. S3). However, membrane migration during engulfment is dependent on two partially redundant mechanisms, peptidoglycan hydrolysis by SpoIID and SpoIIP and the zipper-like interaction of SpoIIQ with SpoIIIAH. In mutants with reduced hydrolase activity, the SpoIIQ/SpoIIIAH system becomes essential (Broder and Pogliano, 2006), so a requirement for muropeptide synthesis for membrane migration could be similarly masked. Consistent with this hypothesis, time-lapse movies revealed that fosfomycin reduced membrane migration in *spoIIQ* mutant cells (Fig. 3C–E and Fig. S3A–C), as 54 out of 72 cells (75%) showed membrane migration in the *spoIIQ* mutant, but only 17 out of 55 (31%) in the *spoIIQ* mutant with fosfomycin. To ensure that fosfomycin did not have pleiotropic effects during sporulation of *spoIIQ* cells, we confirmed that a fluorescent marker under σ^F control was activated in *spoIIQ* cells that showed no membrane migration in the presence of fosfomycin (Fig. S3E).

A fluorescence-based assay to monitor completion of engulfment

The presence of a strong ramoplanin signal at the point of contact between the two engulfing membrane arms (Fig. 2A, iii) suggested that peptidoglycan synthesis was occurring at an appropriate time and place to play a role in the separation of the outer forespore membrane from the mother cell membrane that marks completion of membrane fission during engulfment. We examined this possibility using a strain that expresses CFP only in the forespore along with visualization of membranes by the lipophilic fluorescent dye FM4-64 that was added just prior to microscopy. We expressed CFP under control of a forespore specific promoter (P_{spoIIQ}), which is active only upon completion of the septum and thus CFP-positive cells must have progressed past this point in sporulation. When asymmetric septation was completed in this strain, the forespore contained a CFP signal that was surrounded by an FM4-64 signal (Fig. 4A, panels 'T3.5', 'T4'; numbers indicate the time in hours after the initiation of sporulation). Once engulfment ends, the forespore has detached from the mother cell and since FM4-64 does not cross membranes (Sharp and Pogliano, 1999), the forespore is no longer accessible to the dye. Thus, an engulfed forespore had a CFP signal but no FM4-64 staining (Fig. 4A, panel 'T5', yellow arrow), whereas a forespore that has not completed engulfment and remains attached to the mother cell was stained with FM4-64 (Fig. 4A, panel 'T4.5', green arrow). This assay therefore distinguishes cells at the pre-separation step and cells where the membranes had completed fission and separated.

Inhibition of muropeptide synthesis blocks engulfment membrane fission

This fusion assay was used to determine the effect of inhibiting peptidoglycan synthesis on completion of engulfment. Addition of fosfomycin (5 mM) after asymmetric septation at T2 of sporulation allowed membrane migration but blocked membrane fission (i.e. the detachment of the forespore from the mother cell; Fig. 4B, bottom images). When fosfomycin was added at different times after the start of sporulation, fosfomycin blocked engulfment membrane fission only if it was added before T3, but had no effect when added at T3 (Fig. 4C). A decreasing fraction of cells containing a forespore that

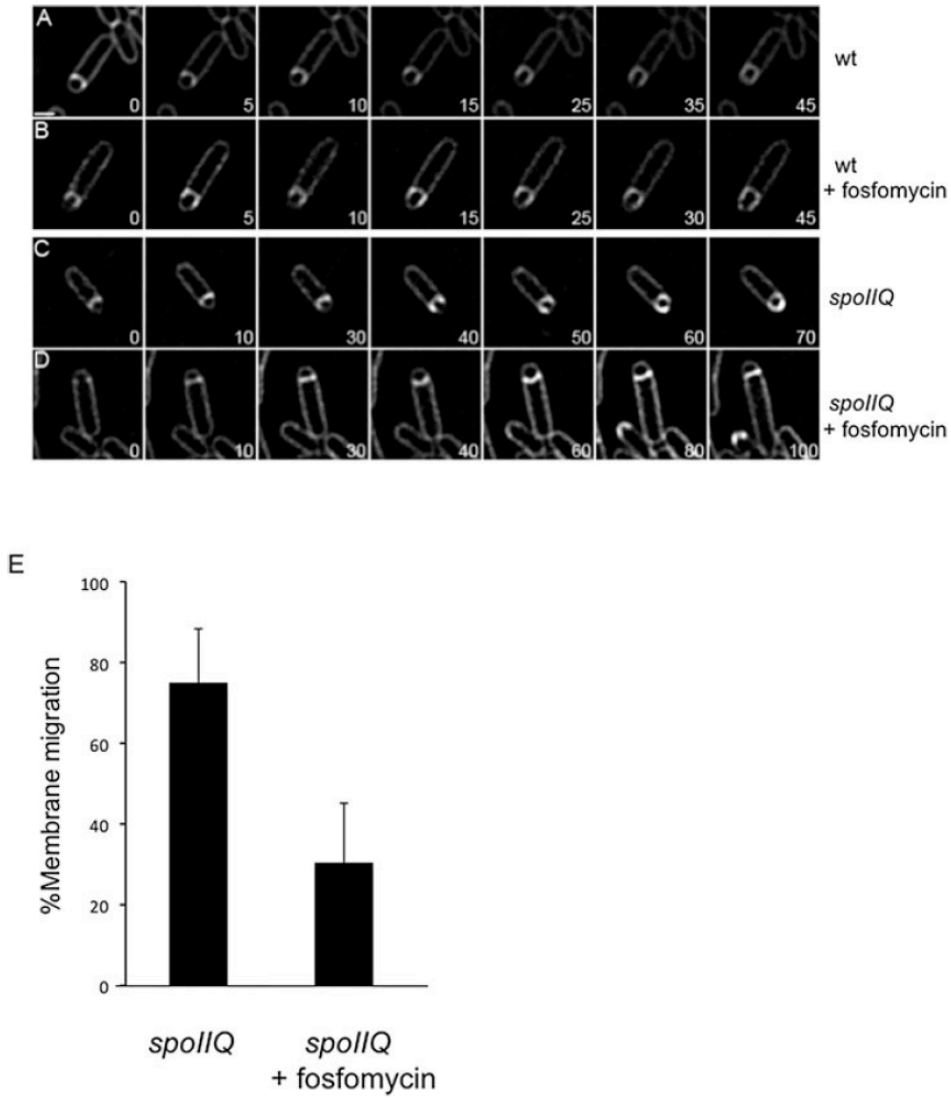

Fig. 3. Inhibition of muropeptide synthesis blocks membrane migration in a *spoIIQ* mutant. All cultures were grown on agarose pads composed of A+B medium at 30°C and stained with FM4-64. The initial image in each sequence was taken at approximately T2 after sporulation initiation and arbitrarily set to t = 0 min. The time of subsequent images of the membrane stain is indicated in minutes in the lower right corner.
A. Wild type (PY79).
B. Wild type + 5 mM fosfomycin added at T1.5 after initiation of sporulation.
C. *spoIIQ* (KP575).
D. *spoIIQ* + 5 mM fosfomycin added at T1.5.
E. Histogram showing the percentage of cells where membrane migrated in Δ*spoIIQ* cells with (17 out of 55 cells or 75 ± 5%) or without (54 out of 72 cells or 30 ± 6%) 5 mM fosfomycin added at T1.5 after initiation of sporulation. Means are significantly different by *t*-test ($P < 10^{-5}$). For complete movies, see Fig. S3. Scale bar = 1 μm.

had detached from the mother cell was observed at fosfomycin concentrations ranging from 1 mM to 10 mM (Fig. S4).

When 5 mM fosfomycin was added at T2 to a strain that expressed an inducible fosfomycin-resistant allele of MurAA (C117D), the fraction of sporulating cells that completed engulfment was significantly higher than a culture where this allele was not expressed (Fig. 4D, Fig. S5). Since the presence of this MurAA mutant allele by itself did not effect engulfment (Fig. S6), fosfomycin must be blocking engulfment membrane fission by directly inhibiting muropeptide synthesis.

Inhibition of peptidoglycan synthesis blocks completion of engulfment

The requirement of muropeptide synthesis to complete engulfment suggests that polymerization of these monomers during formation of mature peptidoglycan was also necessary for engulfment. Vancomycin inhibits transpeptidation and thereby blocks the transglycosylation step necessary for polymerization. Addition of vancomycin at T2 after resuspension blocked engulfment membrane fission (Fig. 5A). Importantly, this was not an effect of blocking septal synthesis since the assay uses a fluorescent reporter whose activity is dependent on the completion of asymmetric septation. This inhibition did depend on when vancomycin was added in sporulation although it still blocked completion of engulfment in 50% of cells when it was added as late as T3.5 (Fig. 5B). Thus, muropeptide polymerization is necessary for completion of engulfment defined as the release of the forespore from the mother cell.

Topology of membrane bulges

Sporulating cells lacking either the SpoIIP or the SpoIID autolysins fail to initiate engulfment and instead produce septal membrane bulges (Fig. 1A, bottom, Fig. S7; Lopez-Diaz *et al*., 1986; Illing and Errington, 1991; Smith and Youngman, 1993; Bylund *et al*., 1994; Frandsen and Stragier, 1995). Time-lapse microscopy of single cells revealed that bulge formation was continuous and occurred over a period of ~30 min (Fig. 6A, Fig. S7). To characterize the topology and origin of these bulges in living cells, we expressed CFP under control of a forespore specific promoter (P_{spoIIQ}). We observed a CFP signal in membrane bulges of a *spoIID* null mutant indicating that they had been, at least transiently, contiguous with the forespore (Fig. 1B, 'bulge'). In some cells, the CFP signal in the forespore and the bulge was not continuous, and the presence of an FM4-64 signal surrounding these discontinuous bulges suggests that the bulge was transformed into a physically distinct membrane-bounded vesicle (Fig. 1B, 'vesicle'; Fig. S8).

Peptidoglycan synthesis in membrane bulges

What is the driving force underlying the formation of these bulges and vesicles? They originated from the septum, a site of prior peptidoglycan synthesis. Bulge-forming *spoIID* cells stained with ramoplanin-FL at T4 of sporulation had a fluorescent signal associated with the septum, indicating the presence of active peptidoglycan synthesis (Fig. 6B). We examined whether peptidoglycan synthesis was necessary for bulge formation by blocking it using fosfomycin. When 5 mM fosfomycin was added at T2 of sporulation to either *spoIID* (Fig. 6C, red) or *spoIIP* (Fig. S9) mutants, many fewer bulges were observed as compared with untreated cells (Fig. 6C, Fig. S9, black). Furthermore, addition of fosfomycin at T2 also blocked formation of vesicles that presumably originated as bulges (Fig. 6D). This effect of fosfomycin was due to a direct inhibition of peptidoglycan synthesis because a *spoIID* strain carrying the MurAA(C117D) allele exhibited bulge formation during sporulation even in the presence of 5 mM fosfomycin (Fig. S10).

While the inhibition of muropeptide synthesis results indirectly in decreased levels of mature, polymerized peptidoglycan, the experiments using fosfomycin do not address the possibility that direct inhibition of synthesis of peptidoglycan polymers from muropeptide monomers would similarly block formation of bulges and vesicles. We used vancomycin to answer this question, and observed that addition of vancomycin (0.5 $\mu g\ ml^{-1}$) at T2 of sporulation blocked bulge (Fig. 6E) and vesicle formation (Fig. S11) in a strain lacking *spoIID*, indicating that synthesis of mature peptidoglycan is necessary for bulge formation. This inhibition by vancomycin could be through an indirect effect on lipid synthesis if reducing lipid synthesis blocked bulge formation. We addressed this possibility by using cerulenin, an inhibitor of an essential enzyme (FadD) in the fatty acid biosynthetic pathway. However, addition of cerulenin had no effect on bulge formation when it was added to *spoIID* cells at the same time in sporulation (T3.5) where the inhibitory effect of vancomycin was observed (Fig. S12). While addition of cerulenin at earlier time points (T2; data not shown) prevented bulge formation in *spoIID* cells, this may be due to the membrane growth that is evident in time-lapse movies of bulge formation (Fig. S7).

A peptidoglycan transpeptidase is necessary for bulge formation

The muropeptide monomer is incorporated into mature peptidoglycan by enzymes mediating transpeptidation

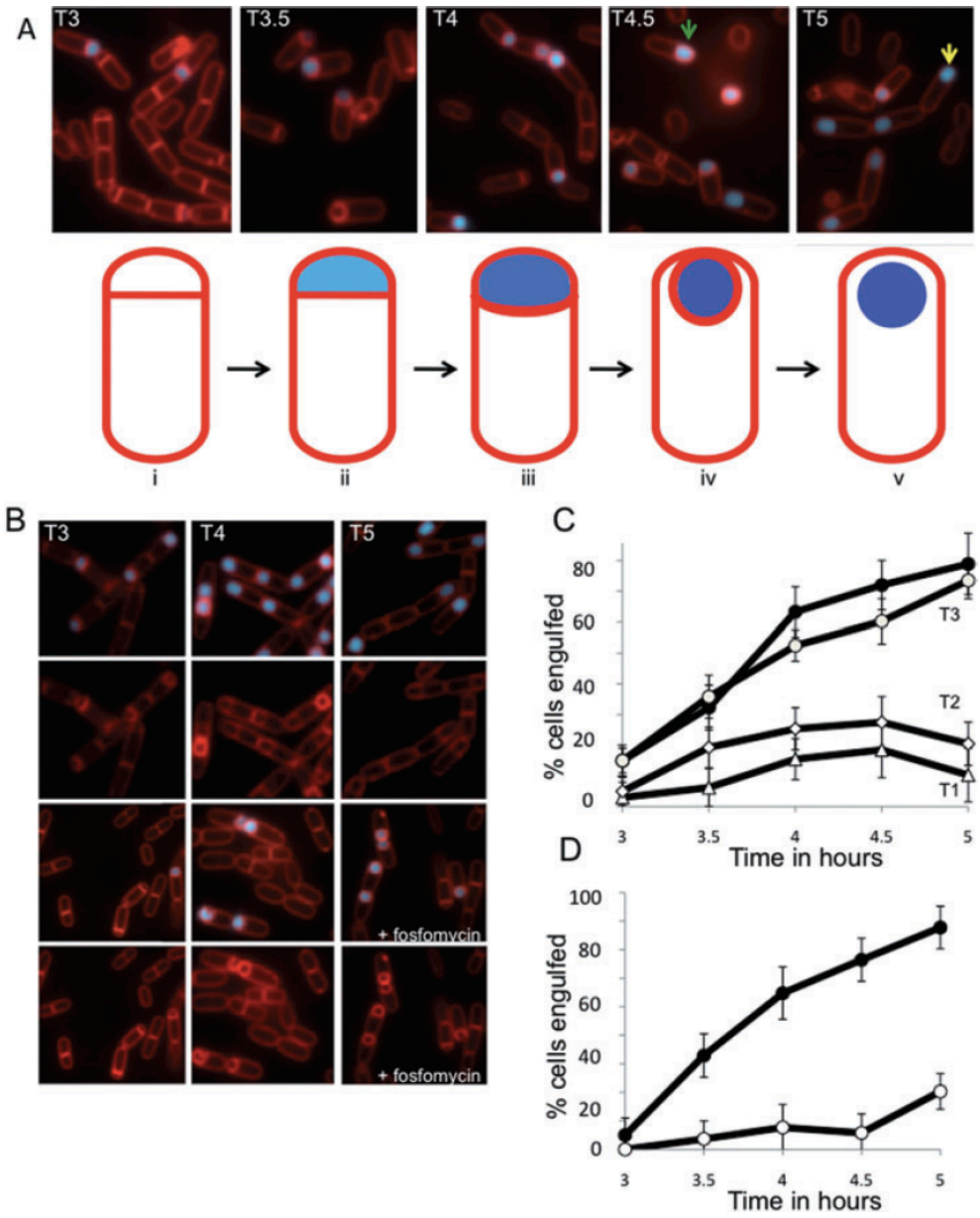

and transglycosylation reactions. During sporulation, the transpeptidase SpoVD is necessary for the production of mature peptidoglycan (Vasudevan *et al.*, 2007). A complementing GFP–SpoVD fusion localizes to septal membrane bulges and vesicles (Fig. 7A), similar to the pattern observed with ramoplanin-FL (Fig. 6B). This similarity suggested that SpoVD is involved, and perhaps necessary, for the peptidoglycan synthesis occurring in the bulges. In fact, bulge formation is reduced in a *spoIIP* strain lacking SpoVD (Fig. 7B, red) as compared with the parent *spoIIP* strain (black). The result is consistent with the inhibition of bulge formation by the transpeptidase inhibitor vancomycin in *spoIID* (Fig. 6E) and *spoIIP* cells (data not shown) and demonstrates that a protein neces-

Fig. 4. Inhibition of muropeptide synthesis blocks membrane fission.
A. Assay of membrane fission. Top, sporulating wild-type cells (AES574) express CFP (blue) under control of a forespore specific promoter (P_{spoIIQ}). Membranes of cells at intermediate stages of engulfment (T3–T4.5, green arrow) are also stained by a membrane impermeant dye (FM4-64, red) just before imaging; upon completion of membrane fission, cells are no longer stained by this dye (yellow arrow). Time after resuspension is indicated. Bottom, cells at different stages of sporulation. Prior to the completion of asymmetric septation (i), no CFP (blue) signal is observed. Following completion of asymmetric septation, a faint CFP signal is observed in the forespore (ii). As the cells proceed through engulfment (iii), the CFP signal increases. When membrane movement is complete (iv), the forespore remains attached to the mother cell and stained with FM4-64 (red). When the forespore is released from the mother cell (v), the CFP signal is no longer surrounded by an FM4-64 signal.
B. Fosfomycin blocks engulfment before membrane separation. Sporulating wild-type cells were either treated with fosfomycin (5 mM) at T2 (bottom panels) or not treated (top panels). Time after resuspension is indicated.
C. Inhibition of membrane fission by fosfomycin is dependent on time of addition. Wild-type cells (AES574) were untreated (filled circles) or fosfomycin (5 mM) was added at T1 (triangles), T2 (diamonds) or T3 (open circles) and the fraction of cells with a CFP signal not surrounded by an FM4-64 signal was determined.
D. Fosfomycin-resistant *murAA* mutant engulfs normally in the presence of fosfomycin. The effect of fosfomycin on engulfment of a merodiploid strain (JDB2426) expressing an IPTG-inducible *C117D murAA* allele and YFP under a forespore-specific promoter (P_{spoIIQ}-*yfp*) was determined. Filled circles, both 1 mM IPTG was added at T0 and 5 mM fosfomycin was added at T2; open circles, only 5 mM fosfomycin at T2.

sary for the synthesis of mature peptidoglycan is also necessary for bulge formation.

Discussion

Muropeptide polymerization during engulfment

Our results allow historical experiments concerning the role of peptidoglycan biosynthesis in engulfment to be put into a mechanistic context. Among the earliest hints of such a role was the observation that removal of the cell wall by lysozyme treatment leads to a block in sporulation, but only when this treatment occurs before engulfment (Fitz-James, 1964). Consistent with this observation, *B. subtilis* exposed to vancomycin during engulfment do not reach a phase bright state, suggesting that peptidoglycan synthesis is required towards the end of engulfment (Dancer, 1979). During engulfment, a thin layer of peptidoglycan known as the germ cell wall is generated adjacent to the inner forespore membrane (Tipper and Linnett, 1976; Meador-Parton and Popham, 2000). Thus, the inhibitory effect of vancomycin on engulfment (Fig. 5) could be due to an inhibition of germ cell wall synthesis.

Consistent with this possibility, our observation that sites of active peptidoglycan synthesis are distributed around the engulfing forespore (Figs 2A and 8A, top) suggests that muropeptide polymerization could be mediating earlier stages of engulfment. Protoplasts of *B. subtilis* that lack peptidoglycan are still able to undergo this membrane movement in a mechanism that depends on the SpoIIQ–SpoIIIAH zipper, which is dispensable for engulfment in intact cells, but which is independent of the SpoIID–SpoIIP peptidoglycan hydrolase proteins that are essential in intact cells (Broder and Pogliano, 2006). Our results demonstrate that the inhibition of muropeptide synthesis blocks membrane migration in intact cells lacking the SpoIIQ–SpoIIIAH zipper (Fig. 3), suggesting that peptidoglycan polymerization comprises a mechanism for membrane migration during engulfment that is essential in the absence of the Q–AH zipper. We therefore propose that peptidoglycan polymerization and the SpoIIQ–SpoIIIAH zipper comprise two redundant mechanisms for force generation (Fig. 8B). Peptidoglycan hydrolysis is required early in engulfment in order to release the asymmetric septum from the cellular cross-wall, and proteins that mediate this event are therefore required for the initiation of engulfment (Abanes-De Mello *et al*., 2002; Morlot *et al*., 2010). Peptidoglycan hydrolysis is required throughout membrane migration (Abanes-De Mello *et al*., 2002; Gutierrez *et al*., 2010), but it remains unclear if it provides force for membrane migration or plays some other role, such as removing steric barriers to the advancing membranes.

During the last step of engulfment, membrane fission, peptidoglycan synthesis was restricted to the zone of contact between the advancing membranes (Fig. 2, panel iii) and inhibition of muropeptide synthesis (Fig. 4) or polymerization (Fig. 5) prevented detachment of the forespore from the mother cell (engulfment membrane fission). The production of a rigid peptidoglycan polymer in this zone of contact could generate a mechanical force that drives elongation of the bud neck, distorting it into a tube, that eventually breaks, leading to cell separation. Then, localized peptidoglycan hydrolysis would allow the membranes to meet and rearrange (Fig. 8C). A membrane protein, SpoIIIE, is necessary for mediating this fission event during engulfment (Sharp and Pogliano, 2003) and our results suggest that SpoIIIE could interact with membrane proteins involved in peptidoglycan synthesis and organize their spatial distribution at the point of membrane fission. Consistent with this possibility, the membrane domain of SpoIIIE is necessary for its localization to the septum and its function in membrane fission (Sharp and Pogliano, 2003) and for the final steps of cytokinesis at the asymmetric septum (Liu *et al*., 2006).

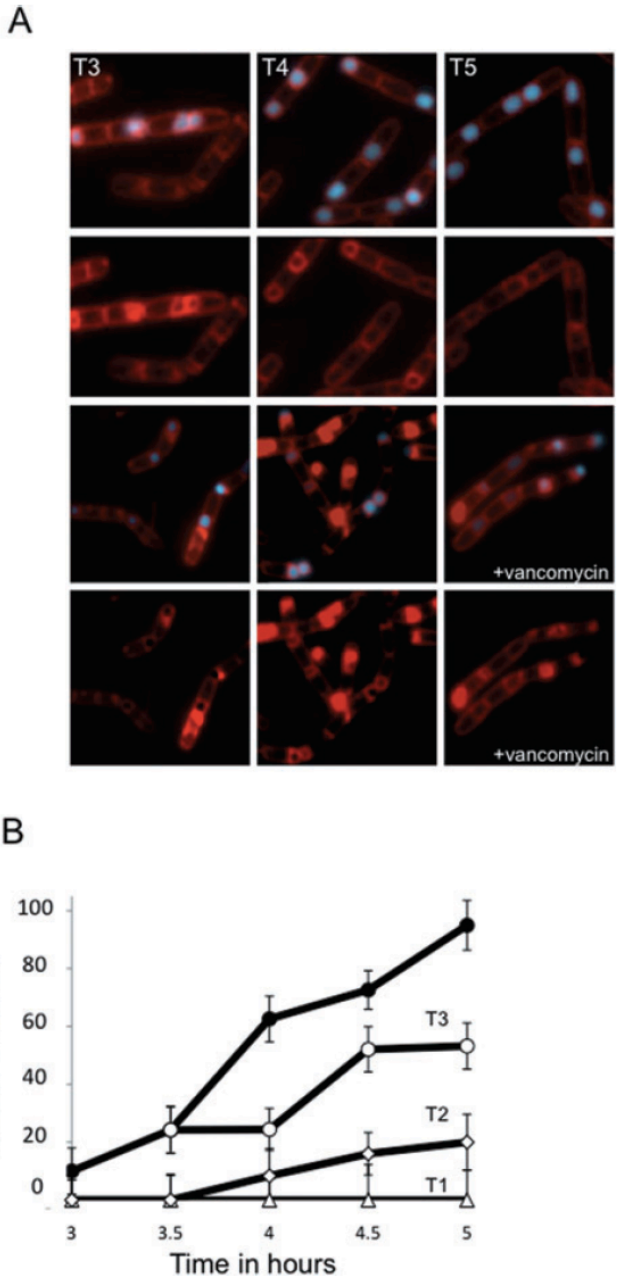

Fig. 5. Inhibition of muropeptide transpeptidation blocks completion of engulfment.
A. Vancomycin blocks engulfment before membrane fission. At T2 of sporulation, cells (AES574) expressing CFP (blue) under control of a forespore-specific promoter (P_{spoIIQ}) were either treated with vancomycin (0.5 μg ml^{-1}; bottom rows) or not treated (top rows). Membranes were visualized with FM4-64 (red). Time after resuspension is indicated.
B. Inhibition of membrane fission depends on the time of addition. The percentage of sporulating cells completing membrane fission was determined for untreated cells (filled circle) or cells incubated with vancomycin (0.5 μg ml^{-1}) at T1 (triangles), T2 (diamonds) or T3.5 (open circles) of sporulation by resuspension.

Muropeptide polymerization during bulge and vesicle formation

Membrane bulges in a *spoIID* or *spoIIP* strain form initially as a deformation of the membrane and then develop into a clear invagination that, at least in some cases, becomes a membrane-bounded vesicle whose cytoplasmic contents are visibly separated from that of the forespore (Fig. 1A, bottom; Fig. 1B). These bulges are sites of active peptidoglycan formation (Fig. 6B) and inhibiting synthesis

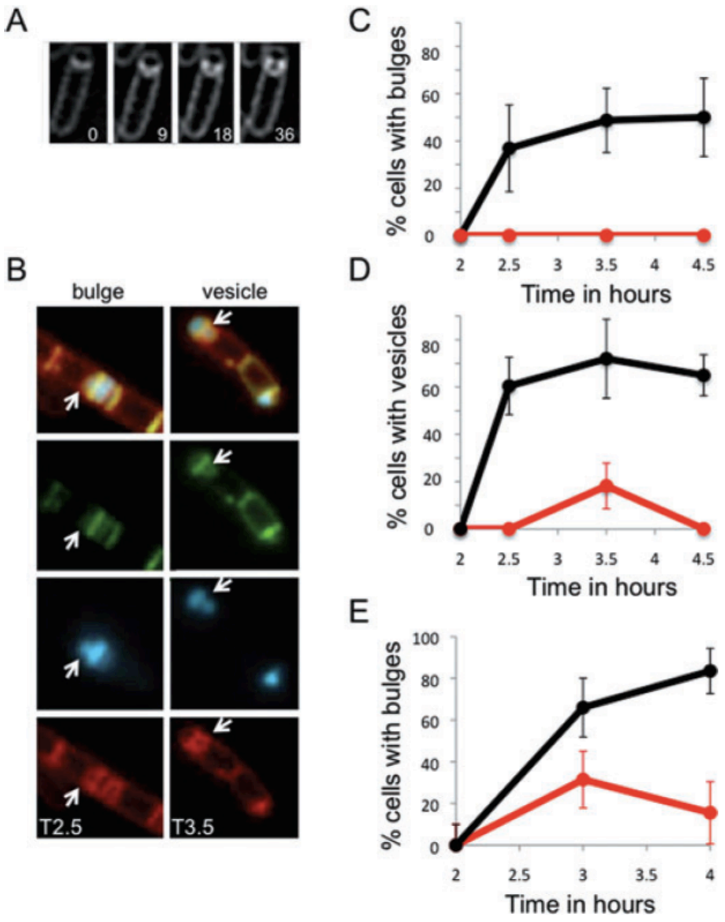

Fig. 6. Muropeptide synthesis and polymerization are required for bulge and vesicle formation.
A. Time-lapse images of a bulge progressively forming in a *spoIID* mutant strain (JDB2395) sporulating in a pad at 30°C and stained with FM4-64. Initial image was taken at approximately T2 after sporulation initiation and arbitrarily set to t = 0 min. The time of subsequent images is indicated in minutes in the lower right corner. See movie Fig. S7.
B. In a *spoIID* mutant strain (JDB2494) expressing CFP (blue) in the forespore, bulge and vesicles (white arrows) are sites of peptidoglycan synthesis. Membranes were visualized with FM4-64 (red) and newly synthesized peptidoglycan identified by ramoplanin-FL, a fluorescent ramoplanin derivative (green). Time after start of sporulation is indicated.
C. Fosfomycin blocks bulge formation. Bulges do not form in a strain (JDB2494) lacking *spoIID* when 5 mM fosfomycin was added at T2 of sporulation (red line) compared with cells where no fosfomycin was added (black line).
D. Fosfomycin blocks vesicle formation. Percentage of cells with vesicles in strains carrying mutations in *spoIID* and expressing CFP at the forespore (JDB2494) in the absence (black) or in the presence of 5 mM fosfomycin added at T2 of sporulation (red).
E. Vancomycin blocks bulge formation. Percentage of *spoIID* cells (JDB2494) with bulges in the absence (black) or in the presence of 0.5 μg ml^{-1} vancomycin (red) added at T2 of sporulation. Bulges and vesicles were identified as defined in Fig. 1B.

of the muropeptide precursor using fosfomycin or of mature peptidoglycan using vancomycin blocks formation of the bulges (Fig. 6C and E). The effect of fosfomycin was on MurAA since a merodiploid strain expressing a resistant mutant protein (MurAAC117D) generated vesicles even in the presence of fosfomycin (Fig. S10). The effect of vancomycin was likely on an inhibition of polymerization directly and not on an inhibition of peptidoglycan hydrolases since inhibition of polymerization in *E. coli* leads to increased muramidase activity (Kohlrausch and Holtje, 1991). Thus, septal peptidoglycan polymerization could exert a mechanical force on the septal membrane that, by analogy to actin polymerization during lamellipodial motility (Mogilner and Oster, 1996), would drive membrane deformations (Fig. 8A, bottom).

The requirement of the SpoVD transpeptidase (Fig. 7A and B) is consistent with the observed inhibition of bulge formation by vancomycin (Fig. 6E) and demonstrates that a protein necessary for the synthesis of mature peptidoglycan is also necessary for bulge formation. In addition, the presence of bulges only on the mother cell side can be explained by this result as SpoVD is under control of σ^E, which is only active in the mother cell. If the forespore had a higher osmotic pressure than the mother cell because of the presence of equally sized chromosomes in the very differently sized compartments, this pressure could push the bulges from the middle of the septum (Perez *et al.*, 2000). However, we did not observe a significant difference in forespore size between the *spoIIP* and the *spoIIP spoVD* strains despite their observed differences in bulge formation (Fig. S13).

Rod-shaped *E. coli* depleted for proteins necessary for cell shape transform into spherical cells that contain large intracellular, membrane-bounded vesicles (Bendezu and de Boer, 2008). The inability of these mutant cells to couple the rate of phospholipid synthesis to changes in shape suggests that vesicle production is caused by overproduction of phospholipids. In *B. subtilis*, a similar coupling is not

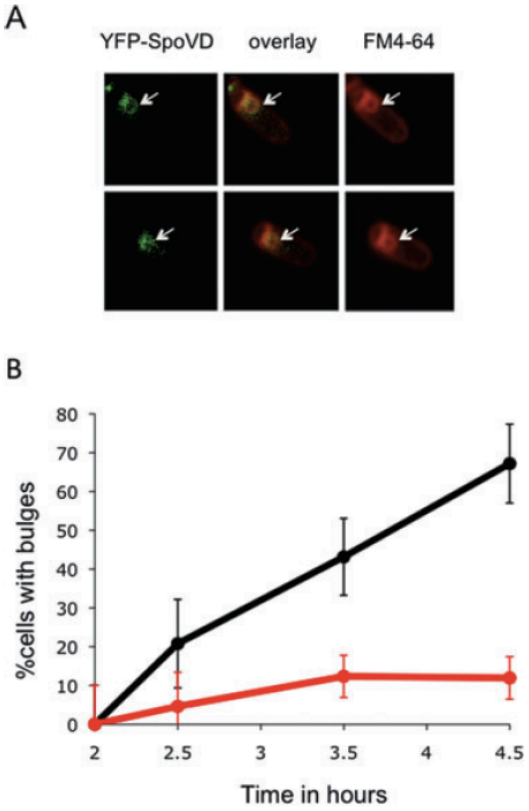

Fig. 7. Muropeptide-polymerizing enzyme is required for bulge formation.
A. The transpeptidase SpoVD localizes to the bulges. A strain lacking *spoIIP* and expressing a YFP–SpoVD fusion (JDB2553) was sporulated by resuspension and images acquired at T4. Two cells are shown. Left, YFP–SpoVD signal; middle is overlay of the YFP–SpoVD and FM4-64 signals; right, FM4-64. White arrows show the bulge.
B. Bulge formation is suppressed by a *spoVD* mutation. Percentage of *spoIIP* (JDB2396; black) and *spoIIP spoVD* (JDB2537; red) cells with bulges was determined. Bulge formation was assessed as defined in Fig. 1B.

known to exist (Paoletti *et al*., 2007), consistent with our observation that fatty acid synthesis was not required at later time points where peptidoglycan synthesis was required for bulge and vesicle formation (Fig. S12) even though it was necessary for initial bulge formation.

Peptidoglycan polymerization as a force-generating mechanism during cytokinesis

A basic question in microbiology is the origin of the force underlying cell division. Although there are well-conserved proteins known to be involved, including the tubulin homologue FtsZ that forms constricting polymeric rings at mid-cell, the source of the force generating these constrictions remains unknown (Weiss, 2004; Margolin, 2005). It has been suggested on theoretical grounds (Lan *et al*., 2007; 2009; Ghosh and Sain, 2008; Allard and Cytrynbaum, 2009) as well as from electron microscopic observations of FtsZ polymer structure *in vivo* (Li *et al*., 2007) that the energetics of FtsZ ring depolymerization could provide such a force. In tubular vesicles, FtsZ forms rings that produce visible constrictions (Osawa *et al*., 2008) consistent with the ability of the constricting Z ring to generate a force. The absence of complete septal closure despite formation of physically distinct compartments seen in some *E. coli* amidase mutants suggests that, at least in these cells, membrane invagination could be mediated solely by constriction of the divisome (Priyadarshini *et al*., 2007).

Gradients of peptidoglycan synthesis generate cell curvature in the bacterium *Caulobacter crescentus* (Cabeen *et al*., 2009), supporting the notion that spatially differentiated peptidoglycan synthesis produces physical force sufficient to generate changes in cell shape that occur during cytokinesis (Huang *et al*., 2008). High-magnification images of dividing *S. aureus* demonstrated the presence of peptidoglycan lying in tight apposition to the membrane. In fact, careful measurement of the diameter of the very tip of the in-growing septum indicated that this site was the locus of peptidoglycan synthesis (Matias and Beveridge, 2007). Thus, this synthesis could provide a driving force for the 'iris-like' movement of the septum from the initial stages of membrane invagination to the completion of septation.

Cell wall polymerization could be used in other systems to generate active and locally controlled forces. Although peptidoglycan is only found in bacteria [and perhaps in the chloroplasts of some plant cells (Machida *et al*., 2006)], yeast and other fungi have rigid cell walls composed of long polysaccharides (Cabib *et al*., 2001) that, similar to peptidoglycan, are polymerized by transglycosylases (Cabib *et al*., 2008). In fact, growing *S. pombe* exerts a large mechanical force at its cell tips that is independent of actin cables and sufficient to play a role in piercing membranes during host invasion (Minc *et al*., 2009). Finally, a variety of cell types such as budding yeasts can undergo cytokinesis in the absence of an actin–myosin contractile ring (Bi *et al*., 1998). Thus, polymerization of fungal polysaccharides could serve a similar function as muropeptide polymerization in providing a force-generating mechanism for cytokinesis.

Experimental procedures

Microbiological methods

Bacillus subtilis strains are derivatives of PY79 (Table S1) and details of their construction are described in *Supporting infor-*

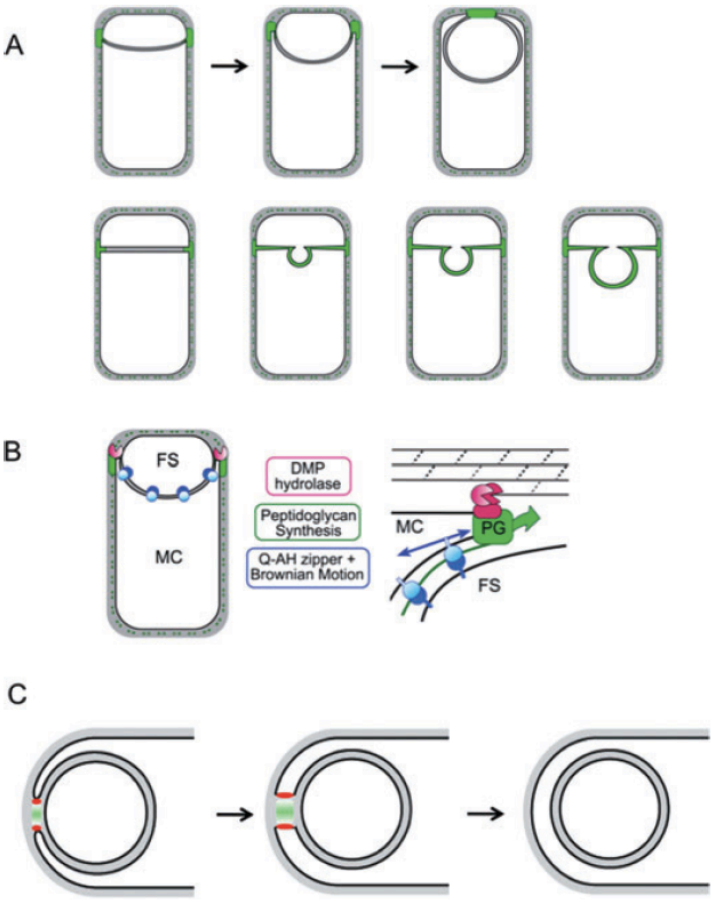

Fig. 8. Role of peptidoglycan polymerization in engulfment.
A. Diagram shows distribution of active peptidoglycan synthesis (green) during membrane migration and before detachment of the forespore from the mother cell (top) as well as during bulge formation (bottom).
B. The polymerization of these newly synthesized muropeptides partially drives membrane movement and results in the separation of the two cells. Our data suggest that membrane movement can be mediated either by peptidoglycan synthesis (PG; green) or by the SpoIIQ–SpoIIIAH proteins (blue) and that peptidoglycan hydrolysis mediated by the DMP proteins (red) plays a necessary role in detaching the septal peptidoglycan from the transverse peptidoglycan. FS, forespore; MC, mother cell.
C. Polymerization of newly synthesized muropeptides into peptidoglycan (green) at the point of contact between the migrating arms of the membranes pushes the septal membranes apart. Following detachment, the forespore becomes an independent membrane-bounded compartment in the cytoplasm. This polymerization is mediated by an unidentified transpeptidase-transglycosylase (red).

mation. Standard procedures were used to prepare and handle recombinant DNA and to transform *E. coli*. *B. subtilis* was transformed using competent cells made by the two-step method (Cutting and Vander Horn, 1990). Sporulation for microscopy was conducted at 30°C and used CH medium or 25% LB for growth and A+B medium for resuspension (Sterlini and Mandelstam, 1969). To measure completion of engulfment, membranes from sporulating cells expressing CFP under control of a forespore-specific promoter (P_{spoIIQ}) were stained with FM4-64 (1 μg ml^{-1}). Every half hour starting at T3 a sample of cells was observed under the microscope. Cells expressing CFP were counted and the fraction of those not exhibiting FM4-64 staining of the forespore was determined.

Reagents

Fosfomycin and vancomycin were obtained from Sigma, cerulenin was obtained from Cayman Chemical, and FM4-64 was from Invitrogen. Ramoplanin-FL and ramoplanin-2c were gifts of Dr Suzanne Walker (Harvard Medical School).

Fluorescence microscopy

One microlitre of FM4-64 (Molecular Probes; 100 μg ml^{-1}) was added to each sample of 100 μl of sporulating cells that were taken at designated times after resuspension, immediately prior to collection by centrifugation. The pellet was resuspended in 10 μl of PBS, and added to a poly-L-lysine pre-treated coverslip. All microscopy (except Fig. 2 and Fig. S2) was performed on a Nikon Eclipse 90i with a 100× objective using phase contrast and captured by a Hamamatsu Orca-ER camera using Nikon Elements BR software. CFP, YFP, FITC (Ramoplanin-FL) and TRITC (FM4-64) exposures were 400 ms. Other microscopy was performed using an Applied Precision Spectris microscope.

Dynamics of engulfing forespores

Time-lapse microscopy was performed as described (Becker and Pogliano, 2007). Briefly, FM4-64 was added to a final concentration of 0.5 μg ml^{-1} in a 1.2% solution of molten

agar/media (A+B) and added to the well of a culture slide and covered with a glass slide. After cooling, the slide was removed and two air pockets were cut out of the agar leaving a 3–5 mm agar bridge in the centre of the well. Sporulating cells suspended in A+B with FM4-64 (0.5 μg ml^{-1}) were added at T2 to the agar bridge and covered by a glass coverslip. To prevent drying during the experiment, 50% glycerol was applied to the region of contact between the slide and the coverslip. The slide equilibrated in an environmentally controlled chamber at 30°C (Precision Control Weather Station) for at least 10 min prior to visualization. Images were acquired using an Applied Precision Spectris microscope.

Finally, the following metric was used for defining membrane migration: 'No migration' is defined as: 40 min of observation with no advancement of the membranes (curvature is acceptable as long as the distance between septum edge and cell pole does not decrease). 'Migration' is defined as: advancement that is maintained for at least 20 min of observation. In addition, cells must be observed for 40 min without going off the screen or lysing.

Acknowledgements

We thank Suzanne Walker (Harvard Medical) for generously supplying fluorescent derivatives of ramoplanin, Avigdor Eldar and Michael Elowitz (Caltech) for strains and Allison Fay for constructing pAF54. This work was supported by NIH R01GM83468 (J.D.) and R01 R01GM57045 (K.P.). P.M. is a Helen Hay Whitney Fellow and J.D. is an Irma T. Hirschl Scholar.

References

Abanes-De Mello, A., Sun, Y.L., Aung, S., and Pogliano, K. (2002) A cytoskeleton-like role for the bacterial cell wall during engulfment of the *Bacillus subtilis* forespore. *Genes Dev* **16:** 3253–3264.

Allard, J.F., and Cytrynbaum, E.N. (2009) Force generation by a dynamic Z-ring in *Escherichia coli* cell division. *Proc Natl Acad Sci USA* **106:** 145–150.

Becker, E.C., and Pogliano, K. (2007) Cell-specific SpoIIIE assembly and DNA translocation polarity are dictated by chromosome orientation. *Mol Microbiol* **66:** 1066–1079.

Bendezu, F.O., and de Boer, P.A. (2008) Conditional lethality, division defects, membrane involution, and endocytosis in *mre* and *mrd* shape mutants of *Escherichia coli*. *J Bacteriol* **190:** 1792–1811.

Bi, E., Maddox, P., Lew, D.J., Salmon, E.D., McMillan, J.N., Yeh, E., and Pringle, J.R. (1998) Involvement of an actomyosin contractile ring in *Saccharomyces cerevisiae* cytokinesis. *J Cell Biol* **142:** 1301–1312.

Broder, D.H., and Pogliano, K. (2006) Forespore engulfment mediated by a ratchet-like mechanism. *Cell* **126:** 917–928.

Bylund, J.E., Zhang, L., Haines, M.A., Higgins, M.L., and Piggot, P.J. (1994) Analysis by fluorescence microscopy of the development of compartment-specific gene expression during sporulation of *Bacillus subtilis*. *J Bacteriol* **176:** 2898–2905.

Cabeen, M.T., Charbon, G., Vollmer, W., Born, P., Ausmees, N., Weibel, D.B., and Jacobs-Wagner, C. (2009) Bacterial cell curvature through mechanical control of cell growth. *EMBO J* **28:** 1208–1219.

Cabib, E., Roh, D.H., Schmidt, M., Crotti, L.B., and Varma, A. (2001) The yeast cell wall and septum as paradigms of cell growth and morphogenesis. *J Biol Chem* **276:** 19679–19682.

Cabib, E., Farkas, V., Kosik, O., Blanco, N., Arroyo, J., and McPhie, P. (2008) Assembly of the yeast cell wall. Crh1p and Crh2p act as transglycosylases *in vivo* and *in vitro*. *J Biol Chem* **283:** 29859–29872.

Cutting, S.M., and Vander Horn, P.B. (1990) Genetic analysis. In *Molecular Biological Methods for Bacillus*. Harwood, C.R. and Cutting, S.M. (eds). New York, NY: John Wiley & Sons, pp. 24–74.

Dancer, B.N. (1979) Requirement for peptidoglycan synthesis during sporulation of *Bacillus subtilis*. *J Bacteriol* **140:** 786–797.

Elbaum, M., Kuchnir Fygenson, D., and Libchaber, A. (1996) Buckling microtubules in vesicles. *Phys Rev Lett* **76:** 4078–4081.

Fitz-James, P.C. (1964) Sporulation in protoplasts and its dependence on prior forespore development. *J Bacteriol* **87:** 667–675.

Francius, G., Domenech, O., Mingeot-Leclercq, M.P., and Dufrene, Y.F. (2008) Direct observation of *Staphylococcus aureus* cell wall digestion by lysostaphin. *J Bacteriol* **190:** 7904–7909.

Frandsen, N., and Stragier, P. (1995) Identification and characterization of the *Bacillus subtilis spoIIP* locus. *J Bacteriol* **177:** 716–722.

Ghosh, B., and Sain, A. (2008) Origin of contractile force during cell division of bacteria. *Phys Rev Lett* **101:** 178101.

Gutierrez, J., Smith, R., and Pogliano, K. (2010) SpoIID peptidoglycan hydrolase activity is required throughout engulfment during *Bacillus subtilis* sporulation. *J Bacteriol* (in press).

Hamburger, J.B., Hoertz, A.J., Lee, A., Senturia, R.J., McCafferty, D.G., and Loll, P.J. (2009) A crystal structure of a dimer of the antibiotic ramoplanin illustrates membrane positioning and a potential Lipid II docking interface. *Proc Natl Acad Sci USA* **106:** 13759–13764.

Hayhurst, E.J., Kailas, L., Hobbs, J.K., and Foster, S.J. (2008) Cell wall peptidoglycan architecture in *Bacillus subtilis*. *Proc Natl Acad Sci USA* **105:** 14603–14608.

van Heijenoort, J. (2001) Recent advances in the formation of the bacterial peptidoglycan monomer unit. *Nat Prod Rep* **18:** 503–519.

Huang, K.C., Mukhopadhyay, R., Wen, B., Gitai, Z., and Wingreen, N.S. (2008) Cell shape and cell-wall organization in Gram-negative bacteria. *Proc Natl Acad Sci USA* **105:** 19282–19287.

Illing, N., and Errington, J. (1991) Genetic regulation of morphogenesis in *Bacillus subtilis*: roles of sigma E and sigma F in prespore engulfment. *J Bacteriol* **173:** 3159–3169.

Inoue, S., and Salmon, E.D. (1995) Force generation by microtubule assembly/disassembly in mitosis and related movements. *Mol Biol Cell* **6:** 1619–1640.

Kim, S.J., Cegelski, L., Stueber, D., Singh, M., Dietrich, E., Tanaka, K.S., *et al.* (2008) Oritavancin exhibits dual mode

of action to inhibit cell-wall biosynthesis in *Staphylococcus aureus*. *J Mol Biol* **377:** 281–293.
Kohlrausch, U., and Holtje, J.V. (1991) Analysis of murein and murein precursors during antibiotic-induced lysis of *Escherichia coli*. *J Bacteriol* **173:** 3425–3431.
Komeili, A., Li, Z., Newman, D.K., and Jensen, G.J. (2006) Magnetosomes are cell membrane invaginations organized by the actin-like protein MamK. *Science* **311:** 242–245.
Lan, G., Wolgemuth, C.W., and Sun, S.X. (2007) Z-ring force and cell shape during division in rod-like bacteria. *Proc Natl Acad Sci USA* **104:** 16110–16115.
Lan, G., Daniels, B.R., Dobrowsky, T.M., Wirtz, D., and Sun, S.X. (2009) Condensation of FtsZ filaments can drive bacterial cell division. *Proc Natl Acad Sci USA* **106:** 121–126.
Li, Z., Trimble, M.J., Brun, Y.V., and Jensen, G.J. (2007) The structure of FtsZ filaments *in vivo* suggests a force-generating role in cell division. *EMBO J* **26:** 4694–4708.
Liu, N.J., Dutton, R.J., and Pogliano, K. (2006) Evidence that the SpoIIIE DNA translocase participates in membrane fusion during cytokinesis and engulfment. *Mol Microbiol* **59:** 1097–1113.
Lopez-Diaz, I., Clarke, S., and Mandelstam, J. (1986) *spoIID* operon of *Bacillus subtilis*: cloning and sequence. *J Gen Microbiol* **132:** 341–354.
Machida, M., Takechi, K., Sato, H., Chung, S.J., Kuroiwa, H., Takio, S., *et al.* (2006) Genes for the peptidoglycan synthesis pathway are essential for chloroplast division in moss. *Proc Natl Acad Sci USA* **103:** 6753–6758.
Margolin, W. (2005) FtsZ and the division of prokaryotic cells and organelles. *Nat Rev Mol Cell Biol* **6:** 862–871.
Matias, V.R., and Beveridge, T.J. (2007) Cryo-electron microscopy of cell division in *Staphylococcus aureus* reveals a mid-zone between nascent cross walls. *Mol Microbiol* **64:** 195–206.
Meador-Parton, J., and Popham, D.L. (2000) Structural analysis of *Bacillus subtilis* spore peptidoglycan during sporulation. *J Bacteriol* **182:** 4491–4499.
Minc, N., Boudaoud, A., and Chang, F. (2009) Mechanical forces of fission yeast growth. *Curr Biol* **19:** 1096–1101.
Mitchison, T.J., and Cramer, L.P. (1996) Actin-based cell motility and cell locomotion. *Cell* **84:** 371–379.
Miyata, H., Nishiyama, S., Akashi, K., and Kinosita, K., Jr (1999) Protrusive growth from giant liposomes driven by actin polymerization. *Proc Natl Acad Sci USA* **96:** 2048–2053.
Mogilner, A., and Oster, G. (1996) Cell motility driven by actin polymerization. *Biophys J* **71:** 3030–3045.
Morlot, C., Uehara, T., Marquis, K.A., Bernhardt, T.G., and Rudner, D.Z. (2010) A highly coordinated cell wall degradation machine governs spore morphogenesis in *Bacillus subtilis*. *Genes Dev* **24:** 411–422.
Osawa, M., Anderson, D.E., and Erickson, H.P. (2008) Reconstitution of contractile FtsZ rings in liposomes. *Science* **320:** 792–794.
Paoletti, L., Lu, Y.J., Schujman, G.E., de Mendoza, D., and Rock, C.O. (2007) Coupling of fatty acid and phospholipid synthesis in *Bacillus subtilis*. *J Bacteriol* **189:** 5816–5824.
Pelham, R.J., and Chang, F. (2002) Actin dynamics in the contractile ring during cytokinesis in fission yeast. *Nature* **419:** 82–86.
Perez, A.R., Abanes-De Mello, A., and Pogliano, K. (2000) SpoIIB localizes to active sites of septal biogenesis and spatially regulates septal thinning during engulfment in *Bacillus subtilis*. *J Bacteriol* **182:** 1096–1108.
Phillips, R., Kondev, J., and Theriot, J. (2009) *Physical Biology of the Cell*. New York: Garland Science.
Priyadarshini, R., de Pedro, M.A., and Young, K.D. (2007) Role of peptidoglycan amidases in the development and morphology of the division septum in *Escherichia coli*. *J Bacteriol* **189:** 5334–5347.
Qualmann, B., Kessels, M.M., and Kelly, R.B. (2000) Molecular links between endocytosis and the actin cytoskeleton. *J Cell Biol* **150:** F111–F116.
Sauvage, E., Kerff, F., Terrak, M., Ayala, J.A., and Charlier, P. (2008) The penicillin-binding proteins: structure and role in peptidoglycan biosynthesis. *FEMS Microbiol Rev* **32:** 234–258.
Scheffel, A., Gruska, M., Faivre, D., Linaroudis, A., Plitzko, J.M., and Schuler, D. (2006) An acidic protein aligns magnetosomes along a filamentous structure in magnetotactic bacteria. *Nature* **440:** 110–114.
Sharp, M.D., and Pogliano, K. (1999) An *in vivo* membrane fusion assay implicates SpoIIIE in the final stages of engulfment during *Bacillus subtilis* sporulation. *Proc Natl Acad Sci USA* **96:** 14553–14558.
Sharp, M.D., and Pogliano, K. (2003) The membrane domain of SpoIIIE is required for membrane fusion during *Bacillus subtilis* sporulation. *J Bacteriol* **185:** 2005–2008.
Smith, K., and Youngman, P. (1993) Evidence that the *spoIIM* gene of *Bacillus subtilis* is transcribed by RNA polymerase associated with sigma E. *J Bacteriol* **175:** 3618–3627.
Sterlini, J.M., and Mandelstam, J. (1969) Commitment to sporulation in *Bacillus subtilis* and its relationship to development of actinomycin resistance. *Biochem J* **113:** 29–37.
Theriot, J.A. (2000) The polymerization motor. *Traffic* **1:** 19–28.
Tipper, D.J., and Linnett, P.E. (1976) Distribution of peptidoglycan synthetase activities between sporangia and forespores in sporulating cells of *Bacillus sphaericus*. *J Bacteriol* **126:** 213–221.
Tiyanont, K., Doan, T., Lazarus, M.B., Fang, X., Rudner, D.Z., and Walker, S. (2006) Imaging peptidoglycan biosynthesis in *Bacillus subtilis* with fluorescent antibiotics. *Proc Natl Acad Sci USA* **103:** 11033–11038.
Vasudevan, P., Weaver, A., Reichert, E.D., Linnstaedt, S.D., and Popham, D.L. (2007) Spore cortex formation in *Bacillus subtilis* is regulated by accumulation of peptidoglycan precursors under the control of sigma K. *Mol Microbiol* **65:** 1582–1594.
Walsh, C.T. (2003) *Antibiotics*. Washington, DC: ASM.
Weiss, D.S. (2004) Bacterial cell division and the septal ring. *Mol Microbiol* **54:** 588–597.
Yao, X., Jericho, M., Pink, D., and Beveridge, T. (1999) Thickness and elasticity of gram-negative murein sacculi measured by atomic force microscopy. *J Bacteriol* **181:** 6865–6875.

Supporting information

Additional supporting information may be found in the online version of this article.

Please note: Wiley-Blackwell are not responsible for the content or functionality of any supporting materials supplied by the authors. Any queries (other than missing material) should be directed to the corresponding author for the article.

Acknowledgments

Chapter II, in full, is a reproduction of the material as it appears in Molecular Microbiology 2010. Meyer, Pablo; Gutierrez, Jennifer; Pogliano, Kit; Dworkin, Jonathan. Blackwell Publishing Ltd, 2010. The dissertation author was a significant contributor to the investigation and writing of the manuscript. Permission of all authors has been obtained.

Supplementary Figures

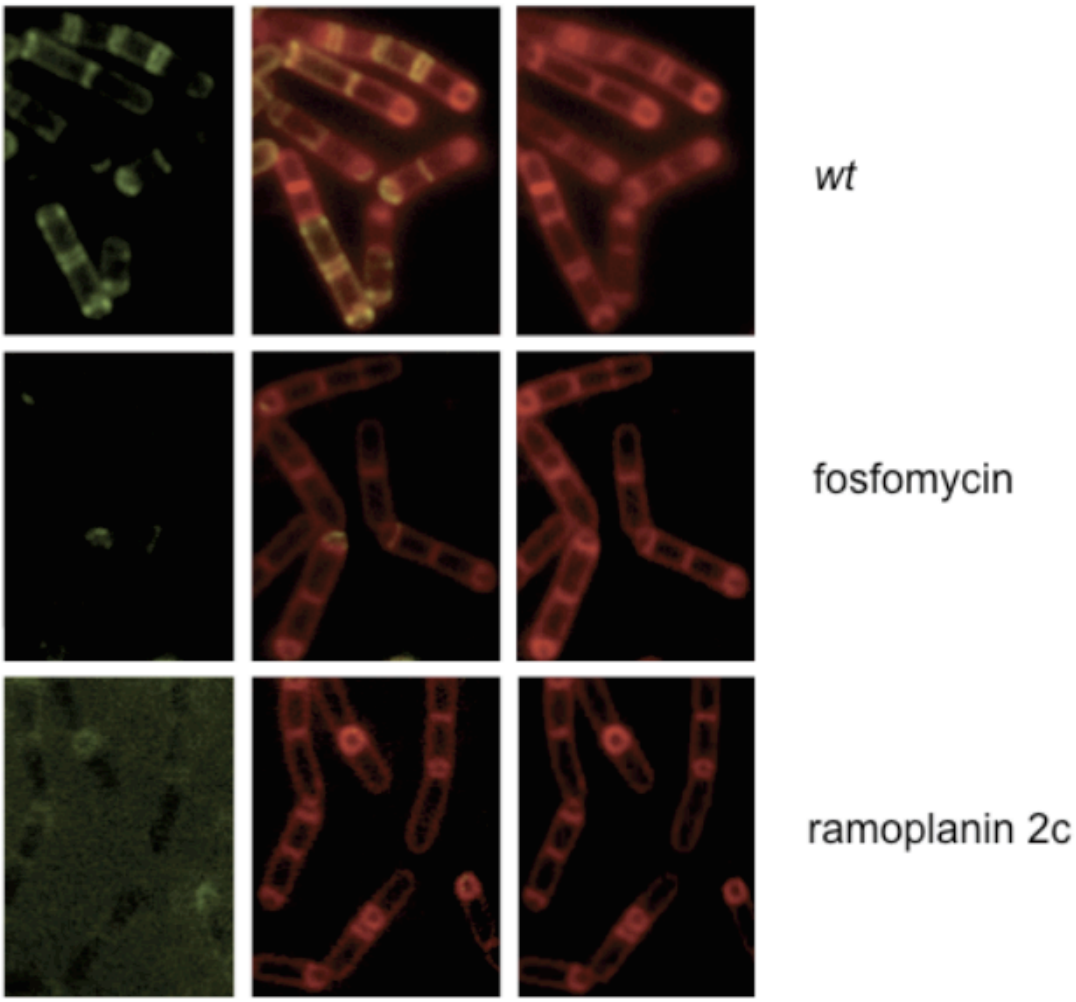

Figure S1. Ramoplanin labels specifically engulfing forespores. Ramoplanin-FL (left), FM4-64 (right) labeling of cells at T3.5 of sporulation. Middle panel is the overlay of both channels. Top, PY79 wild type cells; middle, 5mM fosfomycin was added at T1 to PY79 cells; bottom, wild type *B. subtilis* cells (PY79) were incubated with ramoplanin-2c (1µg/ml) and FM4-64 (1µg/ml) at T3.5 of sporulation.

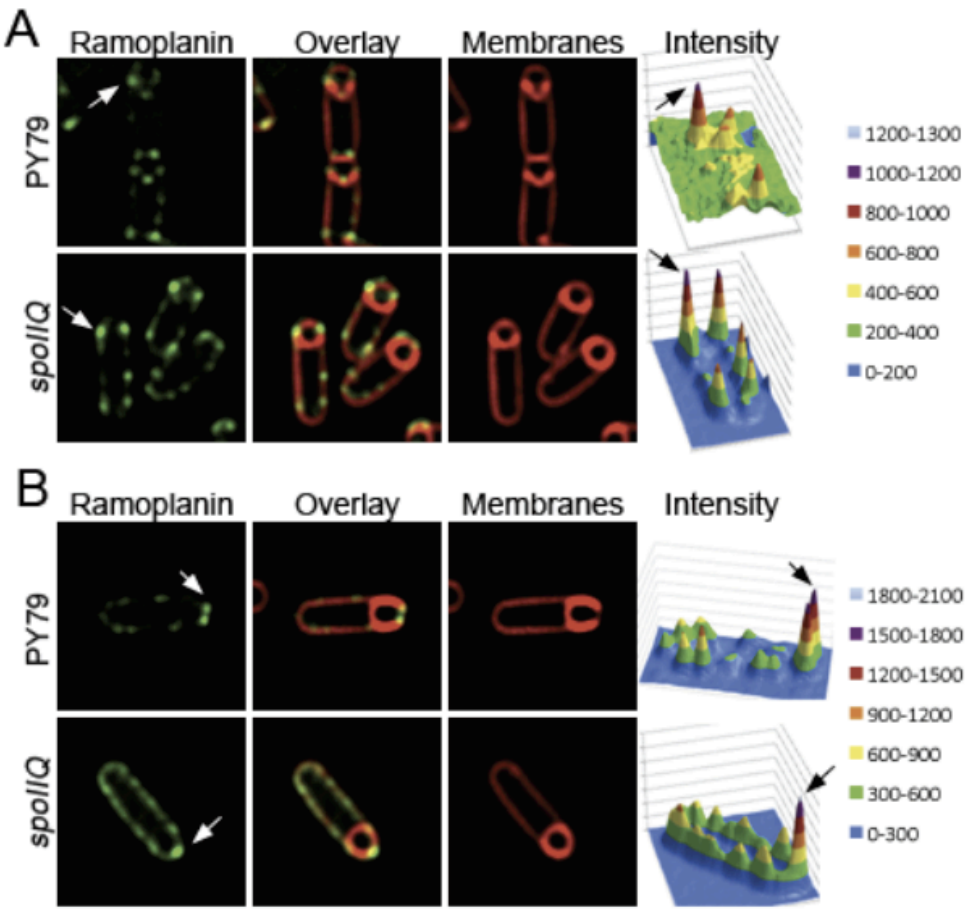

Figure S2. Ramoplanin labeling is not affected by a *spoIIQ* mutation Ramoplanin labelling is the same in wild type and *spoIIQ* mutant strain (KP575). Exposure times for all images were kept constant. Intensity plots were generated in Microsoft Excel using unaltered pixel intensity data and show the Ramoplanin-FL signal in a single cell for each panel. Arrows indicate alignment of the fluorescent image and the intensity plot. **A.** Images taken at T2.5, cells in early stages of migration. **B.** Images taken at T2.5 cells in late stages of migration.

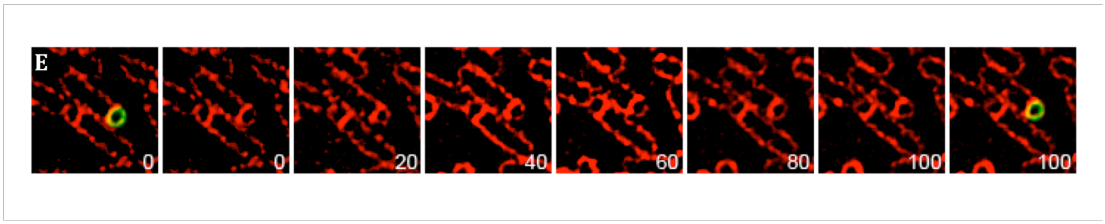

Figure S3 Movies. Time-lapse movies from cells in Fig.3. **A**. Wild type (PY79). **B.** Wild type + 5mM fosfomycin added at T1.5 after initiation of sporulation. **C.** *spoIIQ (*KP575). **D.** *spoIIQ* + 5mM fosfomycin added at T1.5. **E.** *spoIIQ* strain expressing *malF*$_{12}$*-gfp* under P_{spoIIQ} (JFG488) + 5mM fosfomycin added at T1.5. The first and last images show the expression of MalF$_{12}$-GFP superposed on FM4-64 staining. The initial image was taken at approximately T2 after sporulation initiation and arbitrarily set to t=0 minutes. The time of subsequent images of the membrane stain is indicated in minutes in the lower right corner. 12 out of 64 cells expressing MalF$_{12}$-GFP migrated, 37 out of 64 cells had a septa but no GFP.

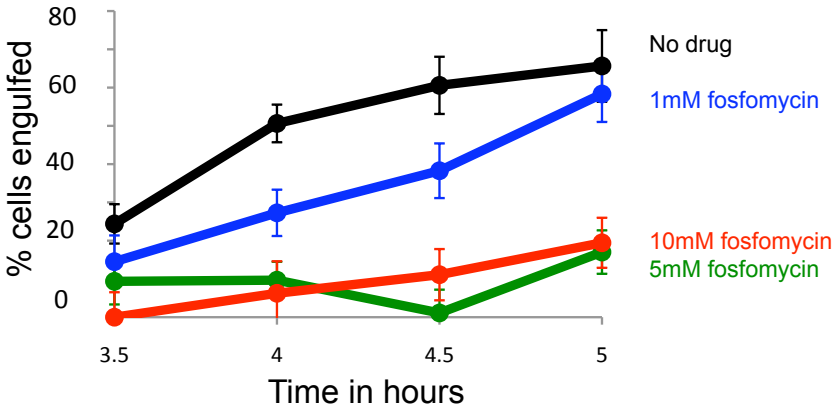

Figure S4. Fosfomycin dose response inhibition of engulfment. Fosfomycin was added at T2 in sporulating cells expressing CFP as a forespore marker (AES574). The fraction of cells showing a CFP signal and not surrounded by an FM4-64 signal was determined. Black, no drug; red, 10mM fosfomycin; green, 5mM; and blue, 1mM.

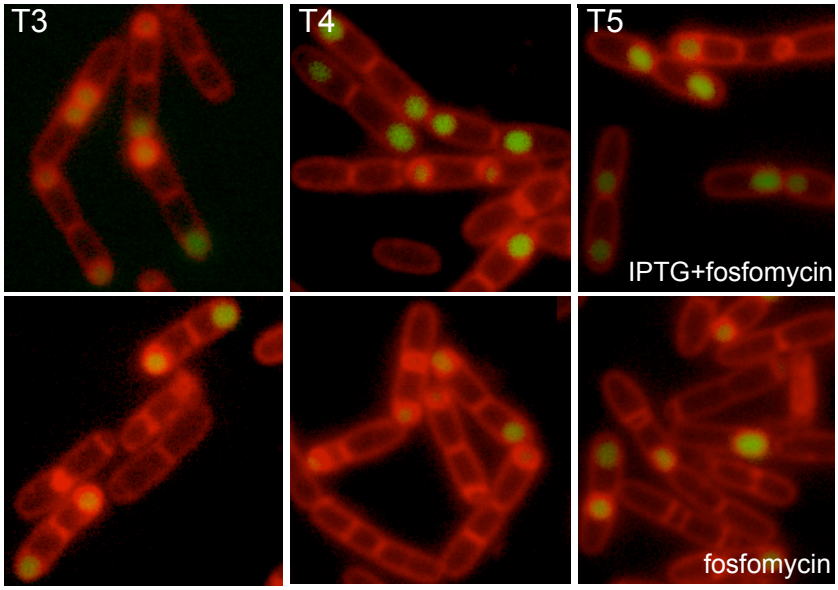

Figure S5. A strain carrying the fosfomycin resistant *murAA* mutant engulfs normally in the presence of fosfomycin. A merodiploid strain expressing inducible *C117D murAA* under IPTG control and *yfp* under (P_{spoIIQ}) control (JDB2426) was sporulated by resuspension. Top, both 1mM IPTG was added at T0 and 5mM fosfomycin at T2; bottom, 5mM fosfomycin was added at T2. Time after start of sporulation is indicated.

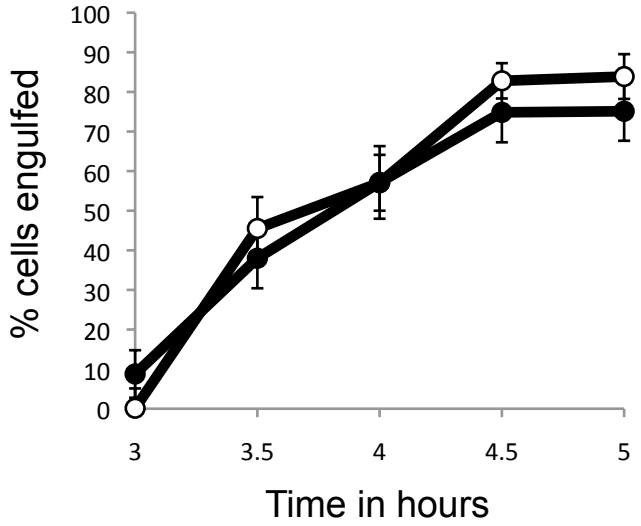

Figure S6. Cells expressing MurAA-C117D engulf normally
Engulfment of a merodiploid strain expressing inducible *C117D murAA* allele under P_{spank} control and *yfp* under (P_{spoIIQ}) control (JDB2426) was sporulated by resuspension and 1mM IPTG was added at T0 (open circles) was compared to a (AES574) strain (closed circles) expressing CFP under control of a forespore specific promoter (P_{spoIIQ}).

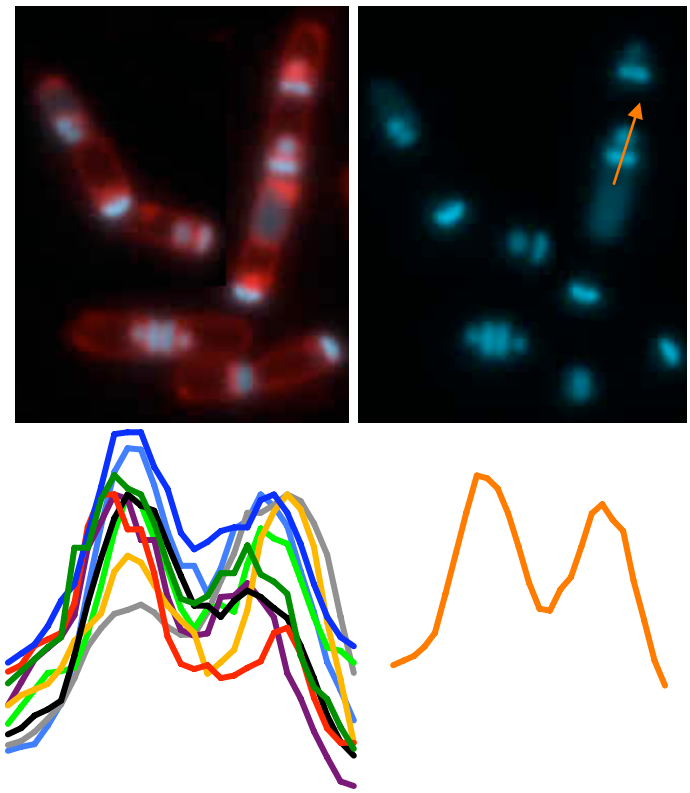

Figure S7. CFP fluorescence distribution in vesicles. A strain (JDB2494) lacking *spoIID* and expressing CFP (blue) under control of a forespore specific promoter (P_{spoIIQ}) as a forespore marker was imaged at T4 of sporulation. Left image is the overlay of CFP with FM4-64 dye in red, right image is CFP only. Bottom left, each trace represents the CFP fluorescence (arbitrary units) across the cell length in nine separate cells. Bottom right, orange trace shows CFP fluorescence (arbitrary units) as a function of distance along the length of the cell indicated by orange arrow.

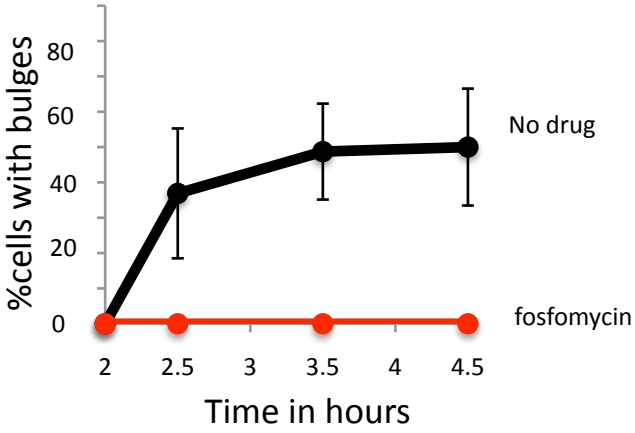

Figure S8. Fosfomycin blocks bulge formation in *spoIIP* cells. Bulges do not form in a strain (JDB2396) lacking *spoIIP* when 5mM fosfomycin was added at T2 of sporulation (red line) compared to cells where no fosfomycin was added (black line).

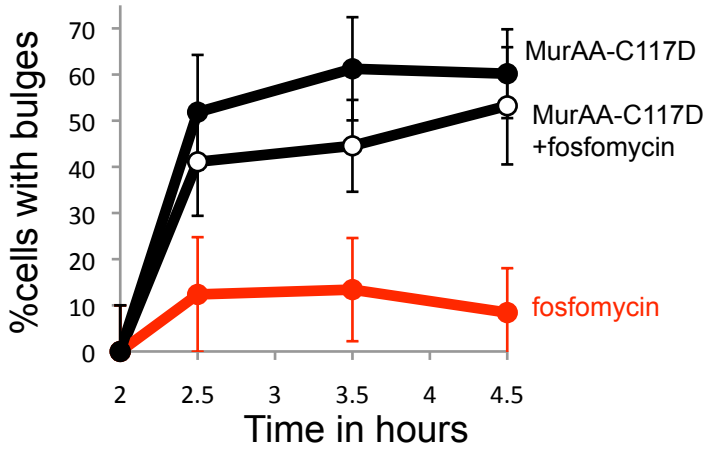

Figure S9. Fosfomycin does not block bulge formation in *spoIID* cells expressing MurAA-C117A. Percentage of bulges in a *spoIID* strain (JDB2535) expressing YFP under control of a forespore-specific promoter and carrying an MurAA-C117A allele under control of P_{spank} in the absence (black circles) or presence of 5 mM fosfomycin (red circles) or in the presence of 1 mM IPTG added at T0 and 5 mM fosfomycin (open circles).

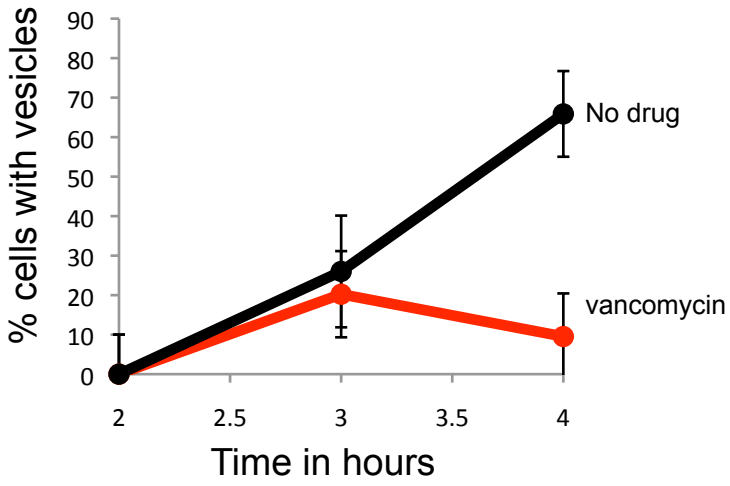

Figure S10. Vancomycin blocks vesicle formation. The percentage of cells containing vesicles of a strain (JDB2494) lacking *spoIID* and expressing CFP as a forespore marker in the absence (black) or presence of vancomycin (0.5 mg/ml) that was added at T2 (red). Vesicles were as defined in Fig. 1B.

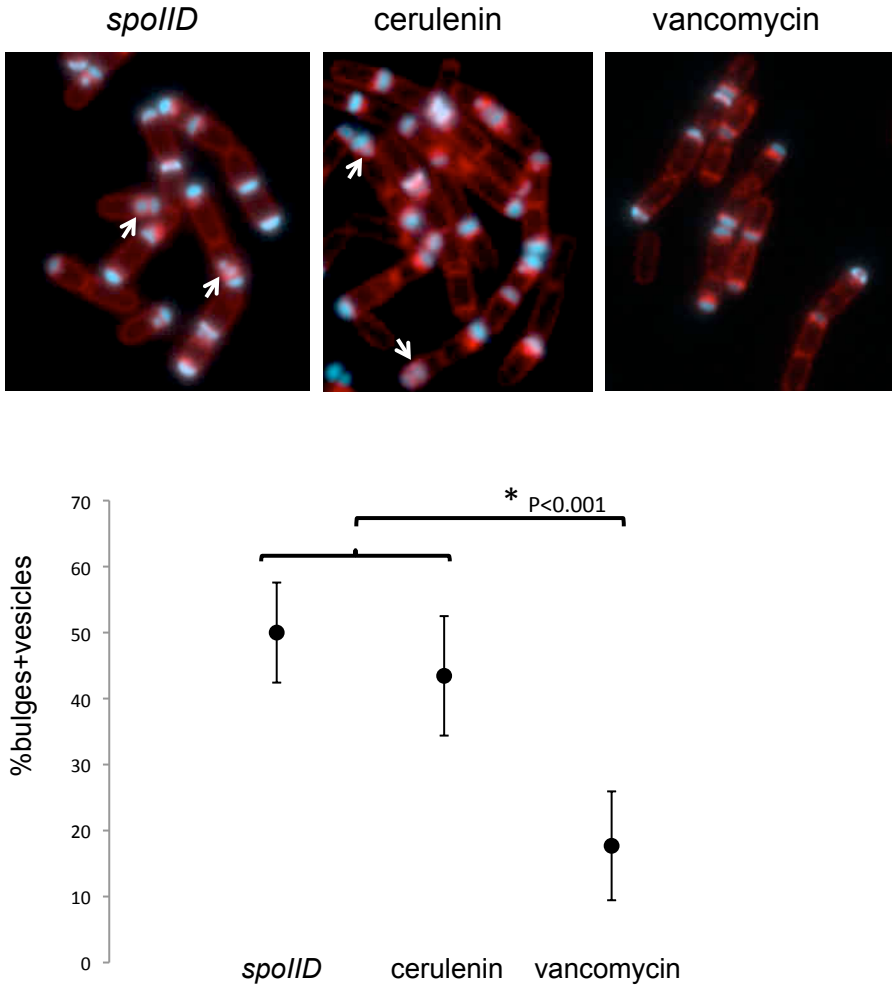

Figure S11. Inhibition of lipid synthesis does not block bulge formation. Images (top) and quantification (bottom) indicate that addition of 10μg/ml cerulenin at T3.5 to a strain (JDB2494) lacking *spoIID* and expressing CFP as a forespore marker does not affect bulge and vesicle formation compared to cells where no drug was added; parallel addition of 0.5μg/ml vancomycin to the same strain at T3.5 blocks bulge and vesicle formation. All observations were made at T4.5 after resuspension. White arrows indicate cells with bulges. Asterisk indicates that for a Pearson's X^2 test with one degree of freedom, the independence hypothesis was true for the number of bulges in vancomycin treated as compared to untreated cells (long bracket, $P<0.001$), but was rejected for cerulenin treated as compared to untreated cells (short bracket, $P>0.1$).

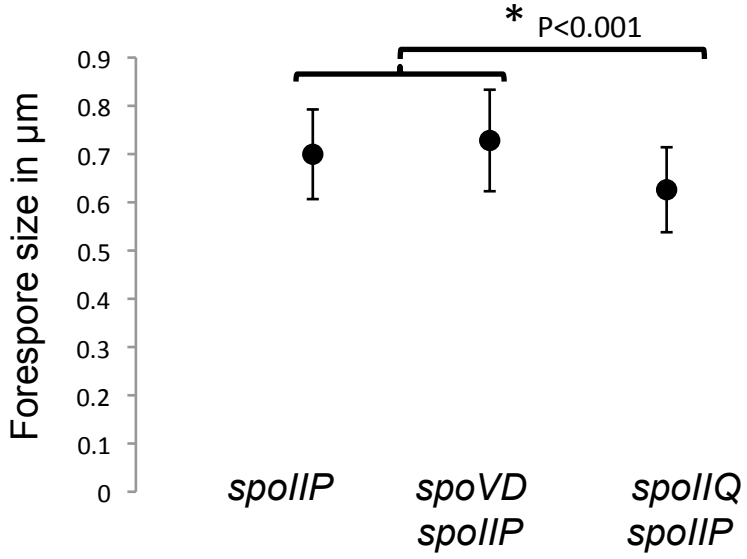

Figure S12. Forespore size measurements. Forespore size at T3 of sporulation was determined by measuring the length of a straight line traced between the forespore tip and the septum. The forespore size in *spoIIP* (KP575) mutant cells (0.69±.09µm) was not different than *spoIIPspoVD* (JDB2537) mutant cells (0.73±.1µm), but was statistically significantly larger than *spoIIPspoIIQ* (JDB2612) mutant cells (0.62±.09µm) by student t-test.

Supplementary Tables

Table S1. Strains used in this study.

Strain	***Genotype***	**Source**
B. subtilis		
PY79	*wt*	Laboratory stock
JGF488	*spoIIQ::spec amyE::P_{spoIIQ}-malF12-gfp*	this work
KP575	*spoIIQ::spec*	(Sun *et al.*, 2000a)
KP1102	*amyE::spoIID(D210A) kan; spoIID298*	(Gutierrez, 2010)
PE177	*spoIID::cm spoIIP::tet spoIIM::erm*	(Eichenberger et al., 2001)
AES240	*sacA::P_{spoIIQ}-yfp cm*	Elowitz lab
AES574	*amyE:P_{spoIIQ}-cfp spec*	Elowitz lab
JDB1213	*spoVD::kan*	(Daniel et al., 1994)
JDB1448	*gltA:P_{spoVE}-yfp-spoVD cm*	(Fay et al., 2009)
JDB2351	*amyE:P_{spank} murAA(C117D) spec*	this work
JDB2395	*spoIID::cm*	this work
JDB2396	*spoIIP::tet*	this work
JDB2426	*amyE:P_{spank}-murAA(C117D) spec sacA:P_{spoIIQ}-yfp cm*	this work
JDB2494	*amyE::P_{spoIIQ}-cfp spec spoIID::cm*	this work
JDB2513	*amyE::P_{spank}-murAA(C117D) spec spoIID::cm*	this work
JDB2535	*amyE::P_{spank}-murAA(C117D) spec spoIID::cm sacA:P_{spoIIQ}-yfp kan*	this work
JDB2537	*spoVD::kan spoIIP::tet*	this work
JDB2546	*sacA::P_{spoIIQ}-yfp kan*	this work
JDB2553	*gltA::P_{spoVE}-yfp-spoVD cm spoIIP::tet*	this work
JDB2612	*spoIIQ::spec spoIIP::tet*	this work
E. coli	*Plasmid*	
BL21		Laboratory stock
	pAF54	this work
	pDG1662	(Guerout-Fleury et al., 1996)
	pMR15	this work
	pKL147	(Lemon & Grossman, 1998)
	pSac-Kan	(Middleton & Hofmeister, 2004)

Chapter III

SpoIID-Mediated peptidoglycan degradation is required throughout engulfment during *Bacillus subtilis* sporulation

JOURNAL OF BACTERIOLOGY, June 2010, p. 3174–3186 Vol. 192, No. 12
0021-9193/10/$12.00 doi:10.1128/JB.00127-10

SpoIID-Mediated Peptidoglycan Degradation Is Required throughout Engulfment during *Bacillus subtilis* Sporulation▽†

Jennifer Gutierrez, Rachelle Smith, and Kit Pogliano*

Division of Biological Sciences, University of California at San Diego, 9500 Gilman Drive, La Jolla, California 92093-0377

Received 4 February 2010/Accepted 31 March 2010

SpoIID is a membrane-anchored enzyme that degrades peptidoglycan and is essential for engulfment and sporulation in *Bacillus subtilis*. SpoIID is targeted to the sporulation septum, where it interacts with two other proteins required for engulfment: SpoIIP and SpoIIM. We changed conserved amino acids in SpoIID to alanine to determine whether there was a correlation between the effect of each substitution on the *in vivo* and *in vitro* activities of SpoIID. We identified one amino acid substitution, E88A, that eliminated peptidoglycan degradation activity and one, D210A, that reduced it, as well as two substitutions that destabilized the protein in *B. subtilis* (R106A and K203A). Using these mutants, we show that the peptidoglycan degradation activity of SpoIID is required for the first step of engulfment (septal thinning), as well as throughout membrane migration, and we show that SpoIID levels are substantially above the minimum required for engulfment. The inactive mutant E88A shows increased septal localization compared to the wild type, suggesting that the degradation cycle of the SpoIID/SpoIIP complex is accompanied by the activity-dependent release of SpoIID from the complex and subsequent rebinding. This mutant is also capable of moving SpoIIP across the sporulation septum, suggesting that SpoIID binding, but not peptidoglycan degradation activity, is needed for relocalization of SpoIIP. Finally, the mutant with reduced activity (D210A) causes uneven engulfment and time-lapse microscopy indicates that the fastest-moving membrane arm has greater concentrations of SpoIIP than the slower-moving arm, demonstrating a correlation between SpoIIP protein levels and the rate of membrane migration.

Endospore formation is an evolutionarily conserved process that allows *Bacillus subtilis* and related Gram-positive bacteria to adapt to changes in the environment, such as nutrient depletion. Many dramatic morphological changes occur during sporulation, each requiring a multitude of specialized proteins (reviewed in references 13 and 17). First, a sporulation septum is formed near one of the cell poles, forming two separate compartments of unequal sizes and with differing fates (Fig. 1A). The smaller of the two, the forespore, will eventually become the spore, while the larger, the mother cell, will ultimately lyse. Next, the mother cell membranes move up and around the forespore in the poorly understood process of engulfment. Although this process is superficially similar to eukaryotic engulfment, it is complicated by the thick cell wall that surrounds and separates the two compartments. After engulfment, the migrating membranes pinch off from the mother cell membrane, thereby releasing the forespore into the cytoplasm of the mother cell, where it can be enveloped with protective coat proteins and eventually released into the environment as a mature spore. Sporulation provides an ideal, nonessential system for understanding how bacterial cells are capable of undergoing dramatic morphological changes.

Engulfment involves dynamic protein localization and large-scale rearrangements of cellular membranes and peptidoglycan to accommodate internalization of the forespore. The physical basis for engulfment remains unclear, but two separate protein machineries that contribute to engulfment have been discovered. The first module involves the only three proteins known to be required for engulfment under all physiological conditions: SpoIID, SpoIIM, and SpoIIP (16, 24, 35). Zymography assays have demonstrated that both SpoIID and SpoIIP degrade peptidoglycan *in vitro* (1, 8), and this function is thought to be essential for engulfment in wild-type cells (1, 2, 8). SpoIID and SpoIIP are membrane-spanning proteins that directly interact both *in vivo* and *in vitro*, as demonstrated by coimmunoprecipitation and affinity chromatography techniques (2, 8). These studies failed to demonstrate an interaction between SpoIIM and either SpoIID or SpoIIP, perhaps because SpoIIM is an integral membrane protein. However, SpoIIM is required for localization of SpoIID and SpoIIP (2, 8), suggesting that all three proteins interact to form a peptidoglycan degradation module that is essential for engulfment.

The second system influencing membrane migration is the SpoIIQ/SpoIIIAH zipper, which is required for engulfment only under certain conditions (2, 7, 38). SpoIIQ is produced in the forespore (23) and SpoIIIAH is produced in the mother cell (19). SpoIIQ and SpoIIIAH interact both *in vitro* and *in vivo* via their extracellular domains (6, 7, 10). Because these two proteins are produced in separate compartments, the only possible place for an interaction is the intermembrane space between the mother cell and forespore, forming a protein-protein zipper between the two cells. This zipperlike interaction is necessary for septal localization of SpoIIIAH and other mother cell proteins (6, 10, 18) and is capable of holding the two cells together when peptidoglycan is removed with lysozyme (7). Surprisingly, digestion of the peptidoglycan with

* Corresponding author. Mailing address: Division of Biological Sciences, University of California at San Diego, 9500 Gilman Drive, La Jolla, CA 92093-0377. Phone: (858) 822-1314. Fax: (858) 822-5740. E-mail: kpogliano@ucsd.edu.

† Supplemental material for this article may be found at http://jb.asm.org/.

▽ Published ahead of print on 9 April 2010.

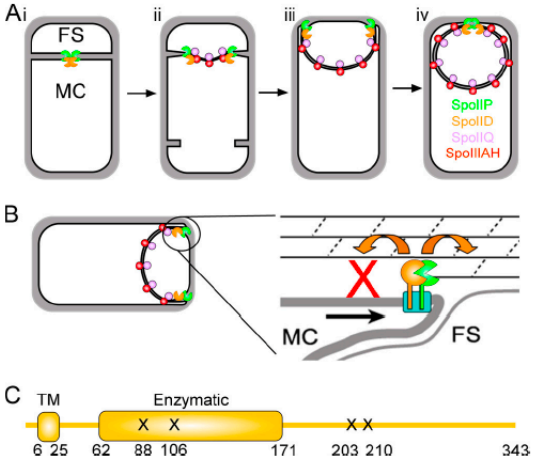

FIG. 1. Engulfment in *B. subtilis*. (A) (i) Engulfment begins with formation of an asymmetric septum that divides the cell into the forespore (FS) and mother cell (MC). SpoIID (orange pacman) and SpoIIP (green pacman) peptidoglycan degradation enzymes localize to the center of the septum. (ii) SpoIID and SpoIIP thin the septal peptidoglycan, starting from the center and moving toward the cell edges. SpoIIQ (purple ball) and SpoIIIAH (red ball) form a zipper across the septum, assembling foci behind the leading edges. (iii) The peptidoglycan degradation enzymes localize to the leading edges during membrane migration, while additional SpoIIQ-SpoIIIAH complexes assemble around the forespore. (iv) Engulfment membrane fission occurs at the top of the forespore, releasing the forespore into the mother cell cytoplasm. (B) Burnt-bridge Brownian ratchet model for membrane migration, adapted from earlier studies (1, 7). (C) Schematic representation of the SpoIID domain structure. The transmembrane domain (TM) and putative enzymatic domain, as defined by Pfam (14), are indicated. Amino acid numbers are below the schematic, and mutations causing *in vivo* phenotypes are indicated by an "X".

lysozyme also allows membrane migration in about half of treated cells, in a process requiring the SpoIIQ/SpoIIIAH zipper but not the SpoIIDMP peptidoglycan degradation module. The SpoIIQ-SpoIIIAH zipper also contributes to engulfment in living cells, since strains lacking SpoIIQ or SpoIIIAH complete engulfment more slowly than the wild type and have synergistic engulfment defects when certain secondary mutations are introduced (2, 7, 38). Together, these results strongly support a role for the SpoIIQ/SpoIIIAH module in engulfment, demonstrating that the zipper contributes to the efficiency of membrane migration even when the SpoIIDMP module is present and functional. They also suggest that the engulfment machinery displays functional redundancy and that the zipper module provides a backup machinery for membrane migration.

The precise role of the SpoIIDMP module during engulfment remains unclear. One model proposes that SpoIID and SpoIIP act as a burnt-bridge Brownian ratchet (Fig. 1B) (1, 7). This model asserts that as SpoIID and SpoIIP degrade peptidoglycan, they eliminate their own enzymatic targets, resulting in the absence of substrate in one direction and therefore, overall movement in the opposite direction. As the enzymes move forward toward new targets, the mother cell membranes are dragged along with them because they are anchored in the membrane. This hypothesis predicts that SpoIID and SpoIIP are processive enzymes and that the SpoIIDMP complex could function as a motor, moving along peptidoglycan as a track and pulling the membranes with it (1, 7). A second model predicts that peptidoglycan degradation could simply remove a steric hindrance to membrane migration (such as links between the forespore membrane and the cell wall) and that some other mechanism provides the force required for membrane migration. Although the SpoIIQ-SpoIIIAH module can contribute to membrane migration, these proteins are not always essential for engulfment in intact cells (7, 38), suggesting that another unidentified system must generate the force required for membrane movement if the DMP module does not act as a burnt-bridge Brownian ratchet. Recent evidence suggests that peptidoglycan biosynthesis, which is localized to the leading edge of the engulfing membrane and necessary for membrane migration in the absence of the SpoIIQ-SpoIIIAH proteins, might be this missing force generating mechanism (26).

Both models predict that the activities of SpoIID and SpoIIP are essential for membrane migration. This requirement has been demonstrated for SpoIIP (8) and, while this work was under review, for SpoIID. SpoIID shows no sequence similarity to any characterized enzyme that degrades peptidoglycan and thus constitutes the founding member of a new class of enzymes that remodel peptidoglycan (1, 27). However, SpoIID does show some similarity to *B. subtilis* LytB (24), a protein that enhances the activity of the amidase LytC (5, 20, 34), while SpoIIP is related to LytC (14). A recent study demonstrated that SpoIIP is both an amidase and endopeptidase and that SpoIID both activates SpoIIP and functions as a lytic transglycosylase, cleaving peptidoglycan between NAG and NAM (27). Together, these two enzymes degrade peptidoglycan into its smallest repeating subunits. However, it remains unclear which of the demonstrated or suggested biochemical functions of SpoIID are required for its various *in vivo* activities (interaction with SpoIIP, localization, septal thinning, and membrane migration), and it is unclear whether peptidoglycan degradation activity is required throughout engulfment or only for the initial stage of septal thinning.

We use site-directed mutagenesis to test the role of 56 conserved amino acids in SpoIID, focusing on hydrophilic amino acids that might be involved in protein-protein interactions and peptidoglycan degradation. We identified one mutation (E88A) that eliminates and three others (R106A, K203A, and D210A) that reduce peptidoglycan degradation activity and show that SpoIID activity is required for the earliest stage of engulfment (septal thinning), as well as throughout membrane migration. Our results confirm and extend those of Morlot et al. (27) and also demonstrate that SpoIID activity is required throughout engulfment. Furthermore, our data indicate that the enzymatically inactive mutant protein (E88A) shows increased septal localization compared to the wild-type protein, suggesting that peptidoglycan degradation contributes to the release of SpoIID from the septum. We propose a modified model for the enzymatic cycle of the SpoIID and SpoIIP complex.

MATERIALS AND METHODS

Bacterial strains, genetic manipulations, and growth conditions. *Bacillus subtilis* strains used in the present study are derivatives of the wild-type strain PY79 (39) and are shown in Table 2. Mutations and plasmids were introduced into PY79 by transformation (12). *B. subtilis* strains were grown and sporulated at 37°C unless otherwise indicated. Sporulation was induced by the modified resuspension method (36) using 25% LB as a growth medium (4) for all cell biological experiments. Heat-resistant spore assays were performed on cultures grown and sporulated in DSM broth (31) for 24 h at 37°C. Cultures were then heated at 80°C for 20 min, serially diluted, and plated on LB. Spore titers were calculated based on colony counts.

Construction of His_6-SpoIID. The His_6-SpoIID overexpression plasmid pSA12 was constructed in pET30a (Novagen). The spoIID region encoding amino acids 27 to 343 was PCR amplified from PY79 chromosomal DNA using the primers: 5′-GAGCCGCATTAGCACCATCATCATCATCATCAGCATA ATAAGGAAGCGGGG and 5′-GCGGCGGTCGACTTACTTTTTCGCCAT ATATTTATT (the NdeI and SalI restriction sites are underlined). pET30a was used as the vector with the N-terminal His_6 tag encoded on the primer. PCR fragments were digested with NdeI and SalI (New England Biolabs) and ligated into NdeI- and SalI-digested pET30a. The ligation mix was transformed into the *Escherichia coli* strain DH5α and transformants selected for on LB-kanamycin (50 μg/ml). All constructs were confirmed to be correct by DNA sequencing.

Targeted mutagenesis of *spoIID*. Mutations in *spoIID* were introduced using a site-directed mutagenesis protocol adapted from an earlier study (30). Plasmid pKP01 (1), an *amyE*-integrating vector that includes *spoIID*, was used as the template for initial QuikChange PCRs. Primers used in the PCRs are listed in Table SA2 in the supplemental material and generally included 12 bp upstream and 12 bp downstream of the mutation that substituted the native codon with a GCA alanine codon. Plasmids were transformed into DH5α or TOP10 cells (Invitrogen). The entire *spoIID* coding region of the mutagenized plasmids was sequenced by EtonBio (San Diego, CA) or Genewiz (San Diego, CA), using the primers JGP2dp or JGPD358 (see Table SA2 in the supplemental material). After transformation into *B. subtilis*, the resultant colonies were purified, patched to DSM, and incubated at 30°C to assess the ability of each construct to support sporulation. Mutations with a sporulation phenotype were subsequently introduced into pRSE15 and pSA12, the latter encoding His_6-tagged SpoIID in an *E. coli* expression construct (Novagen) (construction described above). The *GFP-spoIID* plasmid pRSE15 was constructed from pAAD9 (1), an *amyE* inserting vector containing *spoIID* in frame and downstream of the fusion of green fluorescent protein (GFP) to the *spoIID* promoter, translational initiation sequences, and the first five codons encoded in pMDS14 (33). This plasmid had three mutations in the *spoIID* coding sequence, which were converted to wild type by using QuikChange mutagenesis and primers RMSP12 and RMSP13 to give pRSE10 and then using RMSP10 and RMSP11 (see Table SA2 in the supplemental material) to yield pRSE15.

Microscopy and image analysis. To visualize the GFP, samples from sporulating cultures were taken at the indicated times, stained with a final concentration of 5 μg of FM 4-64/ml and 2 μg of DAPI/ml, and applied to poly-L-lysine-coated coverslips (32). For membrane fusion assays, the cells were stained with a final concentration of 5 μg of FM 4-64/ml and 4 μg of MitoTracker Green (MTG)/ml (32). Images were collected by using an Applied Precision Spectris optical sectioning microscope equipped with a Photometrix CoolsnapHQ charge-coupled device camera. Images were deconvolved by using SoftWoRx software (Applied Precision, Inc.).

Time-lapse microscopy. Time-lapse microscopy was performed as previously described (4). Briefly, cells were grown at 37°C in 25% LB to an optical density at 600 nm (OD_{600}) of 0.5 and resuspended in A+B sporulation salts (36). A 2-ml aliquot of each resuspended culture was shifted to a small culture tube, followed by incubation in a roller at 30°C with FM 4-64 added to a final concentration of 0.5 μg/ml at the time of resuspension, while the remainder of the culture was grown without dye. The unstained culture was spun down 20 min before t_2 and the supernatant used to make a 1.2% agarose/A+B pad containing 0.5 μg of FM 4-64/ml. The stained culture was spread on this pad, covered with a glass coverslip, and equilibrated to 30°C for 10 min prior to viewing. Cells were grown and imaged on the pad in a climate controlled chamber (Precision Control Weather Station) set to 30°C.

His_6-SpoIID overexpression and purification. For purification of His_6-SpoIID, a 250-ml culture of BL21 containing pSA12, or else pSA12 with the indicated single amino acid substitution, was incubated at 37°C until reaching an OD_{600} of 0.6 to 0.8. Cultures were then induced for 3 h with 2 mM IPTG (isopropyl-β-D-thiogalactopyranoside). Cells were harvested by centrifugation, and the pellet was frozen at −80°C. The pellet was resuspended in buffer J (50 mM NaH_2PO_4, 300 mM NaCl, 10 mM imidazole [pH 8.0]) including 2 mM phenylmethylsulfonyl fluoride (PMSF) and sonicated to lyse the cells. Cell debris was removed by centrifugation, and the supernatant was added to equilibrated His-Select Ni/NTA resin (Sigma) and shaken at 4°C overnight. The slurry was added to a column, washed with 10 column volumes of buffer J and 5 column volumes of buffer J plus 40 mM imidazole, and eluted with buffer J plus 250 mM imidazole. His_6-SpoIID protein was further purified by ion-exchange chromatography (except for His_6-$SpoIID^{R106A}$). Protein was dialyzed into buffer A (100 mM NaH_2PO_4, 10 mM TrisHCl, 150 mM NaCl [pH 8]) and run over a column of Q-Sepharose beads. The His-tagged protein was eluted by running buffer A, with stepwise increases in NaCl concentration, over the column. Fractions of 1-ml volume were collected and analyzed for protein content by using a spectrophotometer to monitor the A_{280}. Fractions containing protein were combined and dialyzed into activity buffer (20 mM Tris-HCl, 150 mM NaCl [pH 8.0]). Protein was stored at −80°C until use with an approximate concentration of 0.5 mg/ml.

Renaturing gel electrophoresis assay for peptidoglycan degradation activity. Zymography was performed as previously described (15, 37) using 0.1% *Micrococcus luteus* cells (Sigma) as a substrate. Gels were rocked in renaturing solution (25 mM Tris-HCl, 1% Triton X-100 [pH 7.2]) at 37°C overnight, imaged using an Olympus E-410 Digital SLR camera, stained with fresh 0.01% methylene blue in 0.01% KOH for 3 h at room temperature, and then rinsed. Stained gels were imaged using a Typhoon scanner (GE Healthcare) without an emission filter.

Western blotting. Samples for Western blots were prepared as described in reference 9. Briefly, 1.0 ml of cell culture was harvested at the indicated time points and precipitated by the addition of 110 μl of 50% trichloroacetic acid and frozen overnight. Samples were spun on high for 5 min, washed with Tris buffer (pH 8), and resuspended in 54 μl of Tris sucrose buffer (33 mM Tris [pH 8], 40% sucrose, 1 mM EDTA, 300 μg of PMSF/ml). Lysozyme was added to a final concentration of 1 μg/ml, and the samples were incubated at 37°C for 10 min. An equal volume of 2× sodium dodecyl sulfate (SDS) loading buffer was added to each sample, and the samples were heated to 42°C. Samples were applied to a SDS–10% PAGE gel, transferred to a polyvinylidene difluoride membrane, and probed with previously prepared antibodies to SpoIID at a 1:3,000 dilution (9). Secondary, anti-rabbit antibody conjugated to horseradish peroxidase (GE Healthcare) was added at 1:3,000 and developed using an ECL-Plus kit (GE Healthcare).

In-gel GFP fluorescence. The levels of GFP-SpoIID proteins were assessed using an in-gel GFP fluorescence protocol adapted from Dubnau and Davidoff-Abelson (11). Cultures were sporulated by resuspension. At the indicated times after initiation of sporulation, 1.5-ml samples were collected and resuspended in 45 μl of phosphate-buffered saline plus 300 μg of PMSF/ml. Lysozyme was added to a final concentration of 1 mg/ml, and the samples were incubated at 37°C for 10 min. Then, 50 μl of fresh solubilization buffer (200 mM Tris-HCl [pH 8.8], 20% glycerol, 5 mM EDTA, 0.02% bromophenol blue, 4% SDS, 50 mM dithiothreitol) was added, and the samples were again heated at 37°C for 10 min. A needle and syringe were used to break up DNA and reduce sample viscosity. A 20-μl portion of the sample was applied to a SDS–10% PAGE gel and run at 60 V. GFP fluorescence was visualized by using a Typhoon scanner with 520 BP 40 emission filter and a blue (488-nm) laser.

RESULTS

Site-directed mutagenesis of *spoIID*. SpoIID is a 343-amino-acid, membrane-spanning protein with a short cytoplasmic N terminus, a single transmembrane domain, and a large extracytoplasmic C-terminal domain (Fig. 1C). The SpoIID extracytoplasmic domain is conserved throughout the endospore forming bacteria, with more distant relatives found in many other bacterial phyla (14). Our results indicated that this domain was responsible for the peptidoglycan degradation activity of purified SpoIID in zymography gels (see below), but until recently (27), none of the proteins that are homologous to SpoIID have had characterized activities.

To further investigate the mechanism by which SpoIID cleaves peptidoglycan, we identified conserved amino acids in SpoIID using the CLUSTAL W program (21), which performs multiple HMM alignments of SpoIID homologues (Fig. 2). We selected 56 conserved hydrophilic amino acids for site-directed mutagenesis to alanine, including all conserved amino acids

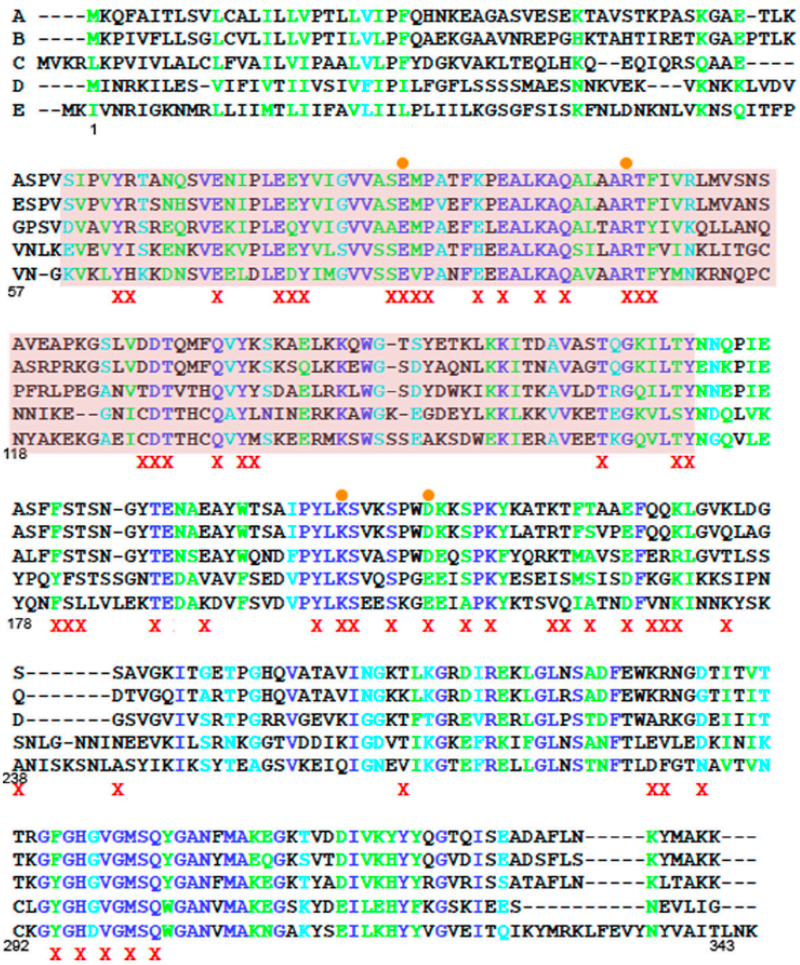

FIG. 2. Amino acids selected for mutagenesis of SpoIID. Alignments of *spoIID* were performed by using CLUSTAL W (21). The species presented here are as follows: A, *Bacillus subtilis*; B, *Bacillus amyloliquefaciens*; C, *Geobacillus thermodinitrificans*; D, *Clostridium perfringens*; E, *Clostridium saccharobutylicum*. Amino acid numbers below the alignment refer to the *B. subtilis* sequence for easier identification of mutations. A red X indicates an amino acid changed to alanine and an orange circle indicates a mutant characterized in the present study. Sequence homology is represented by color, with completely conserved amino acids indicated by royal blue, highly conserved amino acids indicated by green and weakly conserved amino acids indicated by cyan. The putative peptidoglycan degradation domain is highlighted in purple. Recently, an alignment and compilation of all 667 SpoIID family members has become available on Pfam (14). This alignment was used to confirm our earlier alignments and verify that all residues showing significant conservation were mutated during our study. In this more complete alignment, only six amino acids are completely conserved, and just two of these, E88 and R106, resulted in an *in vivo* phenotype when changed to alanine.

identified in the putative enzymatic domain (Pfam 08486, Fig. 2, purple highlight). The entire *spoIID* coding and promoter region was sequenced, and the mutations were screened for the ability to complement a *spoIID*-null strain and support sporulation both by examining pigmentation on DSM plates and by measuring the ability to produce heat resistant spores. This strategy identifies only amino acids that are essential for sporulation. We found three amino acid substitutions within SpoIID that cause severe sporulation blocks: E88A and R106A, conserved residues within the putative enzymatic domain, and K203A, which is on the C-terminal side of this domain and within the extracellular domain (Fig. 1C). Each mutation decreased the viable spore counts 10,000-fold compared to that of the wild type (Table 1). We also identified four amino acid substitutions that cause an intermediate phenotype, ranging from a 10- to a 1,000-fold decrease in spores (Table 1). Of these four, we chose to characterize D210A as a representative of the group. Importantly, all 13 codons that were mutagenized both here and in the study of Morlot et al. (27) had similar effects on sporulation in both studies.

TABLE 1. Spore titers of SpoIID mutants[a]

Strain	SpoIID mutation	Avg spore titer	Avg sporulation (% of wild type)
KP7	*spoIID298*	0×10^8	0.00
PY79	Wild type	1.8×10^8	100.00
KP1124	**GFP-SpoIID**	$\mathbf{2.1 \times 10^8}$	**116.67**
KP1065	Y65A	1.8×10^8	100.00
KP1066	R66A	2.6×10^8	144.44
KP1067	E73A	2.6×10^8	144.44
KP1068	E78A	2.0×10^8	111.11
KP1069	E79A	5.5×10^8	305.56
KP1070	Y80A	8.4×10^7	46.67
KP1071	S87A	2.5×10^8	138.89
KP1072	**E88A**	$\mathbf{3.5 \times 10^4}$	**0.02**
KP1125	**GFP-SpoIID^{E88A}**	$\mathbf{1.5 \times 10^4}$	**0.01**
KP1073	M89A	2.6×10^8	144.44
KP1074	P90A	2.6×10^8	127.78
KP1075	K94A	1.1×10^8	61.11
KP1076	E96A	3.1×10^8	172.22
KP1077	K99A	5.0×10^8	277.78
KP1078	Q101A	1.8×10^8	100.00
KP1079	**R106A**	$\mathbf{6.5M \times 10^4}$	**0.04**
KP1142	**GFP-SpoIID^{R106A}**	$\mathbf{1.1 \times 10^6}$	**0.61**
KP1080	T107A	1.0×10^8	55.56
KP1081	F108A	2.2×10^8	122.22
KP1082	D128A	1.6×10^8	88.89
KP1083	D129A	1.6×10^8	88.89
KP1084	T130A	2.0×10^8	111.11
KP1085	Q134A	1.8×10^8	100.00
KP1086	Y136A	3.0×10^8	166.67
KP1087	K137A	1.5×10^8	83.33
KP1088	T164A	1.3×10^8	72.22
KP1089	T170A	1.8×10^8	100.00
KP1090	Y171A	1.2×10^8	66.67
KP1091	F181A	2.7×10^8	150.00
KP1092	S182A	1.9×10^8	105.56
KP1093	T183A	4.0×10^8	222.22
KP1095	T188A	1.0×10^7	5.56
KP1097	E192A	2.3×10^8	127.78
KP1098	Y201A	1.3×10^8	72.22
KP1099	**K203A**	$\mathbf{1.0 \times 10^4}$	**0.01**
KP1126	**GFP-SpoIID^{K203A}**	$\mathbf{2.2 \times 10^8}$	**122.22**
KP1100	S204A	1.6×10^8	88.89
KP1101	S207A	2.5×10^8	138.89
KP1102	**D210A**	$\mathbf{2.0 \times 10^7}$	**11.11**
KP1127	**GFP-SpoIID^{D210A}**	$\mathbf{1.3 \times 10^5}$	**0.07**
KP1103	S213A	2.4×10^8	133.33
KP1104	K215A	3.8×10^8	211.11
KP1105	T219A	3.3×10^8	183.33
KP1106	K220A	1.3×10^8	72.22
KP1107	T221A	3.5×10^8	194.44
KP1108	T223A	2.6×10^8	144.44
KP1109	E226A	2.6×10^8	144.44
KP1110	Q228A	3.6×10^8	200.00
KP1111	Q229A	3.7×10^8	205.56
KP1112	K230A	2.6×10^8	144.44
KP1113	K234A	1.5×10^8	83.33
KP1114	S239A	1.3×10^8	72.22
KP1115	T262A	1.2×10^8	66.67
KP1116	K282A	2.0×10^8	111.11
KP1117	R283A	2.0×10^8	111.11
KP1118	D286A	1.5×10^8	83.33
KP1119	F295A	2.3×10^8	127.78
KP1120	H297A	1.4×10^5	0.08
KP1121	V299A	1.7×10^8	94.44
KP1122	M301A	2.9×10^7	16.11
KP1123	Q303A	3.1×10^8	172.22

[a] Heat kill assays were performed (31) on strains containing each *spoIID* mutant. Three mutations (E88A, R106A, and K203A) drastically lowered spore titers, while four other mutations lowered spore titers to intermediate levels (T188A, D210A, H297A, and M301A). For this study, we focused on those mutations causing a severe sporulation block and one mutation with an intermediate spore titer as a representative of the intermediate group. Strains further characterized in this study are indicated in boldface.

Characterization of engulfment in the mutant strains. Strains expressing the four mutant proteins SpoIID^{E88A}, SpoIID^{R106A}, SpoIID^{K203A}, and SpoIID^{D210A} were further characterized by using FM 4-64 membrane staining and fluorescence microscopy to determine the stage at which sporulation is arrested. SpoIID^{E88A}, SpoIID^{R106A}, and SpoIID^{K203A} exhibited flat septa and septal bulges with no membrane migration at early time points (Fig. 3C to E), a finding similar to that seen with a *spoIID*-null strain (Fig. 3B). Thus, these mutations block the very earliest stage of engulfment: septal thinning. SpoIID^{D210A}, however, displayed some septal bulging at early time points but also showed significant membrane migration (Fig. 3F), suggesting that this mutant is slow to complete septal thinning but able to initiate membrane migration.

We next used a membrane fusion assay (32) to determine whether strains expressing the mutant SpoIID proteins were able to complete engulfment. This assay uses two membrane stains, MTG, which is membrane permeable, and FM 4-64, which is membrane impermeable and therefore unable to stain the forespore membranes after engulfment. The completion of engulfment is indicated by the staining of the forespore membranes with the membrane permeable dye MTG but not with FM 4-64. In wild-type *B. subtilis*, our observations agree with published data (1, 22, 29) that ca. 65% of cells have completed engulfment by 3 h after the initiation of sporulation by resuspension (t_3) at 37°C (Fig. 3G and see Table SA1 in the supplemental material). In contrast, strains expressing SpoIID^{E88A} (Fig. 3I) or SpoIID^{K203A} (Fig. 3K and Table SA1 in the supplemental material) failed to complete engulfment by t_3, t_4, or t_5. In a strain expressing SpoIID^{D210A}, ca. 4 and 9% of sporangia complete engulfment by t_3 and t_4, respectively (Fig. 3L and see Table SA1 in the supplemental material). This is consistent with spore titer data showing that this strain produces ca. 10% the level of heat-resistant spores as the wild type (Table 1). A strain expressing SpoIID^{R106A} also shows bulges at early time points, but, although migration sometimes initiates, forespores often maintain indents at the original septum site and show evidence of bulge persistence (Fig. 3J, arrow), indicating that dissolution of the septum is less effective than in a strain expressing SpoIID^{D210A}, but more than in a null mutant. Completion of engulfment is very rarely seen in strains expressing SpoIID^{R106A}, reflecting the 10,000-fold reduction in heat-resistant spores compared to the wild type (Table 1). Thus, R106A has a phenotype that is subtly different from *spoIID*-null or *spoIID^{E88A}* strains.

Bulge formation at the sporulation septum is due to a defect in septal thinning, which allows the growing forespore to push through the septal midpoint and into the mother cell (16, 24, 35). Bulges are apparent in all four mutant strains at early time points, indicating that SpoIID^{E88A}, SpoIID^{R106A}, SpoIID^{K203A}, and SpoIID^{D210A} all have a septal thinning defect. However, SpoIID^{E88A} and SpoIID^{K203A} show no membrane migration and significant lysis is observed, exactly mimicking *spoIID*-null strains. Thus, SpoIID^{E88A} and SpoIID^{K203A} have severe early engulfment defects. In contrast, SpoIID^{D210A} shows septal bulges at early time points, indicating decreased septal thinning, but the strain often initiates, and sometimes completes, membrane migration. This phenotype is somewhat similar to that of a *spoIIB*-null strain, which also initially shows septal bulges, followed by the initiation of membrane migra-

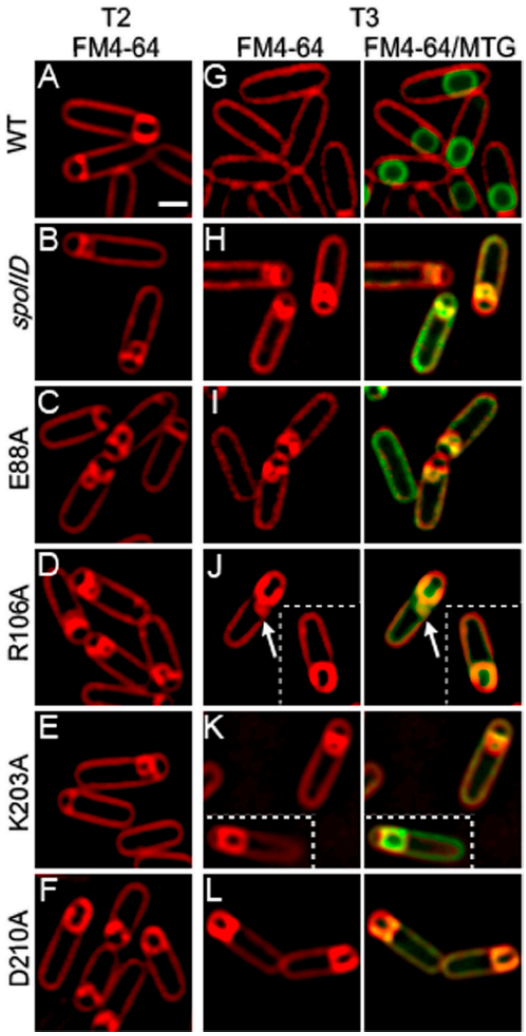

FIG. 3. Mutant SpoIID proteins show engulfment defects. Sporulation was induced by resuspension at 37°C and samples were collected at indicated times of sporulation (in hours). Scale bar, 1 μm. (A to E) Membranes were stained with FM 4-64 in strains expressing a single copy of either wild-type or mutant SpoIID at the *amyE* locus. A, wild type (KP718); B, *spoIID* null (KP7); C, SpoIID^{E88A} (KP1072); D, SpoIID^{R106A} (KP1079); E, SpoIID^{K203A} (KP1099); F, SpoIID^{D210A} (KP1102). Membranes in the wild type (A) show membrane migration and no septal bulges, while membranes in *spoIID* (B), SpoIID^{E88A} (C), and SpoIID^{K203A} (E) show flat or slightly curved septa with bulges. SpoIID^{D210A} (F) shows some open bulges but also membrane migration. Migration is often strikingly asymmetric in this strain. SpoIID^{R106A} (D) shows an intermediate phenotype with slow migration and persistent bulges. (G to L) Fusion assays. Membranes were stained with FM 4-64 and Mitotracker Green (MTG) to examine the completion of engulfment. Forespores that stain green but not red have completed engulfment membrane fission. Wild-type (G) cells have completed engulfment. The *spoIID* null (H), SpoIID^{E88A} (I), and SpoIID^{K203A} (K) show no migration and no fusion but retain septal bulges. SpoIID^{R106A} (J) shows some migration but very little fusion; an arrow illustrates septal bulge persistence even when some migration is present. SpoIID^{D210A} (L) shows significant membrane migration but little fusion (no fusion is shown in this panel, although 3% of cells have fused at t_3; see Table SA1 in the supplemental material).

tion (25, 28). In a *spoIIB* deletion, localization of SpoIIDMP is delayed and is facilitated by SpoIVFA (2). The similarity of the SpoIID^{D210A} and *spoIIB* phenotypes could indicate that the interaction between SpoIID^{D210A} and SpoIIP is impaired and localization of both proteins is delayed or transient, resulting in slow migration. SpoIID^{R106A} has a unique presentation combining elements of both the *spoIID*-null and SpoIID^{D210A} phenotypes with persistent septal bulges, indicating very poor septal thinning even though some membrane migration is evident.

Peptidoglycan degradation activity of the mutant proteins. We used a renaturing polyacrylamide gel assay (zymography) to test whether the proteins could degrade bacterial cell walls incorporated into a gel (1, 15). Briefly, the wild type and the four mutant SpoIID proteins with *in vivo* phenotypes were purified from *E. coli*, and 2- and 1-μg portions of each protein were run on two SDS-PAGE gels, one with *M. luteus* cells suspended in the gel and one without. Prior experiments indicated that *M. luteus* cells are a better substrate for examining SpoIID activity than are purified *B. subtilis* cell walls (1). The recent finding indicating that SpoIID cleaves only glycan strands that have been denuded by SpoIIP (27) suggests that this substrate shows clearing because it consists of a nonuniform mixture of peptidoglycan targets with cells in various stages of division and growth that might have been cleaved by endogenous amidases. After renaturation, the *M. luteus* gel was photographed against a dark background to directly visualize lysis of the *M. luteus* cells as zones of clearing at the positions of the lysozyme control band and SpoIID (Fig. 4A, panel ii), thereby excluding the possibility that an apparent cleavage was caused by exclusion of the methylene blue stain normally used in such assays (as suggested by Morlot et al. [27]). The gel was then stained with methylene blue, rinsed, and then imaged again to more clearly visualize clearing in the gel caused by loss of peptidoglycan and, therefore, peptidoglycan degradation activity (Fig. 4Aiii). As seen in Fig. 4A, the mutant SpoIID proteins display a range of degradation activity. SpoIID^{E88A} showed no clearing on zymography gels, suggesting that it is inactive. Interestingly, SpoIID^{E88A} forms an opaque band on zymography gels (Fig. 4Aii) that is visible prior to staining of the gel, while the other mutants that retain some activity form clear areas. This suggests that SpoIID^{E88A} may be modifying peptidoglycan, but in a way that does not cause cell lysis or support engulfment. This result agrees with the findings of Morlot et al. (27) and reinforces the conclusion that E88 is involved in peptidoglycan degradation.

SpoIID^{D210A} shows minimal but reproducible clearing, suggesting that it has a severe reduction in peptidoglycan degradation activity. The ability of SpoIID^{D210A} to complete engulfment in ~10% of sporangia suggests that the septal thinning system in *B. subtilis* is robust, since enzyme activity levels well below wild-type levels can support membrane migration. SpoIID^{R106A} and SpoIID^{K203A} show intermediate levels of

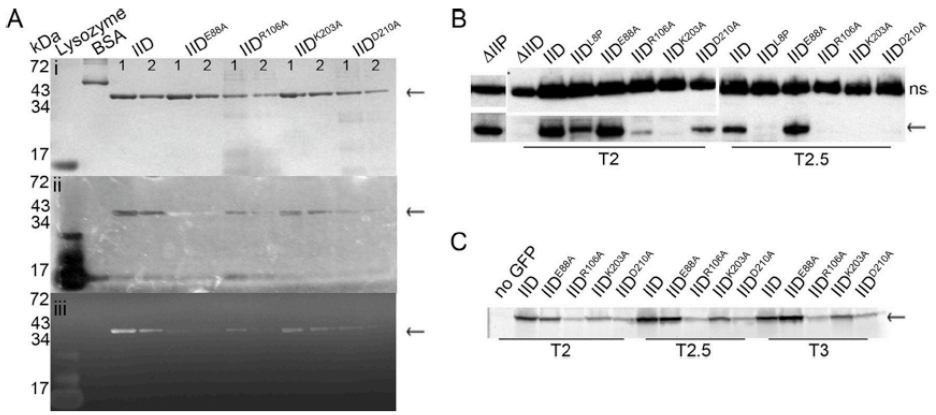

FIG. 4. Biochemical tests of SpoIID. SpoIID is indicated with arrows. (A) Renaturing gel electrophoresis assay for cell wall degradation (zymography). Purified SpoIID and mutant SpoIID proteins were run on two SDS-PAGE gels. Band size is indicated on the left and amount of protein loaded is at the top of each column: lane 1 for each protein contains 2 μg, and lane 2 contains 1 μg. (i) Gel stained with Coomassie blue to visualize protein purity and concentration. (ii) Photograph of gel containing *M. luteus* cells as substrate and incubated overnight in renaturing solution. The gel was imaged without stain and over black paper, with clearing evidenced by the appearance of the black background through the opacity of the gel. SpoIID^{E88A} appears as an opaque band. (iii) Same gel as in panel ii, with the peptidoglycan stained with methylene blue before imaging on a Typhoon scanner. Clearing indicates peptidoglycan degradation. Lysozyme is a positive control for peptidoglycan degradation and bovine serum albumin (BSA) is a negative control. (B) Western blot of SpoIID protein levels. Mutant constructs are inserted at *amyE* and indicated above each column; time of sample collection (after sporulation initiation) is below. The upper panels show a nonspecific (ns) band bound by the SpoIID antibody and used as a loading control. Lower panels show SpoIID. (C) In-gel GFP fluorescence of GFP-SpoIID levels. Cell extracts were collected from cultures containing the GFP-SpoIID fusion protein indicated above each column at the time indicated below. Extracts were run on SDS-PAGE gels, and GFP was visualized directly using a Typhoon imager.

clearing, with more clearing than SpoIID^{D210A} but less than the wild type. This suggests that the reductions in the peptidoglycan degradation activities of these mutant proteins are not sufficient to explain their severe engulfment defect. Although Morlot et al. characterized SpoIID^{R106A} as an inactive mutant based on their mass spectrometry assay, the protein has clear activity on zymography gels. The different results could be due to different buffer conditions or to different substrates present in the *M. luteus* preparation used here compared to purified peptidoglycan.

Variable accumulation of the mutant SpoIID proteins *in vivo*. To determine whether the mutant SpoIID proteins are stably expressed *in vivo*, we used Western blot analysis and SpoIID-specific antibodies to probe the steady-state levels of the proteins throughout sporulation. These experiments showed that levels of SpoIID^{E88A} were greater than wild-type SpoIID (Fig. 4B), either because the inability of this strain to complete engulfment prolonged σ^E activity and SpoIID synthesis or because the mutation increased the proteolytic stability. In contrast, SpoIID^{K203A} was undetectable at all time points tested (Fig. 4B) despite its wild-type expression signals, suggesting that this mutant protein is unstable and quickly degraded. The instability of SpoIID^{K203A} explains the observation that although this mutant protein shows significant peptidoglycan degradation activity, the strain expressing this protein has a phenotype similar to that of the *spoIID*-null strain, with no septal thinning or membrane migration. SpoIID^{D210A} was also detected at levels below that of the wild type (Fig. 4B). However, low protein levels do not explain the low spore titers, because SpoIID^{L8P} (1) accumulates to a level equivalent to that of SpoIID^{D210A} (Fig. 4B), but SpoIID^{L8P} supports ca. 40% wild-type spore production (1), whereas SpoIID^{D210A} produces just 10% of the level of spores compared to the wild type (Table 1). This suggests that SpoIID^{D210A} has an additional defect that reduces spore production, likely its reduced peptidoglycan degradation activity. SpoIID^{R106A} was also detected at levels well below that of the wild type, suggesting that instability of this protein *in vivo* explains the absence of membrane fusion in cells despite retention of peptidoglycan degradation activity *in vitro*. The intermediate level of SpoIID^{R106A}, between that of SpoIID^{K203A} and SpoIID^{D210A}, coupled with its intermediate membrane migration phenotype, suggests that the amount of SpoIID^{R106A} protein available is just below the threshold necessary to complete membrane migration *in vivo*.

Localization of GFP-SpoIID. Wild-type and mutant SpoIID proteins were fused to green fluorescent protein (GFP) in order to directly visualize localization of the mutant proteins. As previously noted (1), GFP-SpoIID does not localize exclusively to the septum (Fig. 5A) but rather shows some enrichment at the leading edge of the engulfing membrane and diffuse fluorescence throughout the mother cell membrane. This localization is dependent on SpoIIP (Fig. 5B) (2, 8). The only GFP-SpoIID construct that exhibited strong septal localization was GFP-SpoIID^{E88A} (Fig. 5C), which localized almost exclusively to the septal membranes. This suggests that GFP-SpoIID^{E88A} is tightly bound at the septum (Fig. 5C, arrow), either to peptidoglycan or to another protein, supporting a model in which SpoIID enzymatic activity is required for movement of the protein around the forespore and also suggesting that this activity releases the protein from the septum. However, GFP-SpoIID^{E88A} was capable of relocalizing to the edge of the septum in ca. 16% of sporulating cells (Fig. 5C,

TABLE 2. Strains used in this study

Strain	Genotype	Source or reference
B. subtilis		
PY79	Wild type	39
KP7	*spoIID298*	24
KP38	*spoIID298 amyE::spoIID38-kan*	1
KP718	*spoIID298 amyE::spoIID-kan*	1
KP719	*spoIIP::tet*	16
KP1065	*spoIID298 amyE::spoIID^{Y65A}-kan*	This study
KP1066	*spoIID298 amyE::spoIID^{R66A}-kan*	This study
KP1067	*spoIID298 amyE::spoIID^{E73A}-kan*	This study
KP1068	*spoIID298 amyE::spoIID^{E78A}-kan*	This study
KP1069	*spoIID298 amyE::spoIID^{E79A}-kan*	This study
KP1070	*spoIID298 amyE::spoIID^{Y80A}-kan*	This study
KP1071	*spoIID298 amyE::spoIID^{S87A}-kan*	This study
KP1072	*spoIID298 amyE::spoIID^{E88A}-kan*	This study
KP1073	*spoIID298 amyE::spoIID^{M89A}-kan*	This study
KP1074	*spoIID298 amyE::spoIID^{P90A}-kan*	This study
KP1075	*spoIID298 amyE::spoIID^{K94A}-kan*	This study
KP1076	*spoIID298 amyE::spoIID^{E96A}-kan*	This study
KP1077	*spoIID298 amyE::spoIID^{K99A}-kan*	This study
KP1078	*spoIID298 amyE::spoIID^{Q101A}-kan*	This study
KP1079	*spoIID298 amyE::spoIID^{R106A}-kan*	This study
KP1080	*spoIID298 amyE::spoIID^{T107A}-kan*	This study
KP1081	*spoIID298 amyE::spoIID^{F108A}-kan*	This study
KP1082	*spoIID298 amyE::spoIID^{D128A}-kan*	This study
KP1083	*spoIID298 amyE::spoIID^{D129A}-kan*	This study
KP1084	*spoIID298 amyE::spoIID^{T130A}-kan*	This study
KP1085	*spoIID298 amyE::spoIID^{Q134A}-kan*	This study
KP1086	*spoIID298 amyE::spoIID^{Y136A}-kan*	This study
KP1087	*spoIID298 amyE::spoIID^{K137A}-kan*	This study
KP1088	*spoIID298 amyE::spoIID^{T164A}-kan*	This study
KP1089	*spoIID298 amyE::spoIID^{T170A}-kan*	This study
KP1090	*spoIID298 amyE::spoIID^{Y171A}-kan*	This study
KP1091	*spoIID298 amyE::spoIID^{F181A}-kan*	This study
KP1092	*spoIID298 amyE::spoIID^{S182A}-kan*	This study
KP1093	*spoIID298 amyE::spoIID^{T183A}-kan*	This study
KP1095	*spoIID298 amyE::spoIID^{T188A}-kan*	This study
KP1097	*spoIID298 amyE::spoIID^{E192A}-kan*	This study
KP1098	*spoIID298 amyE::spoIID^{Y201A}-kan*	This study
KP1099	*spoIID298 amyE::spoIID^{K203A}-kan*	This study
KP1100	*spoIID298 amyE::spoIID^{S204A}-kan*	This study
KP1101	*spoIID298 amyE::spoIID^{S207A}-kan*	This study
KP1102	*spoIID298 amyE::spoIID^{D210A}-kan*	This study
KP1103	*spoIID298 amyE::spoIID^{S213A}-kan*	This study
KP1104	*spoIID298 amyE::spoIID^{K215A}-kan*	This study
KP1105	*spoIID298 amyE::spoIID^{T219A}-kan*	This study
KP1106	*spoIID298 amyE::spoIID^{K220A}-kan*	This study
KP1107	*spoIID298 amyE::spoIID^{T221A}-kan*	This study
KP1108	*spoIID298 amyE::spoIID^{T223A}-kan*	This study
KP1109	*spoIID298 amyE::spoIID^{E226A}-kan*	This study
KP1110	*spoIID298 amyE::spoIID^{Q228A}-kan*	This study
KP1111	*spoIID298 amyE::spoIID^{Q229A}-kan*	This study
KP1112	*spoIID298 amyE::spoIID^{K230A}-kan*	This study
KP1113	*spoIID298 amyE::spoIID^{K234A}-kan*	This study
KP1114	*spoIID298 amyE::spoIID^{S239A}-kan*	This study
KP1115	*spoIID298 amyE::spoIID^{T262A}-kan*	This study
KP1116	*spoIID298 amyE::spoIID^{K282A}-kan*	This study
KP1117	*spoIID298 amyE::spoIID^{R283A}-kan*	This study
KP1118	*spoIID298 amyE::spoIID^{D286A}-kan*	This study
KP1119	*spoIID298 amyE::spoIID^{F295A}-kan*	This study
KP1120	*spoIID298 amyE::spoIID^{H297A}-kan*	This study
KP1121	*spoIID298 amyE::spoIID^{V299A}-kan*	This study
KP1122	*spoIID298 amyE::spoIID^{M301A}-kan*	This study
KP1123	*spoIID298 amyE::spoIID^{Q303A}-kan*	This study
KP1124	*spoIID::cat::tet amyE::gfp-spoIID*	This study
KP1125	*spoIID::cat::tet amyE::gfp-spoIID^{E88A}*	This study
KP1142	*spoIID::cat::tet amyE::gfp-spoIID^{R106A}*	This study
KP1126	*spoIID::cat::tet amyE::gfp-spoIID^{K203A}*	This study
KP1127	*spoIID::cat::tet amyE::gfp-spoIID^{D210A}*	This study
KP1128	*spoIIP::tet amyE::gfp-spoIID-cm*	This study
KP1129	*spoIID298 amyE::spoIID-kan ΔspoIIPtetΩP$_{III}$gfp-spoIIP-erm*	This study
KP1137	*spoIID298 ΔspoIIPtetΩP$_{III}$gfp-spoIIP-erm*	This study
KP1130	*spoIID298 amyE::spoIID^{A}-kan ΔspoIIPtetΩP$_{III}$gfp-spoIIP-erm*	This study
KP1141	*spoIID298 amyE::spoIID^{R106A}-kan ΔspoIIPtetΩP$_{III}$gfp-spoIIP-erm*	This study
KP1131	*spoIID298 amyE::spoIID^{K203A}-kan ΔspoIIPtetΩP$_{III}$gfp-spoIIP-erm*	This study
KP1132	*spoIID298 amyE::spoIID^{D210A}-kan ΔspoIIPtetΩP$_{III}$gfp-spoIIP-erm*	This study
E. coli		
KP1133	BL21; pSA12 (His$_6$-SpoIID$^{27-343}$)	This study
KP1134	BL21; pSA12 (His$_6$-SpoIID$^{27-343}$ E88A)	This study
KP1147	BL21; pSA12 (His$_6$-SpoIID$^{27-343}$ R106A)	This study
KP1135	BL21; pSA12 (His$_6$-SpoIID$^{27-343}$ K203A)	This study
KP1136	BL21; pSA12 (His$_6$-SpoIID$^{27-343}$ D210A)	This study

arrowhead), demonstrating that SpoIID peptidoglycan degradation activity is not always required to move SpoIID across the septum.

Both GFP-SpoIID^{K203A} and GFP-SpoIID^{D210A} localize in a manner similar to that of the wild type, with some enrichment at the leading edge of the engulfing membrane and diffuse fluorescence throughout the mother cell membrane (Fig. 5E and F). Interestingly, fusion of GFP to SpoIID^{K203A} abolished the engulfment defect, allowing membrane migration and restoring spore titers to wild-type levels (Table 1), whereas fusion of GFP to SpoIID^{D210A} enhanced the sporulation phenotype, blocking membrane migration and dropping spore titers to essentially zero (Table 1). GFP-SpoIID^{R106A}, although occasionally seen at the edges of the septal disk, was typically present in the mother cell cytoplasm (Fig. 5D), supporting the conclusion that this SpoIID variant is unstable.

We next examined whether GFP stabilized the mutant proteins using in-gel GFP fluorescence (11). The GFP tag did not change the relative accumulation of SpoIID, SpoIID^{E88A}, SpoIID^{R106A}, or SpoIID^{D210A} compared to Western blots of the untagged protein, since in each case SpoIID^{E88A} accumulated at higher levels than wild-type SpoIID, which accumulated at higher levels than SpoIID^{D210A}, which was higher than SpoIID^{R106} (Fig. 4C). However, GFP-SpoIID^{K203A} accumulated to significantly higher levels than expected, since the untagged protein could not be detected on Western blots (Fig. 4C compared to Fig. 4B). This suggests that the N-terminal GFP tag stabilizes the SpoIID^{K203A} mutant protein, as has been observed for some other proteins (3). The stabilization of SpoIID^{K203A} by the GFP tag likely explains the increased ability of the GFP fusion protein to support engulfment.

Localization of GFP-SpoIIP in the mutant strains. We next investigated the ability of GFP-SpoIIP to localize in strains expressing the mutant SpoIID proteins. SpoIIP and SpoIID interact both *in vitro* (8) and *in vivo* (2) and the absence of either protein alters localization of the other (Fig. 5B and H) (2, 8). GFP-SpoIIP clearly localizes to the leading edges of the migrating membranes during engulfment (Fig. 5G, arrow), becoming more diffusely localized around the forespore membranes after engulfment (Fig. 5G, arrowheads). In a *spoIID*-null strain, GFP-SpoIIP remains as a sharp focus at the center of the septum, without moving the edge of the septal disk (Fig. 5H), suggesting that SpoIID is required to move SpoIIP to the leading edge of the engulfing membrane. These two clearly distinct localization patterns allow minor variations to be distinguished in the mutant SpoIID proteins. In a SpoIID^{E88A} background, GFP-SpoIIP spreads across the septum and sometimes localizes to the edges of the septal disk (Fig. 5I), a phenotype clearly distinct from the tight focus observed in the *spoIID*-null strain (Fig. 5H). Thus, SpoIID^{E88A} is localized at the septum and likely capable of interacting with SpoIIP to mediate its movement across the septum, since SpoIIP localization is distinct from that seen in the absence of SpoIID. However, no membrane migration occurs, suggesting that the activity of both proteins is required for membrane migration.

In the engulfment defective SpoIID^{R106A} and SpoIID^{K203A} strains, GFP-SpoIIP forms a tight focus at the septum center (Fig. 5J and K), identical to the *spoIID*-null strain. This is consistent with Western blot data indicating that SpoIID^{K203A} fails to accumulate in the cell and SpoIID^{R106A} accumulates at

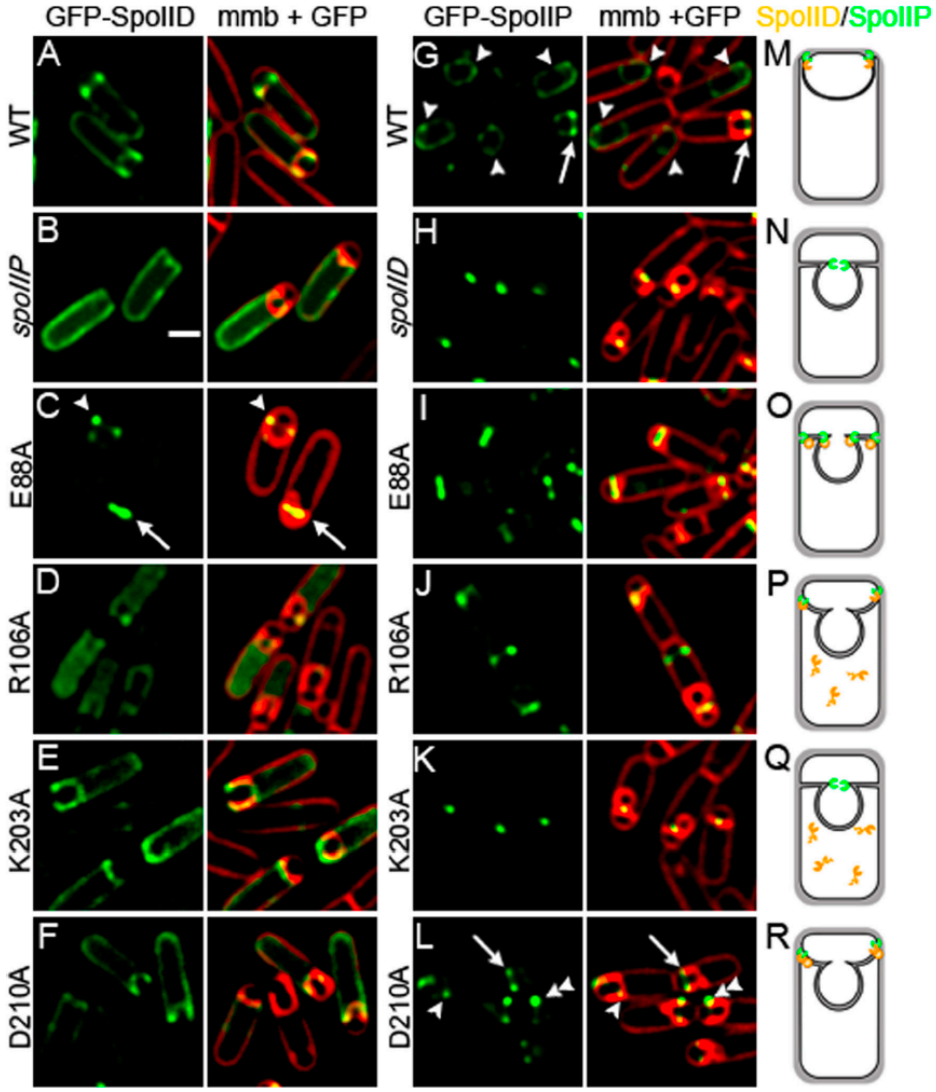

FIG. 5. Localization of GFP fusion proteins. All cells were grown at 37°C and images taken at t_3. Membranes were stained with FM 4-64. Scale bar, 1 μm. (A to E) GFP-SpoIID localization in: A, wild type (KP1124); B, *spoIIP* null (KP1128); C, GFP-SpoIID^{E88A} (KP1125); D, GFP-SpoIID^{R106A} (KP1142); E, GFP-SpoIID^{K203A} (KP1126); and F, GFP-SpoIID^{D210A} (KP1127). GFP-SpoIID shows some enrichment at the leading edge together with diffuse fluorescence throughout the mother cell membranes. The only strain showing significantly enhanced localization is GFP-SpoIID^{E88A} (C), which is almost exclusively localized to the septum (C, arrow) or at the edges of the septum (C, arrowhead), although no membrane migration is seen. Signal is also more diffuse in the *spoIIP*-null strain (B) than in other strains, suggesting that, as previously reported, SpoIID localization depends on SpoIIP (8). GFP-SpoIID^{R106A} (D) is diffuse in the cytoplasm, suggesting protein degradation. (G to L) GFP-SpoIIP localization in: G, wild type (KP1129); H, *spoIID* null (KP1137); I, SpoIID^{E88A} (KP1130); J, SpoIID^{R106A} (KP1141); K, SpoIID^{K203A} (KP1131); and L, SpoIID^{D210A} (KP1132). GFP-SpoIIP localizes to the leading edges of migrating membranes in the wild type (G, arrow), as a diffuse signal after fusion (G, arrowheads) and as a sharp central focus in the absence of SpoIID (H). GFP-SpoIIP localizes across the septum and to the edges of the septal disk in SpoIID^{E88A} (I), as a central focus in SpoIID^{R106A} (J) and SpoIID^{K203A} (K), and similarly to the wild type in SpoIID^{D210A} (L, arrow), although GFP-SpoIIP signal is sometimes uneven (L, double arrowhead) or lagging behind the leading edge in SpoIID^{D210A} (L, arrowhead). (M to R) Diagrams representing SpoIIP (green) and SpoIID (orange) localization at t_3 in: M, wild type; N, *spoIID* null; O, SpoIID^{E88A}; P, SpoIID^{R106A}; Q, SpoIID^{K203A}; and R, SpoIID^{D210A}. Panel Q summarizes the results in the strain expressing untagged SpoIID^{K203A} (which fails to accumulate) and not GFP-SpoIID^{K203A}.

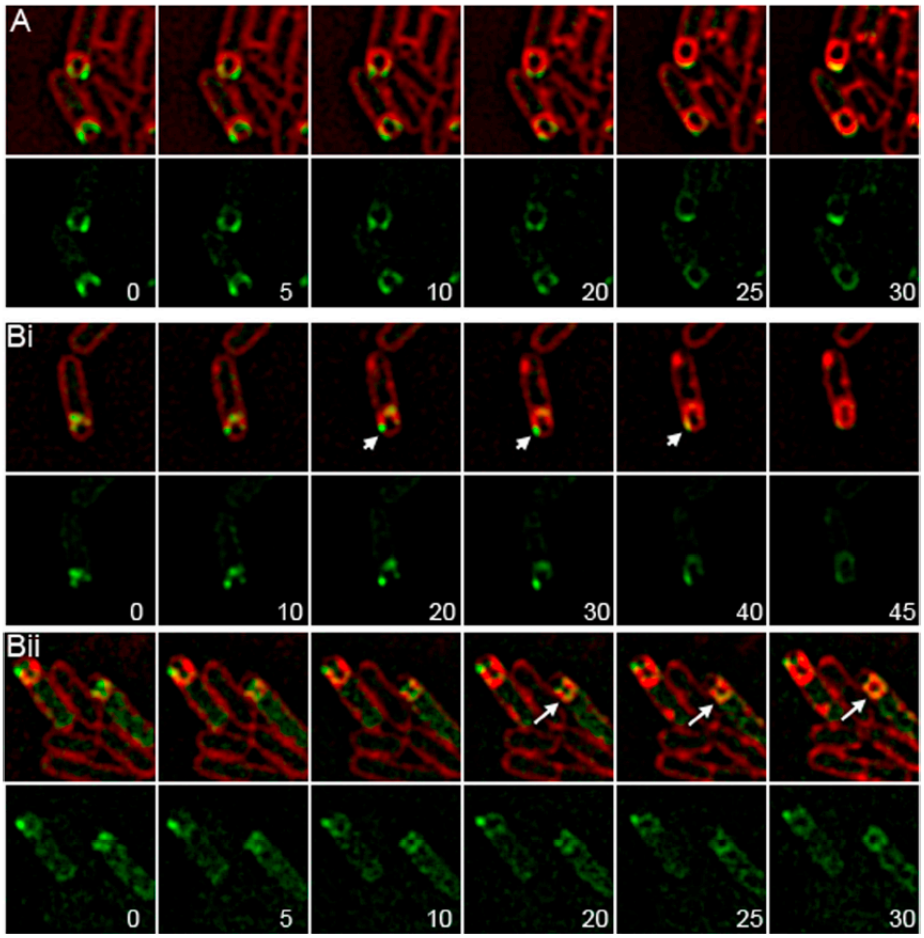

FIG. 6. Time-lapse microscopy of GFP-SpoIIP. Sporulating cells were incubated on agarose pads at 30°C and membranes were stained with FM 4-64. Image sequences were initiated at $t_{2.5}$ after the initiation of sporulation by resuspension and the first image was set to $t = 0$ min. Minutes after $t = 0$ is indicated in lower right of GFP image. The upper panels show FM 4-64 membranes merged with GFP-SpoIIP; the lower panels show GFP-SpoIIP alone. (A) GFP-SpoIIP in wild type (KP1129). GFP-SpoIIP is localized evenly to the leading edges throughout migration and becomes diffuse after the completion of membrane migration. (Bi and ii) Two examples of GFP-SpoIIP in a SpoIID^{D210A} background (KP1132). Localization corresponds with advancement of the membrane, and a faster membrane arm is indicated by arrowheads (i). GFP-SpoIIP is localized unevenly to the leading edges or diffuse throughout blebs; diffuse GFP-SpoIIP is indicated by arrows (ii).

very low levels. In the SpoIID^{D210A} strain, which is slow for both septal thinning and membrane migration, GFP-SpoIIP localizes to the leading edges of the migrating membranes in a manner similar to the wild type (Fig. 5L, arrow), except that some cells appear to have an asymmetric distribution of GFP-SpoIIP at the leading edges (Fig. 5L, double arrowhead) and in others GFP-SpoIIP foci appear to lag behind the leading edge of the engulfing membrane (Fig. 5L, arrowhead). This suggests that the interaction between SpoIIP and SpoIID^{D210A} may be weak or transient, leading to poor GFP-SpoIIP localization.

Time-lapse microscopy of GFP-SpoIIP. If the rate of membrane migration depends on SpoIID and SpoIIP activity, then an increased localization of GFP-SpoIIP on one leading edge in SpoIID^{D210A} cells should correlate with an increased rate of membrane migration on that side of the sporangium. We used time-lapse fluorescence microscopy to test this hypothesis, visualizing GFP-SpoIIP localization and the engulfing membranes in wild-type and SpoIID^{D210A} strains (Fig. 6). In wild-type cells, membrane migration occurs either evenly, with membranes moving around the forespore at similar rates, or in a inch-worm fashion, with membranes on the right side of the forespore moving slightly forward and then membranes on the left side moving slightly forward until meeting at the top middle. GFP-SpoIIP localizes to the leading edges as a focus or

with enrichment at the leading edge together with a gradient along the side of the forespore. Ultimately, GFP-SpoIIP localizes as a cap at the top of the forespore (Fig. 6A and see Movie SA1 in the supplemental material). In a SpoIID^{D210A} strain with GFP-SpoIIP, we observed membrane migration in only 17% of cells, with most cells forming large blebs. These blebs are distinct from the septal bulges seen in *spoIID*-null strains as septal thinning appears to be complete, evidenced by deeply curved septa. However, it appears that membrane synthesis at the edges of the septal disk continues without advancement, leading to membranes blebbing inward that effectively reform a "septum," although there might not be peptidoglycan present in these structures. In such cells, GFP-SpoIIP is localized either in faint foci at the edges of the bleb or diffusely throughout the bleb (Fig. 6Bii, arrows). When membrane migration occurred in this strain, it was often strikingly asymmetric, with one arm advancing far ahead of the other. In these cells, GFP-SpoIIP is localized unevenly, with a brighter focus at the faster moving region of the membrane (Fig. 6Bi, arrowheads; see also Movie SA2 in the supplemental material). This suggests that higher concentrations of the SpoIID/SpoIIP complex are correlated with increased rates of membrane migration.

DISCUSSION

SpoIID peptidoglycan degradation activity is essential for septal thinning and membrane migration. SpoIID degrades peptidoglycan *in vitro* (1), and it was recently demonstrated to have a novel biochemical activity, since it is a lytic transglycosylase that cleaves peptidoglycan only after the peptide side chains have been removed by SpoIIP (27). We identify here an amino acid substitution within the SpoIID protein (SpoIID^{E88A}; also identified by Morlot et al. [27]) that abolishes the peptidoglycan degradation activity (Fig. 4A) and spore formation (Table 1). The membrane morphology of the *spoIID*^{E88A} mutant exactly matches that of the *spoIID*-null strain at t_2 and t_3 (Fig. 3C and I), showing flat septa and slightly curved septa with bulges. These bulges are thought to form due to the lack of septal thinning because in the absence of SpoIID, SpoIIP is trapped at the center of the septum (Fig. 5H) and does not move. This likely causes a weak spot at the center of the septum where SpoIIP is active, allowing membrane protrusion from the forespore and bulge formation. The identical structure of the membranes in a *spoIID*-null and *spoIID*^{E88A} strain strongly suggests that SpoIID-mediated peptidoglycan degradation is essential for septal thinning, the first step in the engulfment process.

We also identified a second mutant protein (SpoIID^{D210A}) that degrades peptidoglycan at a much lower level than wild-type SpoIID (Fig. 4A). This mutation is slow to complete septal thinning, showing transient septal bulges, and ultimately initiates membrane migration and completes engulfment at 10% the level of wild type (Table 1 and see Table SA1 in the supplemental material). By examining cells over a time course and by using time-lapse microscopy to visualize membrane migration in living cells, we found that the movement of the membranes around the forespore was much slower in the *spoIID*^{D210A} strain than in the wild type (Fig. 6B). This indicates that SpoIID activity is required throughout membrane migration. Together, these results show that SpoIID-mediated peptidoglycan degradation is critical throughout engulfment as predicted by both the burnt-bridge and steric barrier models (7).

We also noted that SpoIIP has an altered localization in a strain expressing SpoIID^{D210A}. Specifically, the GFP-SpoIIP signal is more mobile and less symmetrically localized to the leading edge than in the wild type, often showing diffuse localization throughout the blebbing membranes or foci behind the leading edge (Fig. 6). This suggests that SpoIID^{D210A} has a reduced ability to maintain the SpoIID/SpoIIP complex at the leading edge of the engulfing membrane. However, in some mutant cells, GFP-SpoIIP localizes in a manner similar to that of the wild type, and cells exhibiting this pattern show membrane migration, indicating that the correct assembly of the SpoIID/SpoIIP complex is important for rapid membrane migration. The SpoIID^{D210A} mutant strain also frequently shows uneven membrane migration, and in these sporangia, the brighter SpoIIP focus is associated with the most rapidly advancing leading edge, with the less intense focus on the lagging side (Fig. 6Bi, arrowheads). This suggests that, in this strain, peptidoglycan degradation by the SpoIID/SpoIIP complex is rate limiting for membrane migration.

Interaction with SpoIIP is not important for SpoIID stability. In many complexes, the absence of one binding partner causes degradation of the other. Importantly, we show that SpoIID is readily detectable on Western blots in the absence of its binding partner SpoIIP (Fig. 4B). This strongly suggests that the altered levels of mutant SpoIID proteins are not simply due to a defect in SpoIIP interactions. In addition, the promoter region of each of the mutant proteins is identical, suggesting that transcription of the SpoIID region is the same for all proteins and that altered levels of protein are due either to translational differences caused by the specific mutations or to protein misfolding and degradation.

The SpoIIDMP module is robust. Sporulation in *B. subtilis* is a robust process, with multiple redundant pathways contributing to its completion. For example, the SpoIIQ/SpoIIIAH module is normally dispensable for engulfment but is essential when engulfment is compromised by mutations that decrease the activity of the SpoIIDMP complex (7, 18, 38) or when peptidoglycan synthesis is inhibited with antibiotics (26). In addition, the initial localization of SpoIIDMP by the SpoIIB septal landmark protein can also be achieved by a second protein, SpoIVFA, when SpoIIB is absent (2). Finally, synergistic engulfment defects continue to be discovered that are not readily explained by our current models of sporulation (2, 7, 18), indicating as-yet-undiscovered layers of redundancy. It is not surprising, therefore, to discover that the SpoIID, SpoIIM, and SpoIIP proteins are robust as well. SpoIID^{D210A} degrades peptidoglycan at a significantly reduced level compared to the wild type (Fig. 4A), and it accumulates at levels below that of the wild type (Fig. 4B), and yet it still supports membrane migration in 40% of all cells and the completion of engulfment in 10% of cells (see Table SA1 in the supplemental material). In addition, a previously published mutant, SpoIID^{L8P}, accumulates at levels the same as or below that of SpoIID^{D210A}, and yet it supports wild-type levels of sporulation. Together, this indicates that the level of peptidoglycan degradation required for septal thinning and membrane migration is far below what is normally present in wild-type cells

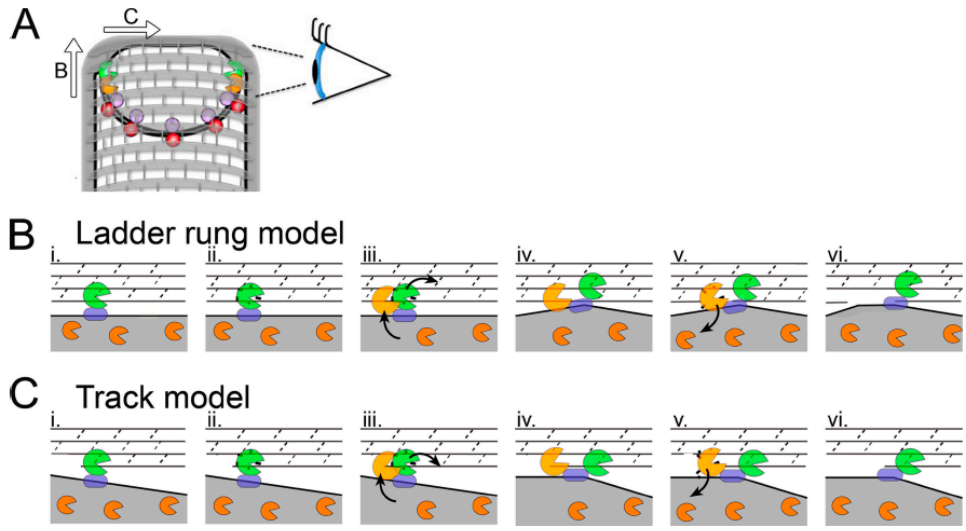

FIG. 7. Model for SpoIIDMP function *in vivo*. (A) An engulfing *B. subtilis* cell with SpoIID (orange), SpoIIP (green), SpoIIQ (purple), and SpoIIIAH (red) indicated. Peptidoglycan is drawn with gray hoops representing glycan strands and short gray rods representing peptide cross-links. The eye orients the reader to the perspective used in panels B and C. As indicated by the arrows, the DMP protein complex can move in one of two directions relative to the long axis of the cell. If the proteins move from one glycan chain to the next (as shown in panel B and proposed by Morlot et al. [27]), each complex would move along the long axis of the cell. If the proteins travel along one glycan chain (as shown in panel C and proposed by Abanes-De Mello et al. [1]), then each complex would move across the short axis of the cell. (B and C) Top-down views of the leading edge of the engulfing mother cell membrane (gray fill) advancing over the forespore peptidoglycan, drawn with gray lines representing the glycan chains and dashed lines representing the peptide cross-links. (B) Ladder rung model, in which SpoIIP moves from one glycan chain to the next. (i) SpoIIP (green) is bound in the membrane by SpoIIM (blue) and to peptidoglycan. SpoIID (orange) is free in the membrane. (ii) SpoIIP cleaves peptide cross-links. (iii) SpoIID is recruited to the recently denuded glycan strands where it displaces SpoIIP to a new target on the next strand, laddering up the peptidoglycan. (iv) Both enzymes are in complex and bound to the peptidoglycan. (v) SpoIID cleaves the glycan strand, loses affinity for either SpoIIP or the peptidoglycan, and exits the complex. (vi) Same as panel i, but membranes have advanced. (C) Track model, similar to panel B, but depicting SpoIIDMP moving along the glycan chain, such that at step iii, SpoIID displaces SpoIIP to the next peptide cross-link on the same glycan strand.

and that the peptidoglycan degradation module can withstand perturbations in both protein levels and protein activity.

Models for the role of SpoIID in engulfment. Our localization data suggest that SpoIID degradation activity causes the protein to be released from the SpoIID/SpoIIP complex, since the enzymatically inactive mutant SpoIID^{E88A} is localized exclusively to the septum, whereas only a fraction of the wild-type protein is localized. This is not the case for wild-type SpoIIP, which is well localized to the septum and leading edge of the engulfing membrane. This suggests that SpoIIP molecules are stably maintained at the leading edge during engulfment, whereas SpoIID moves between a localized pool where it interacts with SpoIIP and cleaves peptidoglycan and a delocalized pool that has little or no peptidoglycan degradation activity (because of the lack of SpoIIP or suitable peptidoglycan substrates). Our data further suggest that movement of SpoIIP across the septum depends on SpoIID and that the inactive SpoIID^{E88A} mutant protein is capable of moving SpoIIP across the septum. Based on these observations and the biochemical data of Morlot et al. (27), we propose a revised model for how the enzymatic activities of these proteins are coordinated and coupled to membrane migration (Fig. 7). First, we propose that SpoIIP binds to SpoIIM and the peptidoglycan at the septum (Fig. 7B, step 1) and cleaves the peptide chains (step 2), producing denuded glycan strands that are a SpoIID substrate. Second, we propose that SpoIID binds this denuded glycan strand (step 3), displacing SpoIIP to the next available substrate and moving the engulfing membrane forward (step 4). SpoIIP might move either along the same glycan strand, using it as a track (if degradation starts at one end of the strand) or by moving to the next glycan strand, using the glycan as a ladder (if degradation can start within a strand). Third, we propose that SpoIID then cleaves the glycan strand (step 5) and is released back into the delocalized membrane pool (step 6), allowing subsequent cycles of binding, degradation, and movement of the SpoIIP/SpoIID complex around the forespore. Our model also provides a potential mechanistic explanation of the previously observed activation of SpoIIP by SpoIID (27). If SpoIID is indeed required to move SpoIIP to a new peptidoglycan target after cleavage, without this push from SpoIID, SpoIIP would have to rely on slow release from the peptidoglycan and diffusion after cleavage to advance. However, if the two enzymes are added together, the rate at which SpoIIP advances should increase due to displacement of SpoIIP by SpoIID, thereby producing more cleavage products in the same amount of time.

This modified model of SpoIIDMP complex organization suggests that the complex could operate as a burnt-bridge

Brownian ratchet, thus providing force for membrane migration (1, 27). However, two additional mechanisms also contribute to membrane migration, the SpoIIQ-SpoIIIAH zipper, which is essential for engulfment in protoplasts and in intact cells when SpoIIDMP activity is reduced (7), and peptidoglycan biosynthesis, which is essential for engulfment in the absence of SpoIIQ (26). The mechanisms by which these three protein complexes contribute to the directionality of engulfment and generate force for membrane movement are important topics for future research.

ACKNOWLEDGMENTS

This research was supported by grants from the National Institutes of Health (R01-GM57045 and F32-GM087864).

The content is solely the responsibility of the authors and does not necessarily represent the official views of the National Institutes of Health or the National Institute of General Medical Sciences.

We thank Richard Losick for strains with GFP-SpoIIP at the native locus that were used to create some of the strains for this study, Stefan Aung and Jon Shum for the creation of some expression plasmids, and James Gregory for the creation of some mutagenesis plasmids.

REFERENCES

1. **Abanes-De Mello, A., Y. L. Sun, S. Aung, and K. Pogliano.** 2002. A cytoskeleton-like role for the bacterial cell wall during engulfment of the *Bacillus subtilis* forespore. Genes Dev. **16:**3253–3264.
2. **Aung, S., J. Shum, A. Abanes-De Mello, D. H. Broder, J. Fredlund-Gutierrez, S. Chiba, and K. Pogliano.** 2007. Dual localization pathways for the engulfment proteins during *Bacillus subtilis* sporulation. Mol. Microbiol. **65:**1534–1546.
3. **Baens, M., H. Noels, V. Broeckx, S. Hagens, S. Fevery, A. D. Billiau, H. Vankelecom, and P. Marynen.** 2006. The dark side of EGFP: defective polyubiquitination. PLoS One **1:**e54.
4. **Becker, E. C., and K. Pogliano.** 2007. Cell-specific SpoIIIE assembly and DNA translocation polarity are dictated by chromosome orientation. Mol. Microbiol. **66:**1066–1079.
5. **Blackman, S. A., T. J. Smith, and S. J. Foster.** 1998. The role of autolysins during vegetative growth of *Bacillus subtilis* 168. Microbiology **144**(Pt. 1)**:** 73–82.
6. **Blaylock, B., X. Jiang, A. Rubio, C. P. Moran, Jr., and K. Pogliano.** 2004. Zipper-like interaction between proteins in adjacent daughter cells mediates protein localization. Genes Dev. **18:**2916–2928.
7. **Broder, D. H., and K. Pogliano.** 2006. Forespore engulfment mediated by a ratchet-like mechanism. Cell **126:**917–928.
8. **Chastanet, A., and R. Losick.** 2007. Engulfment during sporulation in *Bacillus subtilis* is governed by a multi-protein complex containing tandemly acting autolysins. Mol. Microbiol. **64:**139–152.
9. **Chiba, S., K. Coleman, and K. Pogliano.** 2007. Impact of membrane fusion and proteolysis on SpoIIQ dynamics and interaction with SpoIIIAH. J. Biol. Chem. **282:**2576–2586.
10. **Doan, T., K. A. Marquis, and D. Z. Rudner.** 2005. Subcellular localization of a sporulation membrane protein is achieved through a network of interactions along and across the septum. Mol. Microbiol. **55:**1767–1781.
11. **Drew, D., M. Lerch, E. Kunji, D. J. Slotboom, and J. W. de Gier.** 2006. Optimization of membrane protein overexpression and purification using GFP fusions. Nat. Methods **3:**303–313.
12. **Dubnau, D., and R. Davidoff-Abelson.** 1971. Fate of transforming DNA following uptake by competent *Bacillus subtilis*. I. Formation and properties of the donor-recipient complex. J. Mol. Biol. **56:**209–221.
13. **Errington, J.** 2003. Regulation of endospore formation in *Bacillus subtilis*. Nat. Rev. Microbiol. **1:**117–126.
14. **Finn, R. D., J. Tate, J. Mistry, P. C. Coggill, S. J. Sammut, H. R. Hotz, G. Ceric, K. Forslund, S. R. Eddy, E. L. Sonnhammer, and A. Bateman.** 2008. The Pfam protein families database. Nucleic Acids Res. **36:**D281–D288.
15. **Foster, S. J.** 1992. Analysis of the autolysins of *Bacillus subtilis* 168 during vegetative growth and differentiation by using renaturing polyacrylamide gel electrophoresis. J. Bacteriol. **174:**464–470.
16. **Frandsen, N., and P. Stragier.** 1995. Identification and characterization of the *Bacillus subtilis spoIIP* locus. J. Bacteriol. **177:**716–722.
17. **Hilbert, D. W., and P. J. Piggot.** 2004. Compartmentalization of gene expression during *Bacillus subtilis* spore formation. Microbiol. Mol. Biol. Rev. **68:**234–262.
18. **Jiang, X., A. Rubio, S. Chiba, and K. Pogliano.** 2005. Engulfment-regulated proteolysis of SpoIIQ: evidence that dual checkpoints control σ^K activity. Mol. Microbiol. **58:**102–115.
19. **Kellner, E. M., A. Decatur, and C. P. Moran, Jr.** 1996. Two-stage regulation of an anti-sigma factor determines developmental fate during bacterial endospore formation. Mol. Microbiol. **21:**913–924.
20. **Kuroda, A., M. H. Rashid, and J. Sekiguchi.** 1992. Molecular cloning and sequencing of the upstream region of the major *Bacillus subtilis* autolysin gene: a modifier protein exhibiting sequence homology to the major autolysin and the spoIID product. J. Gen. Microbiol. **138**(Pt. 6):1067–1076.
21. **Larkin, M. A., G. Blackshields, N. P. Brown, R. Chenna, P. A. McGettigan, H. McWilliam, F. Valentin, I. M. Wallace, A. Wilm, R. Lopez, J. D. Thompson, T. J. Gibson, and D. G. Higgins.** 2007. CLUSTAL W and CLUSTAL X version 2.0. Bioinformatics **23:**2947–2948.
22. **Liu, N. J., R. J. Dutton, and K. Pogliano.** 2006. Evidence that the SpoIIIE DNA translocase participates in membrane fusion during cytokinesis and engulfment. Mol. Microbiol. **59:**1097–1113.
23. **Londono-Vallejo, J. A., C. Frehel, and P. Stragier.** 1997. SpoIIQ, a forespore-expressed gene required for engulfment in *Bacillus subtilis*. Mol. Microbiol. **24:**29–39.
24. **Lopez-Diaz, I., S. Clarke, and J. Mandelstam.** 1986. spoIID operon of *Bacillus subtilis*: cloning and sequence. J. Gen. Microbiol. **132**(Pt. 2):341–354.
25. **Margolis, P. S., A. Driks, and R. Losick.** 1993. Sporulation gene *spoIIB* from *Bacillus subtilis*. J. Bacteriol. **175:**528–540.
26. **Meyer, P., J. Gutierrez, K. Pogliano, and J. Dworkin.** 1 April 2010. Cell wall synthesis is necessary for membrane dynamics during sporulation of *Bacillus subtilis*. Mol. Microbiol. [Epub ahead of print.] doi:10.1111/j.1365-2958.2010.07155.x.
27. **Morlot, C., T. Uehara, K. A. Marquis, T. G. Bernhardt, and D. Z. Rudner.** 2010. A highly coordinated cell wall degradation machine governs spore morphogenesis in *Bacillus subtilis*. Genes Dev. **24:**411–422.
28. **Perez, A. R., A. Abanes-De Mello, and K. Pogliano.** 2000. SpoIIB localizes to active sites of septal biogenesis and spatially regulates septal thinning during engulfment in *Bacillus subtilis*. J. Bacteriol. **182:**1096–1108.
29. **Perez, A. R., A. Abanes-De Mello, and K. Pogliano.** 2006. Suppression of engulfment defects in *Bacillus subtilis* by elevated expression of the motility regulon. J. Bacteriol. **188:**1159–1164.
30. **Sawano, A., and A. Miyawaki.** 2000. Directed evolution of green fluorescent protein by a new versatile PCR strategy for site-directed and semi-random mutagenesis. Nucleic Acids Res. **28:**78.
31. **Schaeffer, P., J. Millet, and J. Aubert.** 1965. Catabolite repression of bacterial sporulation. Proc. Natl. Acad. Sci. U. S. A. **54:**704–711.
32. **Sharp, M. D., and K. Pogliano.** 1999. An *in vivo* membrane fusion assay implicates SpoIIIE in the final stages of engulfment during *Bacillus subtilis* sporulation. Proc. Natl. Acad. Sci. U. S. A. **96:**14553–14558.
33. **Sharp, M. D., and K. Pogliano.** 2002. Role of cell-specific SpoIIIE assembly in polarity of DNA transfer. Science **295:**137–139.
34. **Shida, T., H. Hattori, F. Ise, and J. Sekiguchi.** 2001. Mutational analysis of catalytic sites of the cell wall lytic *N*-acetylmuramoyl-L-alanine amidases CwlC and CwlV. J. Biol. Chem. **276:**28140–28146.
35. **Smith, K., M. E. Bayer, and P. Youngman.** 1993. Physical and functional characterization of the *Bacillus subtilis spoIIM* gene. J. Bacteriol. **175:**3607–3617.
36. **Sterlini, J. M., and J. Mandelstam.** 1969. Commitment to sporulation in *Bacillus subtilis* and its relationship to development of actinomycin resistance. Biochem. J. **113:**29–37.
37. **Sugai, M., T. Akiyama, H. Komatsuzawa, Y. Miyake, and H. Suginaka.** 1990. Characterization of sodium dodecyl sulfate-stable *Staphylococcus aureus* bacteriolytic enzymes by polyacrylamide gel electrophoresis. J. Bacteriol. **172:** 6494–6498.
38. **Sun, Y. L., M. D. Sharp, and K. Pogliano.** 2000. A dispensable role for forespore-specific gene expression in engulfment of the forespore during sporulation of *Bacillus subtilis*. J. Bacteriol. **182:**2919–2927.
39. **Youngman, P., J. B. Perkins, and R. Losick.** 1984. A novel method for the rapid cloning in *Escherichia coli* of *Bacillus subtilis* chromosomal DNA adjacent to Tn917 insertions. Mol. Gen. Genet. **195:**424–433.

Acknowledgments

Chapter III, in full, is a reproduction of the material as it appears in Jounal of Bacteriology 2010. Gutierrez, Jennifer; Smith, Rachelle; Pogliano, Kit. American Society for Microbiology, 2010. The dissertation author was the primary investigator and author of the manuscript. Permission has been obtained from all authors.

Supplemental Tables

Table S1. Scoring of Engulfment

Strain	Time	Total cells	% Migration	% Fusion
KP718 (WT)	T3	67	7.4	64
	T4	121	5.6	76
KP1072 (E88A)	T3	370	4.2	0
	T4	213	0	0
KP1079 (R106A)	T3	400	19.8	0.8
	T4	302	22.2	2
KP1099 (K203A)	T3	319	1.3	0
	T4	331	3.6	0
KP1102 (D210A)	T3	569	40.2	4.4
	T4	351	39.6	13.4

Quantification of engulfment in the various mutants studied here. Membrane fusion assays were scored for the percent of cells showing exclusion of FM 4-64 from the forespore membrane, indicating the completion of engulfment (% complete). The same images were scored to determine the percent of cells showing significant membrane migration, as indicated by the curving of the septal membrane more than half of the way around the forespore (% migration). This shows that SpoIID^{E88A} and SpoIID^{K203A} have a defect in septal thinning, with no membrane migration or complete engulfment observed at any timepoint. These numbers also demonstrate that SpoIID^{D210A} has a decreased rate of membrane migration, since only 44.6% of cells have migrated more than half of the distance around the forespore or completed engulfment at T3. If this strain was blocked after membrane migration, then one would expect a similar percent of cells with membrane migration as in

wildtype, or 71.4% of cells should show migration at least halfway at T3. SpoIID^{R106A} supports membrane migration at an even slower rate than SpoIID^{D210A}.

Table S2. Primers used in this study		
Primer Name	Sequence	Purpose
JGP58	ACA CAG ATG TTC GCA GTG TAT AAA AGC	Q134A
JGP59	ATG TTC CAG GTG GCA AAA AGC AAA GCG	Y136A
JGP70	ACA AGC AAC GGC TAC GCA GAG AATG CAG AAG CT	T188A
RMSIIDM1	GAA AAC ATT CCG CTT GCG GAG TAT GTG ATT GGA G	E78A
RMSIIDM2	C TCC AAT CAC ATA CTC CGC AAG CGG AAT GTT TTC	E78A
RMSIIDM3	CCT GAA GCG CTG GCG GCC CAG GCG CTT GCC	K99A
RMSIIDM4	GGC AAG CGC CTG GGC CGC CAG CGC TTC AGG	K99A
RMSIIDM5	GCG CTG AAA GCC GCG GCG CTT GCC GCC	Q101A
RMSIIDM6	GGC GGC AAG CGC CGC GGC TTT CAG CGC	Q101A
RMSIIDM7	GCG CTT GCC GCC GCA ACA TTT ATT GTC AG	R106A
RMSIIDM8	CT GAC AAT AAA TGT TGC GGC GGC AAG CGC	R106A
RMSIIDM9	GCC GCC AGA ACA GCG ATT GTC AGA CTG ATG G	F108A
RMSIIDM10	C CAT CAG TCT GAC AAT CGC TGT TCT GGC GGC	F108A
RMSIIDM11	GGC AAA ATC TTA ACG GCC AAC AAC CAG CCG	Y171A
RMSIIDM12	CGG CTG GTT GTT GGC CGT TAA GAT TTT GCC	Y171A
RMSIIDM13	C CCA TAT TTA GCA AGC GTC AAA AGC CC	K203A
RMSIIDM14	GG GCT TTT GAC GCT TGC TAA ATA TGG G	K203A
RMSIIDM15	C CCA TAT TTA AAA GCC GTC AAA AGC CC	S204A
RMSIIDM16	GG GCT TTT GAC GGC TTT TAA ATA TGG G	S204A
RMSIIDM17	GC CCA TGG GCT AAA AAG TCT CCG	D210A
RMSIIDM18	GG GCT TTT GAC GGC TTT TAA ATA TGG G	D210A
RMSIIDM19	C GTC GCC TCC GCA ATG CCG GCA ACC	E88A
RMSIIDM20	GGT TGC CGG CAT TGC GGA GGC GAC G	E88A
RMSIIDM21	GC CGC TGT AAA GGT TTT CGC TGC CTT ATA TTT CGG	T219A
RMSIIDM22	GG GCT TTT GAC GGC TTT TAA ATA TGG G	T219A

Table S2 con't		
JGP71	TTG ATT TGC GGT TCG TGC GAC GGG A	Y65A
JGP72	TTT CAG CGC TTC AGG TGC AAA GGT	K94A
JGP73	CTG GGC TTT CAG CGC TGC AGG TTT	E96A
JGP74	CAG TCT GAC AAT AAA TGC TCT GGC G	T107A
JGP75	TGG GCT TTT GAC GCT TGC TAA ATA T	K203A
JGP76	CCA TGG GCT TTT GAC TGC TTT TAA A	S204A
JGP77	CTT TTT ATC CCA TGG TGC TTT GAC	S207A
JGP78	TGC CTT ATA TTT CGG TGC CTT TTT	S213A
JGP79	TTT CGT TGC CTT ATA TGC CGG AGA	K215A
JGP80	CTG AAA TTC TGC CGC TGC AAA GGT	T223A
JGP81	AAG CTT TTG CTG AAA TGC TGC CGC T	E226A
JGP82	GAC GCC AAG CTT TTG TGC AAA TTC T	Q228A
JGP83	CAG CTT GAC GCC AAG TGC TTG CTG A	K230A
JGP84	GCT AGA TCC ATC CAG TGC GAC GCC A	K234A
JGP85	GGCTCCACTGGTGGCAGATACACAGATG	D128A
JGP86	TCA CTG GTG GAT GCA ACA CAG ATG TTC	D129A
JGP87	CTG GTG GAT GAT GCA CAG ATG TTC CAG	T130A
JGP88	GCG GTA GCC AGT GCA CAA GGC AAA ATC	T164A
JGP89	GGC AAA ATC TTA GCA TAC AAC AAC CAG	T170A
JGP90	AAG GCA ACG AAA GCA TTT ACA GCG GCA	T221A
JGP91	CTG GAT GGA TCT GCA GCA GTA GGG AAG	S239A
JGP92	ATT AAC GGC AAG GCA CTG AAA GGA AGA	T262A
JGP93	AAG CGA AAT GGA GCA AGA ATT ACA GTC	D286A
JGP94	GAT TTT GAA TGG GCA CGA AAT GGA GAC	K282A
JGP95	TTT GAA TGG AAG CGA AAT GGA GAC ACA	R283A
JGP96	ATT CCC GTC TAT GCA ACC GCA AAT CAA	R66A
JGP97	TTC CAG GTG TAT GCA AGC AAA GCG GAG	K137A
JGP98	ACA GAG AAT GCA GCA GCT TAT TGG ACA	E192A
JGP99	TAT AAG GCA ACG GCA ACC TTT ACA GCG	K220A
JGP100	GCA GAA TTT CAG GCA AAG CT GGC GTC	Q229A
JGP101	TCC AAT CAC ATA TGC TTC AAG CGG AAT	E79A
JGP102	GAC TCC AAT CAC TGC CTC TTC AAG CGG	T80A
JGP103	AAA GGT TGC CGG TGC TTC GGA GGC GAC	M89A
JGP104	TTT AAA GGT TGC TGC CAT TTC GGA GGC	P90A
JGP105	GCC GTT GCT TGT TGC GAA AAA GGA TGC	S182A
JGP106	GTA GCC GTT GCT TGC GGA GAA AAA GGA	T183A
JGP107	GAC GCT TTT TAA TGC TGG GAT AGC ACT	Y201A
JGP108	CAT CCC CAC ACC TGC GCC AAA TCC TCT	H297A

Table S2 con't		
JGP109	TTG GCT CAT CCC TGC ACC GTG GCC AAA	V299A
JGP110	TCC GTA TTG GCT TGC CCC CAC ACC GTG	M301A
JGP111	ATT CGC TCC GTA TGC GCT CAT CCC CAC	Q303A
JGP112	AAG CGG AAT GTT TGC TAC GGA TTG ATT	E73A
JGP113	GAA GCA TCC TTT GCA TCC ACA AGC AAC	F181A
JGP116	GGT TGC CGG CAT TTC TGC GGC GAC GAC	S87A
JGP117	CAC ACC GTG GCC TGC TCC TCT CGT CG	F295A
JGPD358	GAAGCTCCTAAAGGCTCACTG	sequencing
JGP2dp	GCTTGTCCCTGCCCATAGACT	sequencing
RMSP10IID	GGCATGGATGAACTATACAAAATGAAACAA TTCGCAATCACAC	GFP-IID
RMSP11IID	GTGTGATTGCGAATTGTTTCATTTTGTATAG TTCATCCATGCC	GFP-IID
RMSP12IID	G CAT AAT AAG GAA GCG GGG GCC AGC G	GFP-IID
RMSP13IID	C GCT GGC CCC CGC TTC CTT ATT ATG C	GFP-IID

Supplementary Movie Captions

Movie A1. GFP-SpoIIP localization in wild type. Cells were sporulated at 30°C in the presence of FM4-64 and placed on a 1.2% agarose/A+B pad containing FM4-64 at t_2 after sporulation initiation. Cells were imaged on the pad inside a climate-controlled chamber at 30°C. Membranes were stained with FM 4-64. Images were collected five minutes apart for 1 hr. Membrane migration is seen in the majority of cells in this strain and engulfment takes approximately 50 minutes to complete. During the early stages of migration, GFP-SpoIIP forms bright foci at the leading edges of the membranes. When the membranes reach halfway, GFP-SpoIIP becomes an elongated focus, forming a gradient that stretches from the leading edge backwards. After completion of migration, GFP-SpoIIP forms a diffuse cap around the top half of the forespore.

Membrane migration is usually symmetric in this strain with the leading edges meeting directly at the top of the cell. However, in some cells, the membranes appear to inchworm up, with the left side moving slightly ahead in one frame and the right side moving slightly ahead in the next. This suggests that the membranes don't move as a single sheet up and around the forespore.

Movie A2. GFP-SpoIIP localization in a SpoIID^{D210A} background. Cells prepared as described for Movie A1. Membrane migration is seen in few cells in this strain. Often, open bulges form early and become closed in later frames. The rate of membrane migration is hard to assess due to the failure of many sporangia to complete engulfment during the data collection period, but is likely to be >60 minutes. GFP-SpoIIP is seen in three distinct patterns corresponding with different membrane migration events. In large blebs, GFP-SpoIIP is diffuse throughout the bleb, sometimes forming a focus at the center of the septum. In evenly migrating membranes, GFP-SpoIIP forms two, equally bright foci, one at each leading edge. In asymmetrically migrating cells, GFP-SpoIIP forms a bright foci at the leading edge that is that migrating more quickly (more advanced) and a weak, or no, focus at the lagging edge. GFP-SpoIIP tends to be dynamic in its localization in this strain, with lower intensity than the wildtype background and with changing intensities in many foci and throughout blebs. Together, these results indicate that the SpoIID^{D210A} mutation is partially defective in the stabilization of SpoIIP to the leading edge and that SpoIIP localization is associated with an increased rate of membrane migration.

Chapter IV

The SpoIIQ landmark protein has different requirements for septal localization and immobilization.

Abstract

The forespore membrane protein SpoIIQ plays a critical role in protein localization during *Bacillus subtilis* sporulation, as it interacts with the mother cell protein SpoIIIAH recruiting the protein to the septum that is the point of contact between the two compartments. The SpoIIQ-SpoIIIAH complex also localizes additional mother cell membrane proteins involved in engulfment dependent gene expression, so the absence of SpoIIQ causes mother cell proteins critical for development to be delocalized and non-functional. It has remained unclear how SpoIIQ itself is targeted during sporulation, since it localizes normally in the absence of its mother cell binding partner, SpoIIIAH. We here demonstrate that septal localization of SpoIIQ is achieved by two separate pathways that are each sufficient for localization, SpoIIIAH and the SpoIID, SpoIIM, SpoIIP engulfment proteins, which interact and are expressed in the mother cell. SpoIIQ shows diffuse localization only in a mutant lacking both protein complexes. Surprisingly, photobleaching experiments demonstrate that, although SpoIIQ localizes normally in the absence of

SpoIIIAH, it is no longer immobilized, demonstrating that the protein is able to exchange subunits within a localized pool. SpoIIQ mobility is further increased by the additional absence of the engulfment proteins, suggesting that this complex interacts with SpoIIQ to slow down diffusion even in the absence of SpoIIIAH. These data suggest that SpoIIQ interacts both with the engulfment proteins and with proteins that control the onset of engulfment dependent gene expression. They further demonstrate that apparently normal localization of a protein in the absence of a partner can mask dramatic alterations in protein mobility.

Introduction

A key task in cell biology is to identify factors that contribute to targeting of proteins to subcellular locales. An amenable system to study this is the sporulation pathway of *Bacillus subtilis*, a developmental program that results in the formation of a durable, dormant endospore and depends on localized proteins. Sporulation commences with the relocalization of cell division proteins from midcell to sites near both cell poles. A polar division event then creates two adjacent cells of unequal size: a smaller forespore that will ultimately become the spore, and a larger mother cell that lyses after contributing to spore development (reviewed in (Errington, 2003, Piggot & Hilbert, 2004)). Next, the forespore is internalized in a phagocytosis-like process called engulfment, during which the mother cell membranes move around the forespore until the leading edges of the engulfing membrane meet and fuse, releasing the forespore into the mother cell cytoplasm (Fig. 1A). The resulting forespore is completely enclosed within the mother cell and is surrounded by two membranes, one derived from the original forespore membrane and one from the engulfing mother cell membrane. Internalization of the forespore allows subsequent steps in spore maturation, such as coat assembly, to occur in a controlled environment, likely contributing to the extreme durability of the final endospore.

Three pathways for protein targeting during sporulation have been identified, all of which are important for the development of the spore. First,

during septation the SpoIIB protein localizes to potential cell division sites and remains at the site of septation thereby forming a landmark for three proteins produced after polar septation in the mother cell (Aung et al., 2007). These three proteins, SpoIID, SpoIIM and SpoIIP, are the only proteins known to be required for engulfment under all conditions (Frandsen & Stragier, 1995, Lopez-Diaz et al., 1986, Smith et al., 1993). Second, the forespore produced protein SpoIIQ and the mother cell produced protein SpoIIIAH interact via their extracellular domains within the septal space (Londono-Vallejo *et al.*, 1997, Kuroda *et al.*, 1992 , Blaylock *et al.*, 2004, Rubio & Pogliano, 2004) (Fig 1C), a process that tethers both proteins to the septum, which is the only potential site of interaction. The SpoIIQ-SpoIIIAH zipper complex subsequently targets proteins involved in engulfment-dependent gene expression to the septum (Fig 1B) (Jiang *et al.*, 2005, Doan *et al.*, 2005). Third, after the onset of the phagocytosis-like process of engulfment, the SpoVM protein targets the convex outer forespore membrane by directly recognizing its lipid architecture and inserting the non-polar face of its amphipathic helix into the bilayer (Ramamurthi *et al.*, 2009, Prajapati *et al.*, 2000). SpoVM then recruits SpoIVA to the outside of the developing forespore (Ramamurthi *et al.*, 2006), together recruiting proteins required for assembly of the spore cortex and spore coat to the outer forespore membranes to create the structures that are critical for the admirable resistance of the spore to heat, dessication and chemical stresses (van Ooij & Losick, 2003, Levin *et al.*, 1993, Driks *et al.*, 1994).

Two of these targeting pathways also comprise redundant pathways for protein localization during the phagocytosis-like process of engulfment. SpoIIB serves as the primary localization pathway for SpoIIM, a five transmembrane domain protein that is synthesized soon after septation and that recruits SpoIIP and SpoIID (Chastanet & Losick, 2007, Aung et al., 2007). However, if SpoIIB is absent, the SpoIIQ/SpoIIIAH zipper acts as a backup mechanism for SpoIIM localization via SpoIVFA (Aung et al., 2007), a mother cell protein targeted to the septum by SpoIIIAH (Jiang et al., 2005, Doan et al., 2005). This redundancy in targeting pathways for the engulfment proteins is mirrored by the existence of redundant pathways for engulfment itself. The SpoIID, SpoIIM, SpoIIP complex is essential for engulfment and includes two enzymes that degrade peptidoglycan (Morlot et al., Chastanet & Losick, 2007, Abanes-De Mello et al., 2002). Two pathways compensate for reduced SpoIID, SpoIIM, SpoIIP activity, peptidoglycan biosynthesis (Meyer *et al.*, 2010) and the SpoIIQ/SpoIIIAH complex (Broder & Pogliano, 2006). SpoIIQ is immobilized during engulfment and the SpoIIQ/SpoIIIAH complex has therefore been proposed to act as a stable scaffold, or ratchet, that resists the backward motion of the engulfing mother cell membranes (Broder & Pogliano, 2006).

Curiously, although SpoIIIAH localization depends on SpoIIQ, SpoIIQ remains localized in the absence of SpoIIIAH, forming foci and helical arcs that look nearly identical to the protein in wild type cells (Jiang et al., 2005).

Genetic evidence indicates that the absence of the mother cell specific sigma factor σ^E causes complete mislocalization of SpoIIQ (Rubio & Pogliano, 2004), suggesting that other proteins produced by σ^E are responsible for SpoIIQ localization. We here demonstrate that septal localization of SpoIIQ is mediated by two redundant systems, SpoIIIAH and the SpoIID/SpoIIM/SpoIIP proteins, either of which are capable of mediating septal localization in the absence of the other. However, we also noted that, although SpoIIQ localizes normally in the absence of SpoIIIAH, it is no longer immobilized and diffuses rapidly within the septum that forms the interface between the forespore and mother cell. Interestingly, when SpoIID, SpoIIM, and SpoIIP are deleted along with SpoIIIAH, SpoIIQ is released from the septum and diffuses even more rapidly, suggesting that the SpoIIDMP engulfment proteins form a secondary tether that helps to localize SpoIIQ to the sporulation septum. Using single mutants and mutations that abolish SpoIID peptidoglcyan degradation activity, we also show that SpoIIM and SpoIIP appear to interact with SpoIIQ whereas SpoIID does not and furthermore, that SpoIIQ is immobilized even in the absence of SpoIIIAH if the SpoIID/SpoIIM/SpoIIP complex is itself trapped at the septum. These findings demonstrate an intimate interaction between the engulfment proteins and the SpoIIQ-SpoIIIAH complex that is required for engulfment-dependent gene expression.

Results

Localization of GFP-SpoIIQ is dependent on both SpoIIIAH and the SpoIIDMP module

Localization of GFP-SpoIIQ is not dramatically affected by the removal of its only known mother cell tether, SpoIIIAH ((Blaylock et al., 2004, Jiang et al., 2005) Fig. 2A-B); only elimination of all mother cell specific gene expression by mutation of *spoIIGB* completely delocalizes GFP-SpoIIQ (Rubio & Pogliano, 2004). We therefore sought to identify members of the σ^E regulon required for SpoIIQ localization. SpoIIQ and SpoIIIAH play an auxillary role in engulfment, and disruption of *spoIIQ* in strains expressing low levels of SpoIID or SpoIIP or expressing GFP fusions to SpoIID, SpoIIM, or SpoIIP (which complement their respective nulls for spore formation) show a synergistic engulfment defect (Broder & Pogliano, 2006). We therefore examined the role of the engulfment proteins, SpoIID, SpoIIM, and SpoIIP, in localization of GFP-SpoIIQ.

Disruption of *spoIID*, *spoIIM,* or *spoIIP* prevents membrane migration and formation of GFP-SpoIIQ foci and arcs, but GFP-SpoIIQ is still retained at the septum indicating that other mother cell proteins restrict its diffusion (Fig 2B-D). GFP-SpoIIQ localized to the septum in most (74-92%) *spoIID*, *spoIIM*, or *spoIIP* single mutant sporangia, forming a bright focus at the center or two foci on either side of the bulges (Fig. 2B-D, J). Three GFP-SpoIIQ localization

phenoytpes were observed in the spoIID, spoIIM, spoIIP triple mutant: 46% of sporangia showed septal localization, 20% were delocalized with a uniform distribution throughout the forespore membrane and 34% showed an intermediate localization phenotype (Fig. 2E, J). This variable and intermediate phenotype suggests that SpoIID, SpoIIM, and SpoIIP contribute to SpoIIQ localization, but that another protein also can mediate SpoIIQ localization.

SpoIIQ localization was next tested in the absence of the engulfment proteins depended on its mother cell binding partner SpoIIIAH by inactivating *spoIIIAH* in the single and triple engulfment mutants. While all three single engulfment/*spoIIIAH* mutant combinations resulted in a variety of GFP-SpoIIQ localization phenotypes, the *spoIID spoIIIAH* strain retained significantly more localization than the other strains (Fig. 2I, M), with the most frequent pattern being a focus at the septum center (32%). This was never observed in *spoIIP spoIIIAH* or *spoIIM spoIIIAH* (Fig. 2G-H, M) strains, which showed either partial or completely delocalized GFP-SpoIIQ. These data suggest that both SpoIIM and SpoIIP contribute to localizing SpoIIQ to the septum (Fig. 2D, J), directly or indirectly. Combination of all three engulfment mutant alleles with the *spoIIIAH* mutation resulted in random localization identical to the σ^E null strain in 93% of sporangia (Fig. 2F, J). These results, which were verified by using immunofluorescence microscopy to localize native SpoIIQ (Fig. S1), indicate that the SpoIID/SpoIIM/SpoIIP and SpoIIIAG/SpoIIIAH complexes

each contribute to GFP-SpoIIQ localization either directly or indirectly via additional factors that they localize.

SpoIIIAH is required for immobility of GFP-SpoIIQ.

GFP-SpoIIQ was previously observed to be immobile during engulfment ((Broder & Pogliano, 2006); confirmed in Fig 3A), but the mechanism for immobilization of SpoIIQ remains unclear. We therefore sought to determine which of the above localization determinants were responsible for immobilization of SpoIIQ by performing a Fluorescence Recovery After Photobleaching (FRAP) analysis on GFP-SpoIIQ in mutants lacking SpoIIIAH and/or the engulfment proteins. Sporulating cells were immobilized on coverslips and a region of the GFP-SpoIIQ fluorescence was bleached with a laser. The bleached region sometimes corresponded to a single focus and sometimes to half of the septum depending the GFP-SpoIIQ localization pattern. Recovery of the bleached region was then observed using timelapse fluorescence microscopy and the images quantified using two different methods. First, to obtain individual cell recovery curves, bleached and unbleached regions were defined using polygons. The amount of fluorescence per pixel was then determined for each region in each image of the timelapse sequence with a correction for background signal (as described in (Broder & Pogliano, 2006)). This allowed the recovery of fluorescence in the bleached region and the loss of fluorescence in the unbleached region to

be plotted for each cell. Second, to obtain average recovery curves of many cells, we calculated the ratio of fluorescence intensity of the bleached region to that of the unbleached region at each timepoint relative to the ratio of the same regions before the bleach to give the corrected recovery index (cRI) (Wu *et al.*, 2006). We then normalized the recovery curves by defining the initial prebleach cRI value as one and the minimum cRI ratio (immediately after photobleaching) as zero to give the corrected fraction recovery (cFR) (as in (Fleming *et al.*, 2010), adapted from (Wu et al., 2006)). These values were directly compared between cells, and averaged when all individual cells formed an obvious group, to obtain the average time to 50% recovery relative to the maximum recovery ($t_{1/2}$ avg) and the average mobile fraction, or amount of protein able to move within the septum, which is represented by the maximum recovery in the cFR.

In wild type cells, GFP-SpoIIQ showed little recovery after photobleaching, even in experiments lasting up to 5 minutes, with an average cFR of 0.2 (20%) versus the 1.0 (100%) expected for a fully mobile protein (Fig 3A). This indicates that that there is no movement of SpoIIQ between the bleached and unbleached regions and that the protein is immobile as previously described (Broder & Pogliano, 2006). As GFP-SpoIIQ appears normally localized in the *spoIIIAH* mutant (Fig. 2B; (Blaylock et al., 2004)), we expected that it would be immobile as in the wild type strain. In contrast, the protein rapidly recovered to 80% the level of prebleach fluorescence, with an

average equilibration half time ($t_{1/2}$) of approximately 12 seconds (Fig. 3B, E). This indicates that, although GFP-SpoIIQ localizes normally in the absence of SpoIIIAH, it shows increased mobility. Strikingly, in many sporangia, GFP-SpoIIQ assembled clear foci and the bleaching of individual foci often resulted in recovery of fluorescence in the same focus as it appeared before photobleaching. Thus, although SpoIIQ appears normally localized in the absence of SpoIIIAH, it displays dramatically increased mobility, indicating that the zipper-like interaction between SpoIIQ and SpoIIIAH immobilizes SpoIIQ.

Next, the possibility that other members of the *spoIIIA* operon affect GFP-SpoIIQ mobility was addressed by examining the effect of a *spoIIIAA::mTn5* mutation that prevents expression of all the genes in the *spoIIIAA-AF* operon, but does not affect expression of the *spoIIIAG-AH* operon (Blaylock et al., 2004). This mutation had no effect on GFP-SpoIIQ mobility (data not shown). We attempted to specifically deplete SpoIIIAH, but found that mutations in *spoIIIAH* destabilized SpoIIIAG, and so were unable to determine if both SpoIIIAG and SpoIIIAH are required for SpoIIQ immobilization. However, we favor the simpler model in which SpoIIQ immobilization primarily depends on SpoIIIAH, since the interaction between these two proteins is remarkably robust.

We next tested if the engulfment proteins are necessary for immobilization of SpoIIQ. FRAP experiments demonstrated GFP-SpoIIQ showed limited mobility in the *spoIID, spoIIM, spoIIP* triple mutant, with the

equilibration half times for most cells longer than the experiment duration of 3 or 5 minutes and with limited recovery similar to the mobility of the protein in wild type cells. Thus, despite the observation that SpoIIQ fails to localize in 17% of sporangia lacking the engulfment proteins, it remains immobilized in this strain (Fig. 3C). Recovery was also very slow in the single engulfment mutants (data not shown) within which GFP-SpoIIQ predominantly localizes as a focus at the septum middle. This indicates that immobilization of SpoIIQ does not depend on the engulfment proteins.

Although GFP-SpoIIQ mobility was increased by the absence of SpoIIIAH, its $t_{1/2}$ (12s) was significantly longer than previously demonstrated for a forespore expressed membrane protein that is not expected to specifically interact with other proteins, MalF-GFP (4s, (Rubio & Pogliano, 2004)). We therefore speculated that, in the absence of SpoIIIAH, GFP-SpoIIQ mobility was restricted by its interaction with other proteins. The engulfment proteins were likely candidates, since GFP-SpoIIQ does not localize in the *spoIID, spoIIM, spoIIP, spoIIIAH* quadruple mutant strain. Indeed, FRAP experiments showed that in this strain, GFP-SpoIIQ showed very rapid and nearly complete fluorescence recovery after photobleaching (Fig. 3D, E) with a $t_{1/2}$ reduced to 2 sec and recovery >60%, similar to that of forespore expressed MalF-GFP (Rubio & Pogliano, 2004). This indicates that, in the absence of SpoIIIAH, diffusion of GFP-SpoIIQ is slowed by SpoIID, SpoIIM, and SpoIIP. These data suggest that one or more of these mothercell

expressed proteins interacts with the forespore expressed SpoIIQ, an interaction that would both slow SpoIIQ diffusion and restrict the protein to the sporulation septum, the only point of contact between the two cells.

SpoIID, SpoIIM, and SpoIIP affect SpoIIQ mobility differently

To further elucidate the individual contributions of the engulfment proteins in SpoIIQ immobilization, we used FRAP to examine GFP-SpoIIQ mobility in mutants lacking SpoIIIAH and either SpoIIP or SpoIID. Interestingly, *spoIID* and *spoIIP* single mutants, when combined with a *spoIIIAH* deletion, resulted in a range of outcomes. Variability was apparent in both the diffusion rate of SpoIIQ, as indicated by the recovery $t_{1/2}$, and in mobile fraction, which represents the amount of SpoIIQ that is free in the membrane and able to diffuse at all. In contrast, the *spoIID, spoIIM, spoIIP, spoIIIAH* quadruple mutant showed a more uniform recovery pattern (Fig 3E). For example, FRAP of the *spoIIP spoIIIAH* double mutant revealed equal numbers of cells either (1) recovering faster than a *spoIIIAH* mutant with an equilibration $t_{1/2}$ of <5 sec but with recovery that did not reach 100%, indicating that only a fraction of SpoIIQ was mobile (Fig 4A), or (2) not recovering at all, with curves mimicking those of wild type, here shown as $t_{1/2}$ > 40sec (Fig 4A). Thus, some *spoIIP spoIIIAH* cells had a fraction of SpoIIQ that was rapidly diffusing, while others showed fully immobilized SpoIIQ. The *spoIID spoIIIAH* double mutants also showed two populations. A smaller subpopulation of cells showed fully immobilized SpoIIQ with no recovery ($t_{1/2}$ >40s), whereas most

cells showed recovery curves similar to a *spoIIIAH* single mutant with a $t_{1/2}$ of 5-20 sec and recovery to 60% of prebleach fluorescence levels (Fig 4A). This indicates that, in the absence of SpoIIIAH and either SpoIID or SpoIIP, another protein can interact with a fraction of the SpoIIQ in the sporangium to restrict its mobility. The observation that a strain lacking all three engulfment proteins shows rapid diffusion and complete recovery and the localization data shown above suggests that SpoIIM and SpoIIP play a more critical role in SpoIIQ immobilization than SpoIID, though how this is mediated (protein-protein interactions, peptidoglycan-SpoIIQ interactions) remains unclear.

SpoIID enzymatic mutants affect SpoIIQ mobility

We recently identified mutants of SpoIID that are either unable to cleave peptidoglycan ($SpoIID^{E88A}$) or have reduced ability to cleave peptidoglycan ($SpoIID^{D210A}$) (Gutierrez et al., 2010). The $SpoIID^{E88A}$ mutant blocks membrane migration and it also traps SpoIID at the septum, suggesting that peptidoglycan degradation contributes to the release of SpoIID from the septum. When these protein variants were introduced into a strain carrying GFP-SpoIIQ, as expected, there was no effect on SpoIIQ mobility, and no recovery was seen during three minute FRAP experiments (data not shown). However, when combined with a *spoIIIAH* deletion, $SpoIID^{E88A}$ resulted in immobilization of SpoIIQ in 20 of the 22 cells tested (Fig 4B) with localization of GFP-SpoIIQ most often confined to a solid line across the septum (Fig 2G). Thus, the enzymatically inactive mutant of SpoIID reduces SpoIIQ mobility in

the absence of SpoIIIAH, whereas the complete absence of SpoIID protein in the null mutant strain increases SpoIIQ mobility in the absence of SpoIIIAH. We previously demonstrated that this enzymatically inactive mutant effectively 'locks down' SpoIID at the septum (Gutierrez et al., 2010), suggesting that peptidoglycan degradation is necessary for SpoIID dynamics. The FRAP data suggest that this protein is capable of also trapping SpoIIQ in an immobile complex, even in the absence of SpoIIIAH, further suggesting that SpoIIQ interacts with one or more members of the SpoIID/SpoIIM/SpoIIP complex.

GFP-SpoIIIAH depends on the same proteins as SpoIIQ for localization and immobility.

Previous results indicated that SpoIIIAH localizes in a manner similar to SpoIIQ, being enriched around the forespore and co-localizing with SpoIIQ (Blaylock et al., 2004, Doan et al., 2005). We were interested in determining if SpoIIIAH was immobilized by interaction with SpoIIQ, and therefore constructed a GFP fusion to the N-terminus of SpoIIIAH. GFP-SpoIIIAH produced striking foci associated with the forespore membrane (Fig 5A). The *spoIIQ* mutation resulted in decreased, though not completely random, localization to the mother cell cytoplasm and membrane as previously reported (Blaylock et al., 2004, Doan et al., 2005). This confirms that SpoIIQ is the primary localization determinant of SpoIIIAH (Fig 5B). Removal of either one or all three essential engulfment proteins, SpoIID, SpoIIM, and SpoIIP, had no effect on GFP-SpoIIIAH localization and the protein localized both to the

septum and to the septal bulges produced in these mutants (Fig. 5C-F). This is in contrast to a previous localization study of epitope-tagged SpoIIIAH by immunofluorescence microscopy, which showed an early localization defect in the absence of the engulfment proteins (Blaylock et al., 2004). We found no evidence for this defect, and suggest that the difference is either due to differences in the procedure or the epitope tag. We conclude that the engulfment proteins do not contribute to apparent residual targeting of SpoIIIAH in the absence of SpoIIQ.

Based on observations of GFP-SpoIIQ dynamics during FRAP experiments, we hypothesized that GFP-SpoIIIAH would also be immobilized in a manner that depends on its partner SpoIIQ. Indeed, photobleaching of GFP-SpoIIIAH resulted in very limited recovery similar to the wild type strain (Fig. 6A). A similar phenomenon was observed in strain missing *spoIIP* (Fig. 6B). In contrast, the absence of SpoIIQ allowed rapid and nearly complete recovery of photobleached GFP-SpoIIIAH, with an 80% mobile fraction and recovery half-times near 25 seconds (Fig 6C, D). Curiously, this recovery was not as fast as that of GFP-SpoIIQ in the absence of SpoIIIAH, suggesting that diffusion of SpoIIIAH is further restricted by some other interaction, perhaps with proteins encoded by the spoIVFA-FB and spoIIIAA-AF operons, which interact with SpoIIIAH and localize to the septum in a SpoIIIAH dependent manner (Blaylock et al., 2004, Doan et al., 2005, Jiang et al., 2005). Further studies are required to determine if any of these proteins interact with

SpoIIIAH in the absence of SpoIIQ. Together our FRAP data indicate that the interaction between SpoIIQ and SpoIIIAH immobilizes both proteins.

Discussion

We here use fluoresecence recovery after photobleaching (FRAP) to demonstrate that the interaction between the forespore protein SpoIIQ and the mother cell protein SpoIIIAH immobilizes both proteins during engulfment. This immobilization is consistent with the ability of this protein complex between the two cells of the sporangium to facilitate engulfment by preventing backwards movement of the migrating membrane (Broder & Pogliano, 2006). Interestingly, although immobilization of each protein depends on the other (Fig 3A, 6A), the septal localization of just one of these proteins, SpoIIIAH, depends on the other. SpoIIQ remains localized in the absence of SpoIIIAH (Blaylock et al., 2004, Rubio & Pogliano, 2004) and it diffuses more slowly than an unfettered membrane protein (Rubio & Pogliano, 2004, Broder & Pogliano, 2006), suggesting that SpoIIQ interacts with atleast one other protein in addition to SpoIIIAH (Fig 2). Indeed, when we eliminated the engulfment proteins, SpoIID, SpoIIM, and SpoIIP, in conjunction with SpoIIIAH, SpoIIQ failed to localize (Fig 2) and its mobility increased to match that of a freely diffusing membrane protein (Fig 3). This strongly suggests that we successfully eliminated all SpoIIQ interacting proteins from the septum. These data indicate that septal localization of the forespore-expressed SpoIIQ protein can be mediated by its interaction with either one of two mother cell tethers, the SpoIIIAH protein or the SpoIID/SpoIIM/SpoIIP complex of engulfment proteins. It also demonstrates that formation of the SpoIIQ-

SpoIIIAH complex that bridges the two cells of the developing sporangia immobilizes both proteins.

Based on these findings, we propose a model where newly synthesized SpoIIQ is inserted into the forespore membrane where it interacts with the engulfment protein complex, SpoIID, SpoIIM and SpoIIP, which localize via the septal landmark protein SpoIIB (Aung et al., 2007). This would create a high concentration of SpoIIQ near the SpoIIDMP complex, which would then facilitate recruitment of SpoIIIAH to the septum. The subsequent interaction immobilizes both SpoIIQ and SpoIIIAH, perhaps because the complex spans septal peptidoglycan that either remains after septal thinning or is synthesized during engulfment (Meyer et al., 2010). Interestingly, SpoIIQ foci and arcs depend on the engulfment proteins rather than on SpoIIIAH. We therefore speculate that these correspond to the deposition and localization of SpoIIQ along the path taken by the engulfment protein complex as it moves around the forespore during membrane migration.

Further evidence that the engulfment proteins interact with SpoIIQ comes from the observation that if SpoIID is unable to be released from the septum (Chapter 3, (Gutierrez et al., 2010)), then SpoIIQ is immobilized even in the absence of SpoIIIAH. This suggests a direct protein-protein interaction between SpoIIQ and one, or more, of the engulfment proteins that is capable of immobilizing SpoIIQ when the engulfment protein complex is locked at the septum by the enzymatically inactive SpoIID mutant. We propose that, in a

wild type cell, the interaction between SpoIIQ and the engulfment proteins is transient and specifically released during the peptidoglycan degradation cycle (Morlot et al., Gutierrez et al., 2010). Our data suggest that SpoIIQ might primarily interact with SpoIIP or SpoIIM, rather than SpoIID. First, in each single engulfment mutant, SpoIIQ localizes to the septum center in most cells (Fig 2), but in the triple *spoIID, spoIIM, spoIIP* mutant, SpoIIQ is diffuse along the septum. The engulfment proteins localize in the sequence SpoIIM, then SpoIIP, then SpoIID (Chastanet & Losick, 2007, Aung et al., 2007), so the SpoIIQ localization pattern suggests that the first two engulfment proteins to arrive at the septum (SpoIIM then SpoIIP) likely interact redundantly with SpoIIQ. Second, the FRAP recovery curves for the *spoIID spoIIIAH* and *spoIIP spoIIIAH* double mutant strains each show variable mobilization of SpoIIQ, with each strain having a subpopulation of cells with immobilized SpoIIQ, as well as those with increased SpoIIQ mobility. The immobile population suggests that the remaining engulfment protein, SpoIIM, can interact with SpoIIQ and sometimes immobilizes it in the absence of SpoIIIAH, perhaps suggesting that SpoIIIAH competes with the engulfment proteins for SpoIIQ binding. The second population of *spoIIP spoIIIAH* cells revealed freely diffusing SpoIIQ with individual cell recovery $t_{1/2}$ <5s (Fig 4), but with variable amounts of SpoIIQ free in the membrane, suggesting that SpoIIM might bind SpoIIQ until it becomes saturated, leaving different amounts of SpoIIQ free in the membrane depending perhaps on how much SpoIIQ has been produced.

The second population of curves in the *spoIID spoIIIAH* background recovered at rates similar to the *spoIIIAH* single mutant (Fig 4), suggesting that SpoIIQ interacts with both SpoIIP and SpoIIM, and that these interactions are sufficient to explain the reduced recovery rates observed in the *spoIIIAH* mutant compared to a freely diffusing membrane protein.

The immobilization of SpoIIQ and SpoIIIAH observed here demonstrates that the interaction between the two proteins is very strong and not easily reversible, and thus that monomers do not cycle in and out of the complex. It also demonstrates that the complex does not diffuse around the membrane as a unit. Hence, we propose that the large SpoIIQ/SpoIIIAH complex that is predicted to form in the intermembrane space (Camp & Losick, 2009, Camp & Losick, 2008, Meisner *et al.*, 2008) could be held in place by septal peptidoglycan. Though individual monomers of SpoIIQ diffuse freely between the foci in the absence of SpoIIIAH, once the complex is formed, it could be too big to follow the track potentially left by SpoIID, SpoIIM, and SpoIIP on their way up and around the forespore during engulfment.

Materials and Methods

Strains, genetic manipulations and growth conditions

Strains (Table 1) are derivatives of *B. subtilis* PY79 (Youngman *et al.*, 1984). Mutations were introduced by transformation (Dubnau & Davidoff-Abelson, 1971). Sporulation was induced by resuspension (Sterlini & Mandelstam, 1969) at 37°C with the modification that initial growth was performed using 0.25X LB in most cases. When used, CH medium was prepared using casein hydrolysate from EMD, due to variability in the ability of Oxoid brand casein hydrolysate to support sporulation.

Genetic constructions

An N-terminal GFP fusion to SpoIIIAH expressed from the *spoIIIAA* promoter was created as follows. A 600 bp fragment encoding the *spoIIIAA* promoter was amplified via PCR with Pfu polymerase using oligonucleotides DB121 (5'-ACTGAAAGGATCCGGGCTTGTTGTAAACGTGCCG-3') and DB209 (5'-TTT ATC ATT ACT AGT TTG TTT TTT AAG CAT CAG AGC CTC CTC CTT TCT ACC G-3'), digested with BamHI and SpeI, and ligated into BamHI/SpeI-digested pMDS14 (Sharp & Pogliano, 2002) to create plasmid pDB141. The 654 bp *spoIIIAH* gene was then amplified using oligonucleotides DB177 (5'-GGAGGATGGGCCCATGCTTAAAAAACAAACCG-3') and DB178 (5'-TCCCTCATTCGGGCCCTTATTTAGAGGGTTC-3'), digested with PspOMI,

and ligated into EagI-digested pDB141 to create plasmid pDB142. DNA sequencing was performed by Eton Bioscience Inc. (San Diego, CA). The various *spoIID* mutants were inserted at the *thrC* locus by subcloning out of pKP01 or PCR products from the amyE locus of strains KP1102 and KP1072 (Gutierrez et al., 2010). SpoIID constructs were digested using enzymes BamHI and SfoI and inserted into pDG1664 (Guerout-Fleury et al., 1996) digested with BamHI and SnaBI, eliminating the erm^R cassette on the plasmid. All plasmids were initially transformed into PY79 and verified to be kan^R, erm^S, spc^S to ensure proper integration of the plasmid at the *thrC* locus. These mutant were combined with a *spoIIIAH* knockout generated from pDB102. pDB102 is pMutinFLAG with a KpnI/HindIII-digested PCR product created with primers DB163 and DB164 cloned in. When campbelled in this interrupts the *spoIIIA* operon after *spoIIIAG*, creating a *spoIIIAH* null.

Microscopy, deconvolution, image analysis, and Fluorescence Recovery After Photobleaching (FRAP)

Imaging of FM 4-64 stained cells was performed as described (Rubio & Pogliano, 2004), using an Applied Precision Spectris microscope equipped with a Quantified Laser Module (described in (Liu *et al.*, 2006)). Image files were deconvolved using SoftWoRx (15 iterations on conservative setting). TIFFs were saved from medial focal planes, adjusting the GFP images to eliminate background fluorescence in vegetative cells that do not express

GFP, and the FM 4-64 images to eliminate fluorescence outside the cells. Photobleaching experiments to assess GFP-SpoIIQ or GFP-SpoIIIAH mobility used cells from $t_{2.5}$ or t_3 of sporulation, that were concentrated, stained with FM 4-64 and applied to poly-$_L$-lysine treated coverslips. Prebleach images were collected for both FM 4-64 and GFP. Photobleaching was achieved using a 0.05 sec pulse of a 488 nm argon laser at 50% power or a 0.3 second pulse at 30% power, and subsequent GFP images were collected at appropriate intervals for either 30, 82, 125, 180 or 300 seconds, depending on the observed recovery time of the GFP fusion. Three sec exposure times were used for GFP-SpoIIIAH, 0.5 sec for GFP-SpoIIQ. Quantification of FRAP experiments was performed as described (Fleming et al., 2010). Control experiments demonstrated that identical mobility was observed on timelapse pads (Becker & Pogliano, 2007), which are made without poly-$_L$-lysine.

Tables

Table 1. Strains used in this study

Strain	Genotype	Reference or source
AR126	*ΔspoIIQ::spec, amyE::P_{spoIIQ}.GFP-spoIIQ-cm*	Lab collection
AR139	*ΔspoIIQ::spec, amyE:: P_{spoIIQ}. GFP-spoIIQ-cm, ΔspoIIP::tet*	Lab collection
AR140	*ΔspoIIQ::spec, amyE::P_{spoIIQ}.GFP-spoIIQ-cm, spoIIM-mls*	Lab collection
AR200	*ΔspoIIQ::spec, amyE:: P_{spoIIQ}.GFP-spoIIQ-cm, spoIID298, spoIIM-mls, ΔspoIIP::tet*	Lab collection
DB149	*ΔspoIIQ::spec, amyE:: P_{spoIIQ}.GFP-spoIIQ-cm, spoIID298, spoIIM-mls, ΔspoIIP::tet, spoIIIAGH-kan*	This work
DB150	*ΔspoIIQ::spec, amyE::P_{spoIIQ}.GFP-spoIIQ-cm, spoIIIAGH-kan, spoIIM-mls*	This work
DB151	*ΔspoIIQ::spec amyE::P_{spoIIQ}. GFP-spoIIQ-cm r ΔspoIIIAGH-kan ΔspoIIP::tet*	This work
DB153	*ΔspoIIQ::spec amyE:: P_{spoIIQ}. GFP-spoIIQ-cm ΔspoIIIAGH-kan, spoIID::cat::tet*	This work
DB188	*spoIID298, spoIIM-mls, ΔspoIIP::tet*	Lab collection
DB284	*ΔspoIIQ::spec, amyE:: P_{spoIIQ}. GFP-spoIIQ-cm, spoIID298*	This work
DB351	*spoIID298, spoIIM-mls, ΔspoIIP::tet, spoIIIAGH-kan*	This work
DB542	*spoIIIAG::pMutinFLAG-erm, amyE::$P_{spoIIIA}$.GFP-spoIIIAH-cm*	This work
DB553	*amyE::$P_{spoIIIA}$.GFP-spoIIIAH-cm*	This work
DB554	*amyE::$P_{spoIIIA}$.GFP-spoIIIAH-cm, ΔspoIIQ::spec*	This work
DB555	*amyE::$P_{spoIIIA}$.GFP-spoIIIAH-cm, ΔspoIIP::tet*	This work
DB556	*amyE::$P_{spoIIIA}$.GFP-spoIIIAH-cm, spoIIM-mls*	This work
DB557	*amyE::$P_{spoIIIA}$.GFP-spoIIIAH-cm, spoIID298, spoIIM-mls, ΔspoIIP::tet*	This work
DB558	*amyE::$P_{spoIIIA}$.GFP-spoIIIAH-cm, spoIIB::erm*	This work
DB631	*spoIIIAG::pMutinFLAG-erm, amyE::$P_{spoIIIA}$.GFP-spoIIIAH-cm, ΔspoIIQ::spec*	This work
DB632	*spoIIIAG::pMutinFLAG-erm, amyE::$P_{spoIIIA}$.GFP-spoIIIAH-cm, ΔspoIIP::tet*	This work
KP845	*ΔspoIIQ::spec, amyE::P_{spoIIQ}.GFP-spoIIQ-cm (same As AR126)*	Lab collection

Table 1 con't

XJ459	*spoIIIAGH-kan*	Lab collection
XJ461	*ΔspoIIQ::spec, amyE:: P_{spoIIQ}.GFP-spoIIQ-cm, spoIIIAGH-kan*	Lab collection
JFG510	*ΔspoIIQ::spec; amyE:: P_{spoIIQ}. GFP-spoIIQ-cm; spoIID298; thrC::P_{spoIID}-spoIID^{E88A}-kan*	This work
JFG513	*ΔspoIIQ::spec; amyE:: P_{spoIIQ}. GFP-spoIIQ-cm; spoIID298; thrC::P_{spoIID}-spoIID^{D210A}-kan*	This work
JFG514	*ΔspoIIQ::spec; amyE:: P_{spoIIQ}. GFP-spoIIQ-cm; spoIID298; thrC::P_{spoIID}-spoIID-kan*	This work
JFG520	*ΔspoIIQ::spec; amyE:: P_{spoIIQ}. GFP-spoIIQ-cm; spoIID298; thrC::P_{spoIID}-spoIID^{D210A}-kan; spoIIIAG::pMutinFLAG-erm*	This work
JFG522	*ΔspoIIQ::spec; amyE:: P_{spoIIQ}. GFP-spoIIQ-cm; spoIID298; thrC::P_{spoIID}-spoIID-kan; spoIIIAG::pMutinFLAG-erm*	This work
JFG524	*ΔspoIIQ::spec; amyE:: P_{spoIIQ}. GFP-spoIIQ-cm; spoIID298; thrC::P_{spoIID}-spoIID^{E88A}-kan; spoIIIAG::pMutinFLAG-erm*	This work
JFG526	*ΔspoIIQ::spec; amyE:: P_{spoIIQ}. GFP-spoIIQ-cm; spoIID298; spoIIIAG::pMutinFLAG-erm*	This work
pDB102	spoIIIAG::pMutinFLAG-erm (spoIIIAH-)	This work
pDB142	$P_{spoIIIAH}$.GFP-SpoIIIAH-Cm	This work
pJFG77	thrC::P_{spoIID}-spoIID-kan	This work
pJFG78	thrC::P_{spoIID}-spoIID^{D210A}-kan	This work
pJFG79	thrC::P_{spoIID}-spoIID^{E88A}-kan	This work

Figures

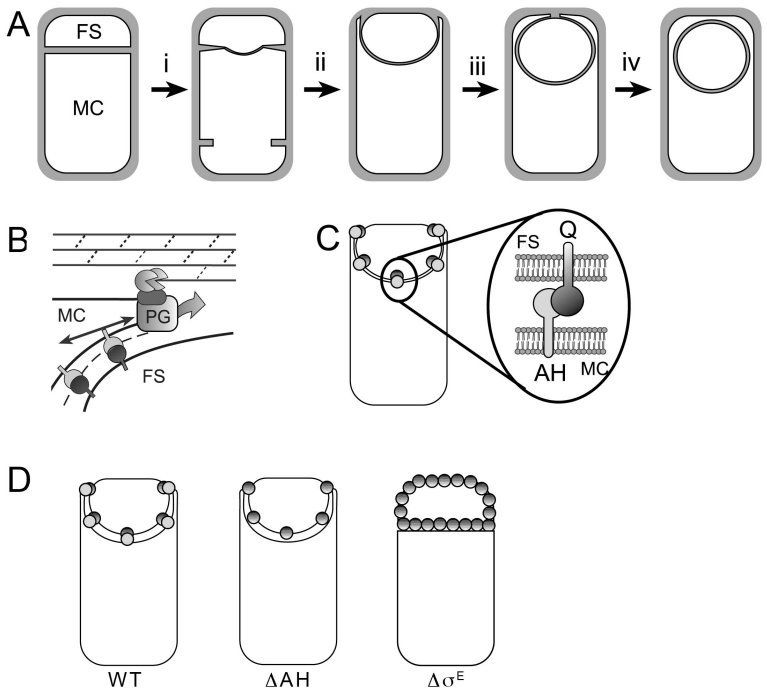

Figure 1. The process of engulfment during *Bacillus subtilis* sporulation

(A) The smaller forespore (FS) and larger mother cell (MC) initially lie side by side. Engulfment commences with septal thinning (i), during which septal peptidoglycan (light gray) is degraded. The mother cell membrane then migrates around the forespore (steps ii-iii), until it meets and fuses to release the forespore into the mother cell cytoplasm (step iv). (B) Engulfment in intact cells requires three mother cell membrane proteins, SpoIID (pacman), SpoIIM (oval), and SpoIIP (pacman) that localize to the septum and leading edge of the engulfing membrane. SpoIID and SpoIIP degrade peptidoglycan, suggesting that engulfment might be mediated by the processive degradation of the peptidoglycan adjacent to the forespore membrane, which could move the mother cell membrane around the forespore. The SpoIIQ (dark gray) and SpoIIIAH (light gray) ratchet provides a backup mechanism for membrane migration (Broder & Pogliano, 2006). Membrane movement facilitated by peptidoglycan synthesis is indicated by the PG box and arrow, this machinery becomes required if SpoIIQ is deleted (Chapter 2/ (Meyer et al., 2010)). Figure adapted from (Chapter 2/(Meyer et al., 2010)). (C) The zipper-like interaction between the forespore membrane protein SpoIIQ (labeled Q, gradient) and the mother cell membrane protein SpoIIIAH (labeled AH, grey) localizes SpoIIIAH (Blaylock et al., 2004, Doan et al., 2005), which recruits additional mother cell proteins (Doan et al., 2005, Blaylock et al., 2004). (D) Localization of SpoIIQ in wt, a *spoIIIAH* deletion, and σ^E deletion.

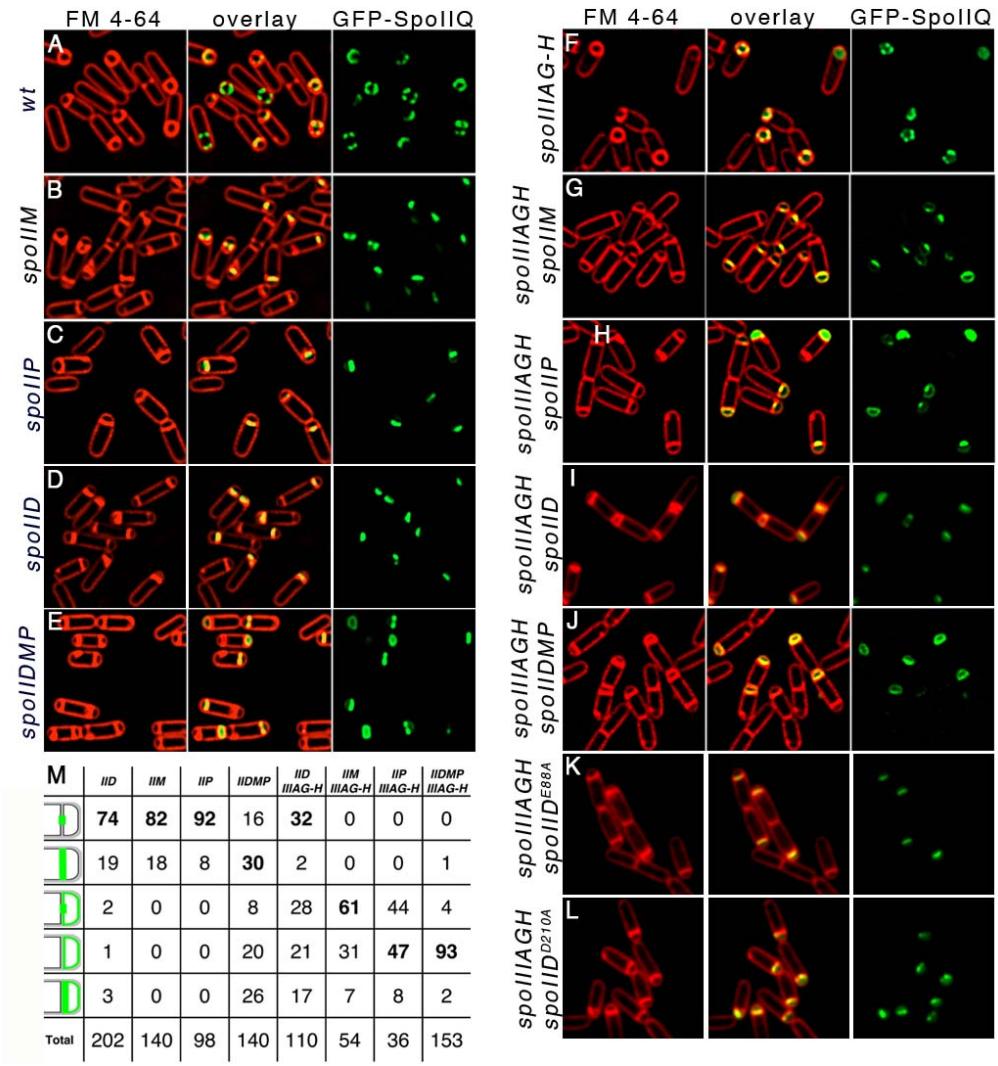

M	*IID*	*IIM*	*IIP*	*IIDMP*	*IID IIIAG-H*	*IIM IIIAG-H*	*IIP IIIAG-H*	*IIDMP IIIAG-H*
	74	**82**	**92**	16	**32**	0	0	0
	19	18	8	**30**	2	0	0	1
	2	0	0	8	28	**61**	44	4
	1	0	0	20	21	31	**47**	**93**
	3	0	0	26	17	7	8	2
Total	202	140	98	140	110	54	36	153

Figure 2. Localization of GFP-SpoIIQ in different *spo* backgrounds.

Samples were taken at $t_{2.5}$ after resuspension at 37°C and stained with FM 4-64 (red, left column) to visualize membranes. GFP images (green) are on the right with overlaid images in the middle. (A) AR126 (Δ*spoIIQ, gfp-spoIIQ*) (B) AR140 (*spoIIM-mls*, Δ*spoIIQ, gfp-spoIIQ)* (C) KP848 (*spoIIP::tet*, Δ*spoIIQ, gfp-spoIIQ)* (D) DB284 (*spoIID298,* Δ*spoIIQ, gfp-spoIIQ)* (E) AR200 (*spoIID298, spoIIM-mls , spoIIP::tet*, Δ*spoIIQ, gfp-spoIIQ*), (F) XJ461 (Δ*spoIIIAG-H-kan*, Δ*spoIIQ, gfp-spoIIQ),* (G), DB150 (Δ*spoIIIAGH-kan, spoIIM-mls,* Δ*spoIIQ, gfp-spoIIQ*), (H) DB151 (Δ*spoIIIAGH-kan, spoIIP::tet,* Δ*spoIIQ, gfp-spoIIQ)* (I) JFG526 (spoIID298, Δ*spoIIIAGH-erm),* (J) DB149 (*spoIID298, spoIIM-mls , spoIIP::tet,* Δ*spoIIIAGH-kan,* Δ*spoIIQ, gfp-spoIIQ*), (K) JFG526 (*spoIID*^{E88A}, Δ*spoIIIAGH-erm),* (L) JFG520 (*spoIID*^{D210A}, Δ*spoIIIAGH-erm),* (M) Summary of GFP-SpoIIQ localization in *spo* backgrounds.

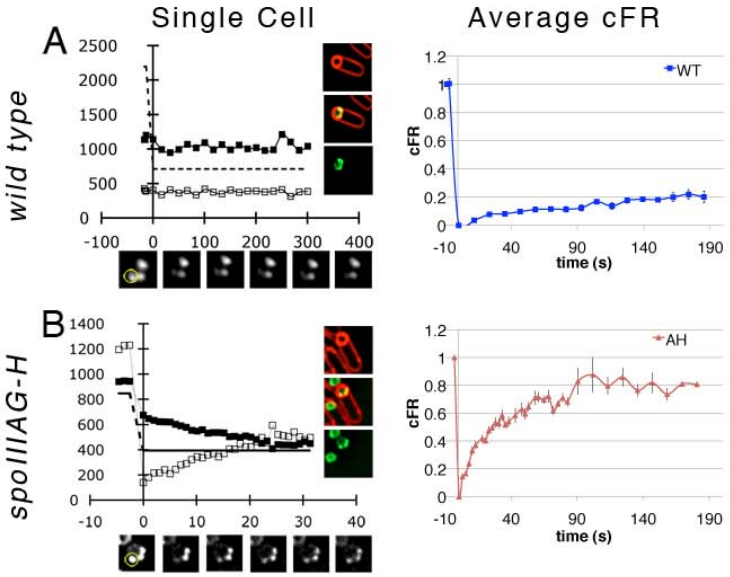

Figure 3. (Part 1) Photobleaching experiments demonstrate that immobility of GFP-SpoIIQ is primarily dependent on SpoIIIAH.

Left column: After photobleaching, images were collected, quantified and plotted (see Experimental Procedures) to show the adjusted mean pixel intensity of the bleached (black squares) and unbleached (unfilled squares) regions and the theoretical pixel intensity value following equilibration between these regions (dashed line). Images of GFP-SpoIIQ (green) and FM 4-64-stained membranes (red) of photobleached cells are shown to the right of each graph. Images below each plot show GFP-SpoIIQ during the experiment. Bleached regions are indicated by a yellow circle.

Right column: Individual photobleached cell recovery curves were generated and normalized using the equations in (Wu et al., 2006), then averaged at each timepoint. The average curve including standard error bars is shown with corrected fraction recovery (cFR) on the y-axis and time on the x-axis. A cFR of 1 represents complete recovery.

(A) KP845 (ΔspoIIQ::spc, gfp-spoIIQ), (B) XJ461 (ΔspoIIQ::spc, gfp-spoIIQ, spoIIIAGH-kan),

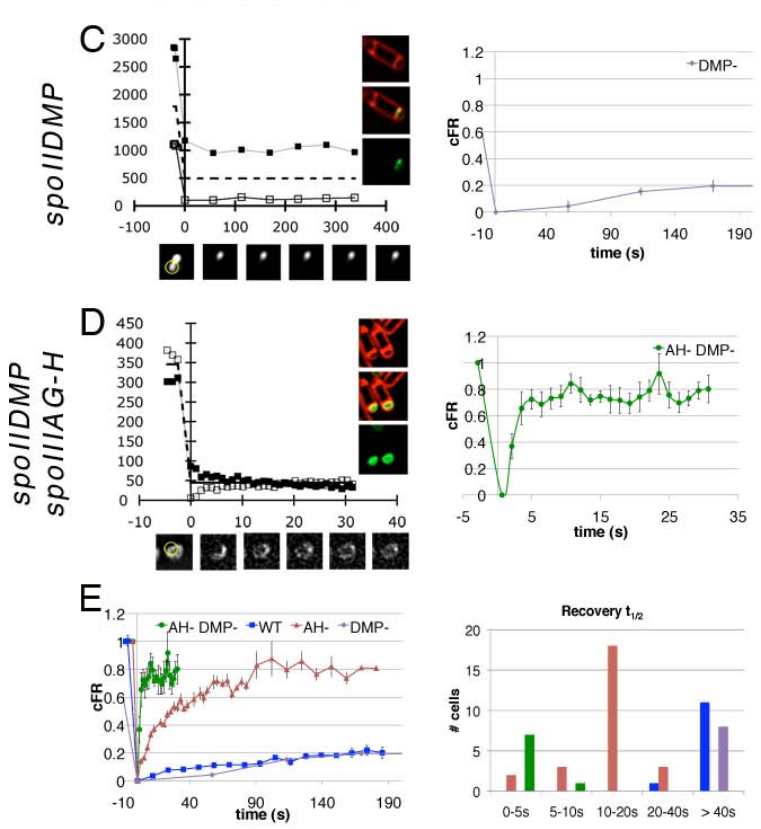

Figure 3. (con't) Photobleaching experiments demonstrate that immobility of GFP-SpoIIQ is primarily dependent on SpoIIIAH.

Columns defined in caption for Figure 3, Part 1. (C) AR200 (ΔspoIIQ::spc, gfp-spoIIQ, spoIID298, spoIIM-mls, ΔspoIIP::tet), (D) DB149 (ΔspoIIQ::spc, gfp-spoIIQ, spoIIIAGH-kan, spoIID298, spoIIM-mls, ΔspoIIP::tet), (E) Frequency with which the various phenotypes were observed in individual cells subjected to FRAP. Bars indicate time for fluorescence to reach 50% of the whole cell fluorescence value after the first post-bleach time point. This is also shown in cFR format for easy comparison.

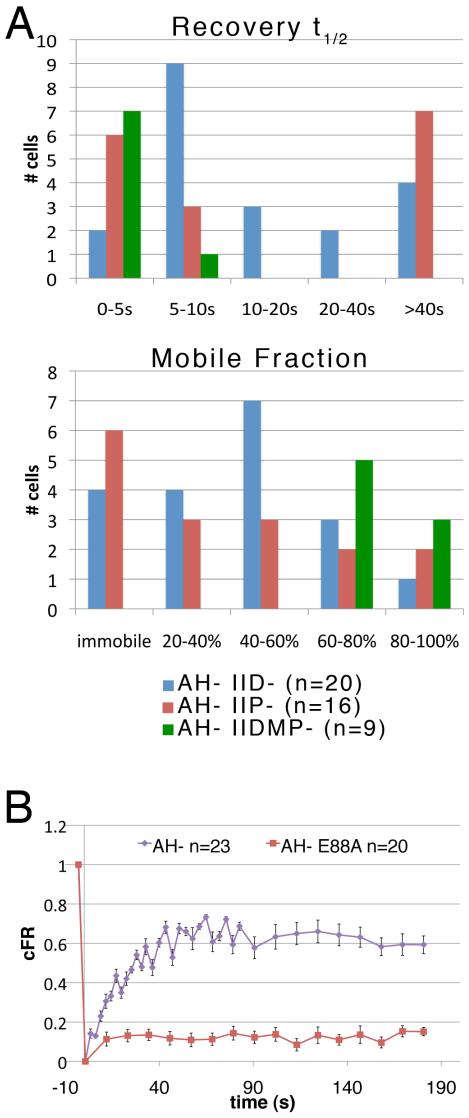

Figure 4. GFP-SpoIIQ dynamics in mutant backgrounds

Histograms representing (A, upper) the distribution of time to 50% recovery relative to each cell's maximum recovery and (lower) mobile fraction (level of recovery/free IIQ) of GFP-SpoIIQ in JFG526 (AH- IID-, blue), DB151 (AH- IIP-, red), and DB149 (AH- IIDMP-, green). DB151 shows a tightly grouped population at fast $t_{1/2}$ but a broad range of mobile fraction whereas JFG526 shows a slower $t_{1/2}$ and more tightly grouped, higher mobile fraction. (B) Average cFR of GFP-SpoIIQ in XJ461 (AH-) compared to JFG524 (AH-, IID^{E88A}), a strain with a SpoIID variant incapable of cleaving peptidoglycan.

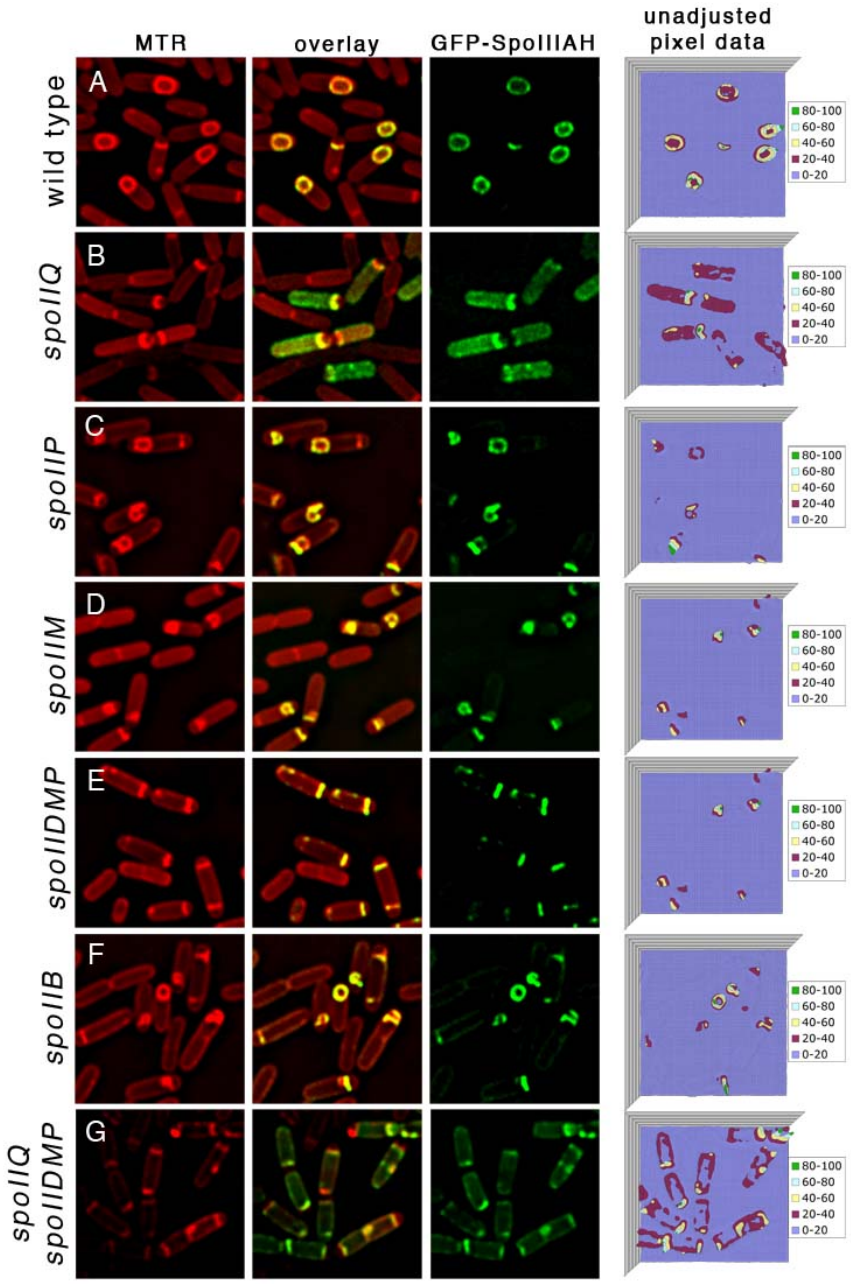

Figure 5. Localization of GFP-SpoIIIAH in different *spo* backgrounds.

Samples were taken at $t_{2.5}$ (A-F) after resuspension and stained with FM 4-64 (red, left column). GFP images (green) are on the right with overlaid images in the middle. (A) DB553 (*gfp-spoIIIAH*) (B) DB554 (*ΔspoIIQ::spc*, *gfp-spoIIIAH),* (C) DB555 (*ΔspoIIP::tet*, *gfp-spoIIIAH)* (D), DB556 (*spoIIM-mls*, *gfp-spoIIIAH*), (E) DB557 (*spoIID298, spoIIM-mls, ΔspoIIP::tet*, *gfp-spoIIIAH*), (F) DB558 (*spoIIB::erm*, *gfp-spoIIIAH)*.

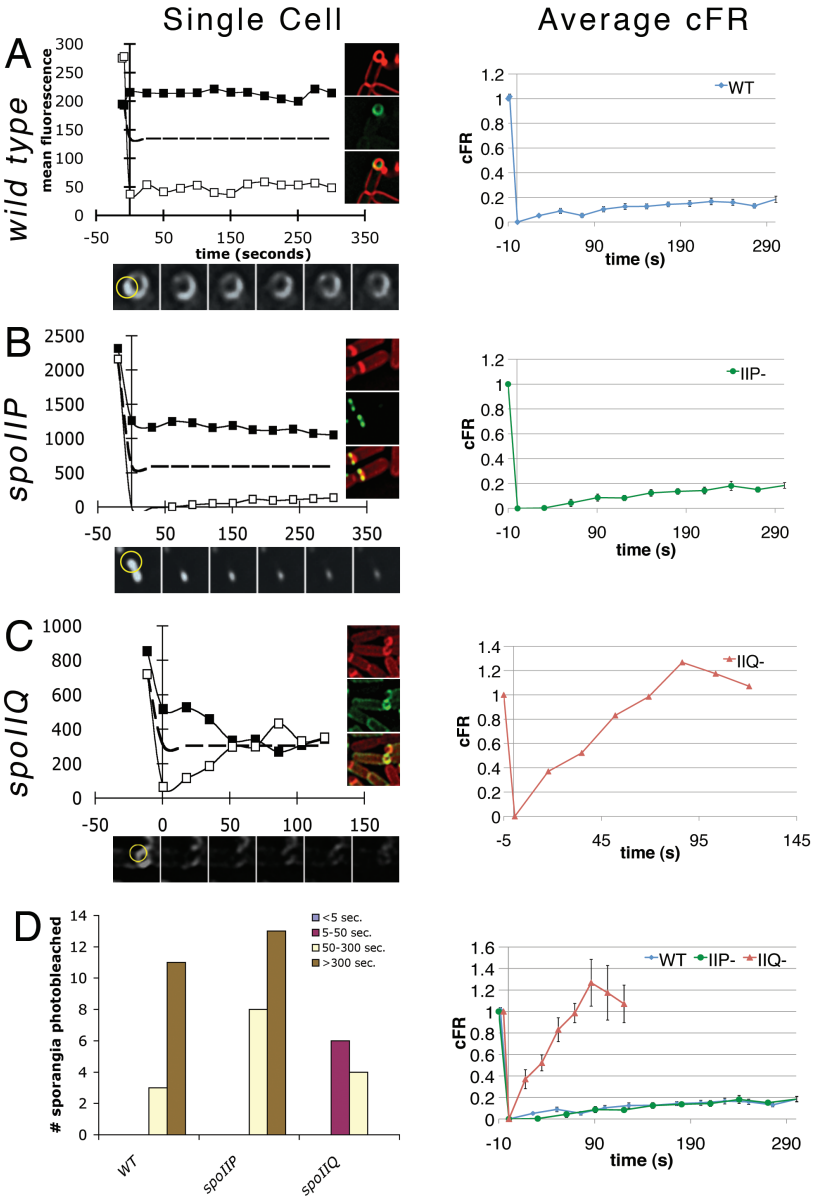

Figure 6. Immobility of GFP-SpoIIIAH is primarily dependent on SpoIIQ.

Left column shows an example of one cell of each strain with the black squares representing the unbleached region and white squares representing the bleached region, while the right column shows the averaged corrected fraction recovery. (A) DB542 (*spoIIIAH, gfp-spoIIIAH*), (B) DB632 (*ΔspoIIP, spoIIIAH, gfp-spoIIIAH)*, (C) DB631 (*ΔspoIIQ, spoIIIAH, gfp-spoIIIAH)*, (D) Frequency with which the various phenotypes were observed in individual cells subjected to FRAP and comparison cFR graph.

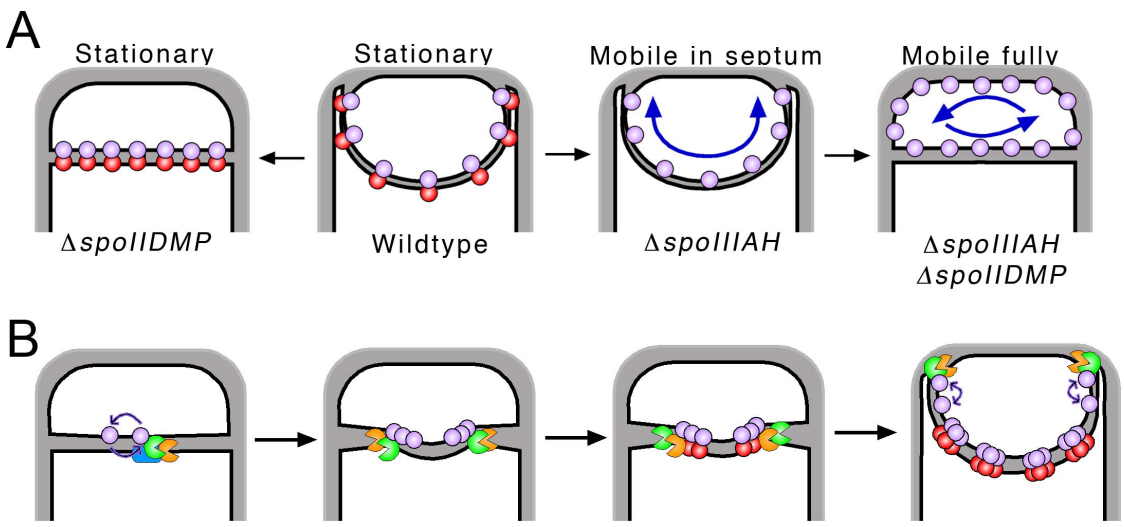

Figure 7. Model of SpoIIQ/SpoIIIAH/SpoIIDMP interactions.

Cartoon depicting proposed interactions at the sporulation septum and SpoIIQ/SpoIIIAH localization. (A) When SpoIIIAH (red) is present, SpoIIQ (purple) localizes into a higher order structure independent of SpoIIDMP. When SpoIIIAH is missing, SpoIIQ organizes into a higher order structure across the septum and is highly mobile within that framework. When SpoIIIAH and SpoIIDMP are deleted, SpoIIQ is diffusely localized and freely mobile within the forespore membranes. (B) At the start of septal thinning, SpoIIQ transiently interacts with the SpoIID (orange), SpoIIP (green) and SpoIIM (blue) complex. A local concentration of SpoIIQ is created near the engulfment proteins, which localizes SpoIIIAH. SpoIIQ and SpoIIIAH for a complex behind the leading edges dictated by the concentration gradient, which forms continuously during engulfment.

Supplementary Figures

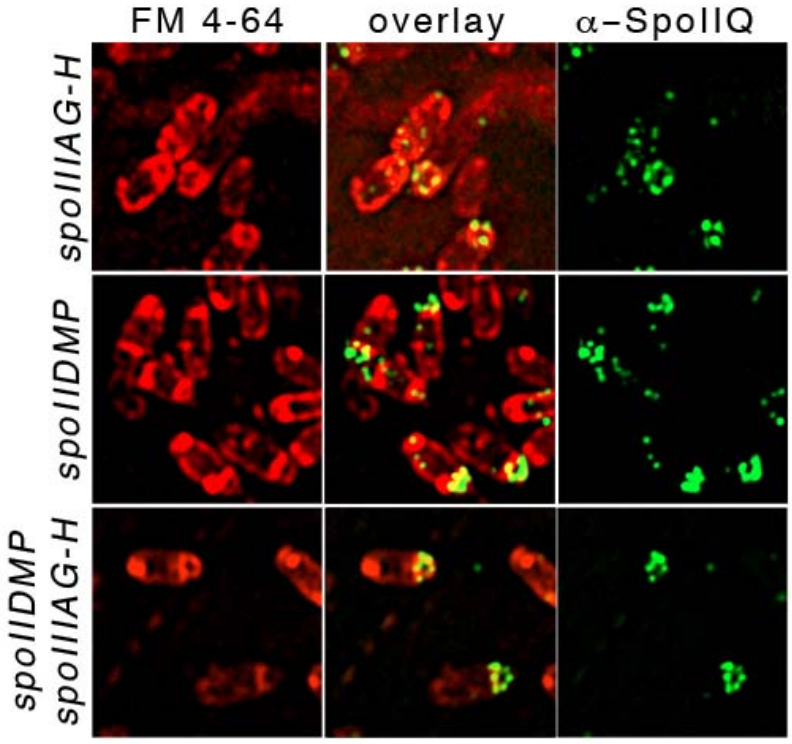

Figure S1. Immunofluorescence of SpoIIQ

To verify GFP-SpoIIQ localization in these mutant backgrounds, native SpoIIQ localization was analyzed using immunofluorescence with antibody raised to the soluble domain of SpoIIQ. As we observed for GFP-SpoIIQ, native SpoIIQ appeared punctate in the *spoIIIAG-AH* background, showed smooth septal localization in the *spoIID, spoIIM, spoIIP* triple mutant background, and exhibits more random localization in the *spoIIIAG-AH*, *spoIID, spoIIM, spoIIP* background. These experiments suggest that GFP-SpoIIQ reliably mimics untagged, native SpoIIQ. Samples were processed for immunofluorescence as described in Materials and Methods. Immunofluorescence samples were taken at $t_{2.5}$ and stained with FM 4-64 (membranes in red), DAPI (DNA in blue) and SpoIIQ (in green). (A) XJ459 (*ΔspoIIIAG-H-kan*), (B) DB188 (*spoIID298, spoIIM-mls , spoIIP::tet*), (C) DB351 (*spoIID298, spoIIM-mls , spoIIP::tet* , *ΔspoIIIAG-H-kan*). Localization patterns for GFP-SpoIIQ observed for fixed cells are the same as with live cells.

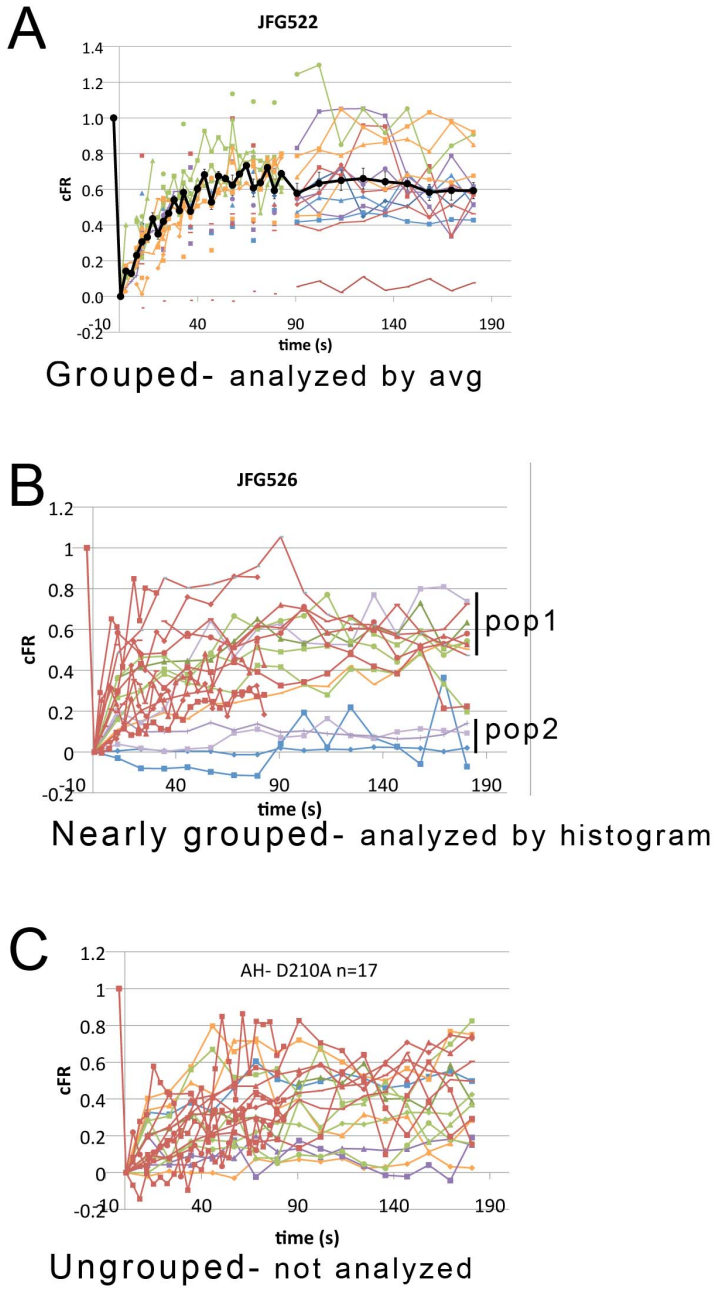

Figure S2. Examples of groupings of individual FRAP curves and how they were analyzed.

Acknowledgement

Chapter IV, in full, is currently being prepared for submission to Molecular Microbiology. Gutierrez, Jennifer; Broder, Dan; Pogliano, Kit. The dissertation author was the primary investigator and author of the manuscript. Permission of all authors has been obtained.

Chapter V

Conclusions and perspectives

Sporulation in *B. subtilis* provides an attractive model system to study the normally essential cellular processes of division and growth. Septum formation, peptidoglycan synthesis, peptidoglycan degradation, membrane movement, membrane fission, and DNA translocation all occur during sporulation, but can be perturbed and studied without killing the cell. Engulfment, one of the early steps during sporulation, provides a non-essential system to examine the mechanisms by which protein complexes and peptidoglycan biosynthesis are localized within the cell, and to elucidate the mechanisms by which peptidoglycan biosynthesis and degradation are coupled.

Although it has long been known which proteins are required for engulfment, recent advances in imaging technology have allowed visualization of these proteins, leading to a deeper understanding of their functions (Aung et al., 2007, Chastanet & Losick, 2007, Camp & Losick, 2008, Doan et al., 2005, Broder & Pogliano, 2006, Jiang et al., 2005, Blaylock et al., 2004, Rubio & Pogliano, 2004, Abanes-De Mello et al., 2002). The localization patterns of SpoIID, SpoIIM, and SpoIIP and biochemical data demonstrating peptidoglycan degradation has led to the popular proposal that these proteins

act as a motor, localizing to the leading edges of the engulfing mother cell membranes and using pepdidoglycan as a track to physically pull the membranes around the forespore (Abanes-De Mello et al., 2002). The localization of SpoIIQ and SpoIIIAH (Blaylock et al., 2004, Rubio & Pogliano, 2004) combined with cell morphology during protoplast assays demonstrated that SpoIIQ and SpoIIIAH have a strong enough interaction to hold the forespore and mother cell compartments together when peptidoglycan is removed (Broder & Pogliano, 2006). This strongly supports a model where SpoIIQ and SpoIIIAH act as a zipper to facilitate membrane migration and localize other proteins to the septum (Broder & Pogliano, 2006). Thus, the prevailing view is that engulfment is mediated by the peptidoglycan degrading activities of SpoIID and SpoIIP, in a process supported by the strong interaction between SpoIIQ and SpoIIIAH. However, a significant deficit in current models for engulfment is the lack of direct evidence in support of SpoIID/SpoIIM/SpoIIP motor activity. As SpoIIQ and SpoIIIAH are not essential for engulfment, if SpoIID, SpoIIM and SpoIIP are not part of a motor complex, other machinery must support membrane movement.

My studies of SpoIID, peptidoglycan synthesis, and the SpoIIQ/SpoIIIAH zipper helped clarify what happens at the leading edges of the migrating membranes during engulfment. First, I identified that peptidoglycan synthesis serves as a novel back-up mechanism for engulfment that is required for membrane migration in the absence of the zipper, thereby

filling one gap in current models. Second, I demonstrated that the lytic transglycoslase activity of SpoIID is required throughout engulfment and proposed a mechanism that explains how SpoIID, SpoIIM, and SpoIIP might provide force for the migrating membranes. This model also accounts for the current localization and biochemical data. Third, I have shown that both members of the SpoIIQ/SpoIIIAH zipper are primary localization determinants for each other and are responsible for immobilizing each other. I have also shown that the SpoIID/SpoIIM/SpoIIP complex interacts with SpoIIQ to localize it during engulfment. This finding also suggests coordination between the different machineries that facilitate engulfment during *B. subtilis* sporulation.

Peptidoglycan synthesis is conditionally required for engulfment

My studies demonstrate that peptidoglycan synthesis is required for membrane migration when the SpoIIQ/SpoIIIAH zipper is absent (Chapter 2), and this fills a significant gap in current models for engulfment. Specifically, if the SpoIID/SpoIIM/SpoIIP degradative machinery does not function as a motor, previous models could not provide an alternative machinery that might generate force and thereby explain why the SpoIIQ/SpoIIIAH zipper was dispensible. Now, peptidoglycan synthesis is predicted to provide a mechanism of force generation through polymerization of glycan strands immediately behind the leading edges, substituting for the ratchet created by the zipper. Thus, this finding suggests that the SpoIID, SpoIIM, and SpoIIP

proteins might not provide force for engulfment, but could instead simply remodel the peptidoglycan to accommodate membrane migration that is promoted either by Brownian motion that is captured by the SpoIIQ/SpoIIIAH zipper or by new peptidoglycan synthesis.

Based on regulation of peptidoglycan precursors in the mother cell, cortex synthesis cannot begin until engulfment is complete (Vasudevan et al., 2007), strongly suggesting that it is specifically germ cell wall synthesis that is required for engulfment. The arrangement of the peptidoglycan synthesis enzymes relative to the SpoIID/SpoIIM/SpoIIP machinery is unknown, but they likely trail behind the degradative enzymes and provide force during engulfment. Though the germ cell wall may provide a track ahead of SpoIID/SpoIIM/SpoIIP, this seems unlikely given that blocking peptidoglycan synthesis in the presence of the zipper has no effect on rate of membrane migration (Chapter 2) and if the track were eliminated, a decrease in rate of membrane migration would be expected. It will be interesting to see if the forespore-expressed peptidoglycan synthesis enzymes interact directly with the SpoIID/SpoIIM/SpoIIP degradation enzymes, as they both localize to the leading edges. If so, this would be the first example of a peptidoglycan holoenzyme containing both biosynthetic and degradative enzymes in a model organism. It may be possible to explore this question using the SpoIID^{E88A} mutant that abolished peptidoglycan degradation in co-immunoprecipitation experiments. SpoIID^{E88A} is stuck at the septum (Chapter 3) and immobilizes

other proteins, including SpoIIQ, that normally appear to have weak or transient interactions with the engulfment proteins (Chapter 4).

Beyond its requirement for membrane migration, we also showed that peptidoglycan synthesis is required for engulfment membrane fission (Chapter 3). Use of peptidoglycan synthesis to create force is a novel mechanism, but is supported by the rigidity of the molecule (Theriot, 2000). Similar effects have likewise been seen for polymerization of cytoskeletal filaments in yeast and other eukaryotes (Yao et al., 1999, Francius *et al.*, 2008). The implications for this are far-reaching and suggest that peptidoglycan synthesis could play a role in membrane fission during bacterial cell division, although it does not appear to serve this function in *E. coli* (Priyadarshini et al., 2007). Perhaps force generation by peptidoglycan polymerization requires a thicker layer of peptidoglycan, as is present in Gram positive organisms, in order to generate force.

Roles of the SpoIID, SpoIIM, SpoIIP complex during engulfment

It has long been known that SpoIID, SpoIIM, and SpoIIP are the only essential proteins for engulfment (Frandsen & Stragier, 1995, Lopez-Diaz et al., 1986, Smith et al., 1993, Sun *et al.*, 2000b, Abanes-De Mello et al., 2002, Driks & Losick, 1991), but their biochemical roles in this process have only recently been elucidated. Chastanet and Losick (Chastanet & Losick, 2007),

were able to show that the peptidoglycan hydrolysis activity of SpoIIP was required for septal thinning *in vivo* using mutants that were unable to cleave peptidoglycan. I utilized a similar strategy in my studies, first identifying SpoIID variants that did not support sporulation *in vivo* and then investigating their activity *in vitro*. SpoIID variants were found that were either unable to cleave peptidoglycan or had limited activity *in vitro*, and then phenotypes were monitored by fluorescence microscopy to show that SpoIID peptidoglycan degradative activity is required throughout engulfment *in vivo*. This was the first demonstration of SpoIID *in vivo* requirements, as previous studies had only examined *in vitro* activity (Abanes-De Mello et al., 2002).

Through examination of protein localization and biochemical assays and incorporation of recent data elucidating the peptidoglycan cleavage mechanisms of SpoIID and SpoIIP (Morlot et al.), I proposed a mechanism for the sequential degradation of peptidoglycan by SpoIID, SpoIIM, and SpoIIP (Chapter 3). This model proposes that SpoIIP binds to and cleaves peptidoglycan allowing SpoIID binding, which moves SpoIIP around the forespore. SpoIID then cleaves peptidoglycan and is released from the complex. This mechanism fits with models suggesting SpoIID/SpoIIM/SpoIIP can use peptidoglycan as a track to generate force and move the mother cell membranes up and around the forespore during engulfment (originally proposed by (Abanes-De Mello et al., 2002)). A logical next step will be to finally determine whether SpoIID/SpoIIM/SpoIIP act as a motor. Processivity is

a key requirement of the motor model and kinetic experiments using purified proteins on synthetic or homemade substrates (similar to what was done in (Morlot et al. 2010)) using varying amounts of protein and substrate would help to demonstrate whether the complex is processive, at least *in vitro*.

SpoIIQ localization versus immobilization

I showed that immobilization of SpoIIQ in the membrane, a property required for the proposed ratchet function of the SpoIIQ/SpoIIIAH zipper, is dependent primarily on SpoIIIAH and vice versa (Chapter 4). However, in the absence of SpoIIIAH, SpoIIQ maintained a wildtype localization pattern that was dependent on SpoIID, SpoIIM, and SpoIIP. This finding is significant for two reasons: first, it shows interaction between the engulfment machineries, and second, it highlights the limitations inherent when imaging fluorescent proteins. Although the GFP-SpoIIQ localization pattern is identical with and without SpoIIIAH, SpoIIQ mobility and function is vastly different. By taking a single still image, although we gain the extremely useful knowledge about where a protein is within the cell, we have no way of knowing whether it is active, inactive, mobile, immobile, or enroute to its site of action. This reinforces the requirement for using a variety of complementary techniques (biochemical, epifluorescence, FRAP) to verify conclusions.

Interactions between engulfment machineries

An important aspect of my studies is that interactions have now been demonstrated between two of the three engulfment machineries and further interactions can be predicted and investigated using models presented here. First, the SpoIID/SpoIIM/SpoIIP engulfment complex is responsible for the helical pattern and foci that are displayed by SpoIIQ-GFP (Chapter 4). As SpoIIQ and SpoIIIAH have been hypothesized to function as large complex (Camp & Losick, 2009, Meisner et al., 2008), this interaction could be important in facilitating localization to areas where peptidoglycan has been recently degraded and prior to synthesis of the germ cell layer. It is also possible that SpoIID, SpoIIM, and SpoIIP interact with peptidoglycan synthesis enzymes to direct new insertion and that the newly made peptidoglycan localizes SpoIIQ. One way to distinguish the two is to localize GFP-SpoIIQ in the presence of antibiotics that block peptidoglycan synthesis: if localization is normal, then it is likely that SpoIIQ localization is not dependent on peptidoglycan synthesis, only on SpoIID/SpoIIM/SpoIIP. This could be further investigated using FRAP and examining SpoIIQ mobility in a *spoIIIAH* mutant with peptidoglycan synthesis inhibitors, if there is an interaction between SpoIID/SpoIIM/SpoIIP and the peptidoglycan synthesis machinery or between SpoIIQ and peptidoglycan synthesis machinery, the rate of SpoIIQ recovery should increase. Coupled with localization data, this should elucidate the specific interactions occurring during engulfment.

Appendix I

Role of SpoIIB during engulfment

Introduction

Engulfment in *B. subtilis* is known to require only three proteins: SpoIID, SpoIIM, and SpoIIP (Frandsen & Stragier, 1995, Lopez-Diaz et al., 1986, Smith et al., 1993). It was recently shown that the localization of these proteins depends primarily on the SpoIIB septal landmark protein and secondarily on SpoIVFA (Aung et al., 2007), which relies on the SpoIIQ/SpoIIIAH zipper ((Doan et al., 2005), Chapter 4). SpoIIB itself has a similar localization pattern to the engulfment proteins, initially localizing at the septum center, relocalizing to the edges of the septal disk and following the migrating membranes up and around the forespore (Aung et al., 2007). SpoIIB is not essential and *spoIIB* mutant strains show an early bleb phenotype that is eventually overcome, presumably due to the late localization of SpoIID and SpoIIP as SpoIVFA is produced later than SpoIIB.

SpoIIB is a 37kD, single-transmembrane protein with a coiled-coil domain both inside and outside the cell. It is expressed under the SpoOA promoter (Margolis *et al.*, 1993) and therefore is present before septation begins during sporulation. The extracytoplasmic coiled-coil is implicated in recruitment of SpoIIM (Shum, unpublished results), but is not required for SpoIIB localization to the septum, suggesting that either the cytoplasmic domain or putative cell wall binding domain of SpoIIB is responsible for its initial localization.

How SpoIIB arrives at the septum is an important question for understanding engulfment efficiency as it directly affects SpoIIDMP localization. SpoIIB is known to localize to the septum in an FtsZ dependent manner, since it gives no signal at potential division sites, as determined by DAPI staining of the chromosome, if FtsZ is depleted (Aung et al, 2007). However, it remains unclear what division protein specifically recruits SpoIIB or even if protein-protein interactions mediate this step. An alternate and interesting possibility is that the septal peptidoglycan itself is being used as a signal similar to divisome assembly in *Streptococcus pneumoniae* (Morlot et al, 2004). Because the the cell wall is stationary, it is possible that it is modified in some way by a sporulation protein or a division protein so that SpoIIB can recognize it. In support of this, SpoIIB contains a putative cell wall binding domain similar to the autolysin CwlC (Errington et al, 2003). Analogously, SpoIIB has not been seen to directly interact with SpoIIDMP, leading to the hypothesis that SpoIIB localizes SpoIIDMP by further modifying the peptidoglycan so that it is recognized by the hydrolase complex.

Another intriguing aspect of SpoIIB function in engulfment is the characteristic cleavage pattern observed on western blots (Abanes-De Mello et al., 2002). Perhaps the SpoIIB cleavage is important during engulfment due to the timing: it is not seen until timepoints corresponding to the initiation of engulfment (2 hours at 37°) even though SpoIIB is transcribed and localized to the center of the polar septum before this event. This is also the approximate

time at which SpoIIB-mCherry, a fluorescent fusion protein (Shaner *et al.*, 2004), changes its localization pattern from the center of the sporulation septum to the leading edges (Aung et al., 2007).

Results

SpoIIB-mCherry localization in late-divisome mutants

The divisome in *B. subtilis* is composed of FtsZ, a group of early division proteins that arrive at the septum shortly after FtsZ, and a group of four late division proteins that all interact with each other and are largely co-dependent for localization (reviewed in (Errington et al., 2003)). The late division proteins, PBP2b, FtsL, DivIC and DivIB, are all essential except DivIB, which is only required at high temperatures. To investigate which late-division protein might interact with SpoIIB and recruit it to the septum, I obtained a series of genetic constructs with specific domains of each late division protein swapped out for unrelated *E. coli* protein domains ((Thompson *et al.*, 2006, Bramkamp *et al.*, 2006)). These constructs were created in such a way as to determine which domains of the late-division proteins were important for vegetative growth and are under inducible promoters.

First, I examined SpoIIB-mCherry, a red fluorescent protein fusion (Shaner et al., 2004), in the presence of DivIB and DivIC domain swaps that contained only the extracytoplasmic portion of each protein fused with the cytoplasmic and transmembrane domain from an unrelated *E. coli* protein, TolR. In both the control and domain swap strains, SpoIIB-mCherry localized to the septum in wildtype fashion (Fig 1A-D), suggesting that these proteins do not facilitate SpoIIB localization. I next examined SpoIIB-mCherry in a strain containing an FtsL chimera at amyE that has an unrelated cytoplasmic domain

but still retained its own transmembrane and extracytoplasmic domains. Again, SpoIIB-mCherry localized properly in this background (Fig 1E-F). I was unable to test SpoIIB-mCherry in a PBP2b deletion as all parts of that protein are essential for growth of the cell. However, based on process of elimination, PBP2b seems a likely candidate to interact with SpoIIB. It should be noted that these experiments do not completely rule out DivIB, DivIC, and FtsL as SpoIIB interacting partners, as the constructs tested here cannot provide useful information if SpoIIB localization is facilitated by its putative cell wall domain, which is extracytoplasmic.

SpoIIB bacterial two-hybrid assays

Because the division proteins are essential and localization experiments were inconclusive, I used bacterial two-hybrid assays to further probe SpoIIB localization determinants (Karimova *et al.*, 1998). SpoIIB was cloned into both bait and prey vectors for screening against a library of all the division proteins. This was part of a collaborative effort with the Jeff Errington lab, that created and curates the library. First, the C and N-terminal domains of SpoIIB were cloned separately into each vector and later the full-length SpoIIB protein was cloned. When screened against each other, the SpoIIB constructs showed no B-galactosidase activity (Fig 2A), suggesting that they did not self interact. When screened against the division protein library, there were only two positive hits. These hits were not replicated in the corresponding bait/prey switched vectors and may be non-specific. However, the only hits were with

PBP2b, one with the full-length SpoIIB construct and one with the C-terminal, extracytoplasmic domain of SpoIIB (Fig 2B and data not shown). Though considerably weak, this evidence supports the hypothesis that PBP2b localizes SpoIIB to the septum.

Identification of the SpoIIB cleavage site

Western blots have shown that SpoIIB is cleaved following localization to the sporulation septum. In order to investigate this cleavage event, it was necessary to identify the proteolysis site. I therefore immunoprecipitated SpoIIB-FLAG from samples collected 3.5 hours after the initiation of sporulation, a timepoint after the cleavage event (Fig 3). The purified eluent was transferred to a PVDF membrane and stained with Ponceau to reversibly visualize the protein. The major band corresponded to cleaved SpoIIB-FLAG based on size (approx 32 kDa) and was sent for N-terminal sequencing which identified the cut site as between A58 and A59, in close agreement with earlier estimates of its location based on the apparent size of the proteolytic products on SDS PAGE. This cleavage event should release a soluble, 58 amino acid, N-terminal product from the 275 amino acid, transmembrane-containing, C-terminal region of SpoIIB.

The specific protease that recognizes and cleaves SpoIIB at A58 is also unknown and examination of the sequence adjacent to the cut site revealed no clues. To determine if proteolysis is regulated by sporulation, Western blot analysis of SpoIIB was performed on strains lacking either σ^F, σ^E, SpoIVFA,

SpoIVB, SpoIID, or SpoIIP and revealed that SpoIIB cleavage is under the control of the early mother cell transcription factor, σ^E, which becomes active immediately after polar septation. However, cleavage was not directly mediated by SpoIVFA, SpoIVB, SpoIID, or SpoIIP themselves, as cleavage of SpoIIB did occur in these mutant backgrounds (Fig 4B-C).

To further investigate the cleavage event, I constructed a truncated version of SpoIIB on a plasmid that is missing amino acids 5-58, which simulates the cleaved protein. This construct contains 600 bp of upstream DNA to include the promoter and any other regulatory elements, and was inserted in the dispensable *amyE* locus in *B. subtilis* to examine its effects on engulfment. I also created and inserted the corresponding full-length SpoIIB cassette. To assay the ability of these mutants to support sporulation, they were moved into a strain that lacked *spoIIB* at its native site and was missing *spoIVFA*, the secondary localization pathway for SpoIIDMP (Aung 2007). I performed heat kills on these mutants and found that neither the full-length or truncated construct supported sporulation (Fig 5), suggesting that either important regulatory elements for SpoIIB are more than 600 bp upstream of the start, or that the mRNA was unstable because enough downstream sequence was not included during the construction.

SpoIIP localization requires the extracytoplasmic domain of DivIB

Interestingly, GFP-SpoIIP localized normally in a strain with a DivIB domain swap, but was diffuse throughout the mother cell membranes in a

DdivIB strain (Fig 6). This was unexpected as SpoIIB-mCherry localized normally in both backgrounds and SpoIIB is the primary localization determinant of SpoIIM, which localizes SpoIIP (Chastanet, Aung). Maintentance of this localization pattern at later timepoints (up to t4) suggests that SpoIVFA, the backup mechanism for SpoIIDMP localization (Aung et al., 2007), also is not localized at the septum.

Conclusions

Attempts made here to determine how SpoIIB recognizes the septum were unsuccessful. However, I was able to demonstrate that SpoIIB localization to the sporulation septum is not dependent on the intracellular domains of the late division proteins DivIB, DivIC, and FtsL, nor the transmembrane domains of DivIB and DivIC (Fig 1). As SpoIIB localization is dependent on the late division proteins (Shum), if the intracellular domain of SpoIIB is responsible for its localization, these results suggest that PBP2b interacts with SpoIIB. Consistent with this, bacterial two-hybrid assays showed a weak interaction between some SpoIIB constructs and PBP2b (Fig 2).

As well, I showed that the extracytoplasmic domain of DivIB is required for SpoIIP localization but not SpoIIB localization (Fig 6). This is unexpected as SpoIIP localizes in a cascade downstream from SpoIIB (Aung et al. 2007) and suggests that simply the presence of SpoIIB is not what localizes later proteins, but that SpoIIB either functions in some way at the septum, possibly acting on the peptidoglycan, or is modified after arriving at the septum. Whatever occurs after SpoIIB localizes seems to require the extracytoplasmic domain of DivIB.

The cleavage site of SpoIIB was also identified and corresponds to the alanine at position 58. This cleavage would completely remove the cytoplasmic coiled-coil domain of SpoIIB suggesting that an interaction

between SpoIIB and another protein is terminated, as coiled-coils are known to mediate protein-protein interactions. This could allow for altered SpoIIB localization or could prime SpoIIB for an interaction with SpoIIDMP by causing a conformational change or simply creating more space at the membrane. However, other possibilities for the role of the cleavage event exist. Proteolysis is known to play a role in other aspects of sporulation, namely σ^K activation, where cleavage of SpoIVFA in the mother cell membrane by SpoIVB causes a destabilization of the SpoIVFB inhibition complex, allowing the SpoIVFB protease to cleave pro-σ^K, thereby activating σ^K in the mother cell (reviewed in (Errington, 2003)). This mechanism provides an example within sporulation that cleavage can both end a protein function (SpoIVFA) or initiate a protein function (σ^K), suggesting many interesting possibilities for the role of SpoIIB cleavage in engulfment initiation.

Materials and Methods

Bacterial strains, genetic manipulations and growth conditions.

Bacillus subtilis strains used here are derivatives of the wild type strain PY79 (Youngman et al., 1984) and are shown in Table 1. Mutations and plasmids were introduced into PY79 by transformation (Dubnau & Davidoff-Abelson, 1971). *B. subtilis* strains were grown and sporulated at 30°C unless otherwise indicated. Sporulation was induced by the CH resuspension method (Sterlini & Mandelstam, 1969) for all cell biological experiments. Heat-resistant spore assays were performed on cultures grown and sporulated in DSM broth (Schaeffer *et al.*, 1965) for 24 hrs at 37°C. Cultures were then heated at 80°C for 20 minutes, serially diluted and plated on LB.

Construction of *amyE::spoIIB* and *amyE::spoIIBtrunc* vectors.

spoIIB plus 600 bp upstream DNA was PCR amplified from PY79 chromosomal DNA using primers JGP39 and JGP40 (Table 2), digested with EcoRV and inserted in the pSMART vector from Lucigen to create pJFG12. This plasmid was mutagenized using a modified QuickChange protocol ((Chiba *et al.*, 2007), Chapter 3) and primers JGP53 and JGP54 to delete DNA corresponding to amino acids 5-58 of SpoIIB and create pJFG27. JGP56 and JGP57 (containing engineered BglII sites) were then used to amplify full-length spoIIB off pJFG12 and truncated spoIIB off pJFG27. PCR products were cleaned and inserted in the pCR2.1 TOPO vector (Invitrogen) to create pJFG38 and pJFG30 respectively. pJFG38 and pJFG30 were digested with

BglII and inserted into the amyE integrating vector pDG1730 (Guerout-Fleury et al., 1996) digested with BamHI to create pJFG39 and pJFG40.

Construction of bacterial two-hybrid vectors.

Either the N-terminal region, C-terminal region or full-length SpoIIB was amplified off of PY70 chromosomal DNA and inserted in the vectors associated with the BACTH kit (Karimova et al., 1998), all digested with XbaI and KpnI. All full-length clones were generated using primers JGP7 and JGP23. N-terminal clones were generated using primers JGP7 and JGP22 for insertion into all vectors. C-terminal clones were generated using primers JGP6 and JGP23 for insertion into pUT18 and pKT25N and with primers JGP6 and JGP8 for insertion into pKT25 and pUT18C.

Co-Immunoprecipitation of SpoIIB-FLAG.

Co-immunoprecipitation was performed as described in (Blaylock et al., 2004). Briefly, 1L cultures of PY79 and DB157 were grown to t3.5 and spun down. The pellet was washed once with 40mL SMM buffer and respun. The pellet was washed with 10mL SMM and lysozyme added to a final concentration of 1mg/mL. The solution was incubated at 37°C for 15min, pelleted and stored at -80°C overnight. The pellet was resuspended in 12 mL SolnB (20mM HEPES, 150mM NaCl, 1mM EDTA, pH 7.5) with leupeptin (1uL/mL), pepstatin(1uL/mL) and PMSF (5ul/mL) plus 200uL 10%DDM and iced 30 min. The lysate was spun at 40,000rpm, 30min, 4°C. The

supernatant was saved and mixed with M2mouse anti-FLAG beads (Sigma) overnight at 4°C. The slurry was centrifuged gently to separate the unbound fraction, washed with Soln B, then eluted by resuspension of the beads in 2X SDS loading buffer and incubated 42°C for 15 min.

Microscopy and image analysis.

To visualize GFP, samples from sporulating cultures were taken at the indicated times, stained with a final concentration of 5 mg/mL FM 4-64, 2 mg/mL DAPI and applied to poly-L-lysine coated coverslips (Sharp & Pogliano, 1999). To image mCherry, cells were stained with a final concentration of 4 mg/mL Mitotracker Green (Sharp & Pogliano, 1999). Images were collected using an Applied Precision Spectris optical sectioning microscope equipped with a Photometrix CoolsnapHQ CCD camera. Images were deconvolved using SoftWoRx software (Applied Precision Inc.).

Western blotting.

Samples for Western blots were prepared as described in (Chiba et al., 2007) and Chapter 3. Briefly, 1.0 mL of culture was collected at the indicated timepoints and precipitated by addition of 110 μL 50% tri-chloro-acetic acid (TCA) and frozen overnight. Samples were spun on high, washed with Tris buffer (pH 8) and resuspended in 54 mL Tris Sucrose Buffer (33 mM Tris, pH 8, 40% Sucrose, 1 mM EDTA, 300 μg/mL PMSF). Lysozyme was added to a final concentration of 1 μg/mL and samples were incubated at 37°C, 10 minutes. An equal volume of 2X SDS loading buffer was added to each

sample and samples were heated to 42°C. Samples were applied to a 12% SDS-PAGE gel, transferred to a PVDF membrane and probed with antibodies to SpoIIB at a 1:1000 dilution (R320, bleed3) or antibodies to FLAG (Sigma) at a 1:5000 dilution. Secondary, anti-rabbit antibody conjugated to HRP (GE Healthcare) was added at 1:3000 and developed using the ECL kit (GE Healthcare).

Tables

Table 1. Strains used in this study		
strain	genotype	source
PY79	wt	ref
JFG30	*spoIIB-mCherry-kan; murB::pVK3::divIBcat(Pspac-BBB)*	this work
JFG31	*spoIIB-mCherry-kan; murB::pVK12::divIBcat(Pspac-RRB)*	this work
JFG32	*spoIIB-mCherry-kan; amyE::pVK13::cat(Pspac-RRC); ΔdivIC-spc*	this work
JFG33	*spoIIB-mCherry-kan; amyE::pVK14::cat(Pspac-CCC); ΔdivIC-spc*	this work
JFG34	*amyE::pVK14::cat(Pspac-CCC); ΔdivIC-spc; spoIIB-FLAG-erm*	this work
JFG35	*amyE::pVK13::cat(Pspac-RRC); ΔdivIC-spc; spoIIB-FLAG-erm*	this work
JFG40	*murB::pVK3::divIBcat(Pspac-BBB); spoIIB-FLAG-erm*	this work
JFG41	*murB::pVK12::divIBcat(Pspac-RRB); spoIIB-FLAG-erm*	this work
JFG42	*spoIIB-FLAG-erm; spoIIP::tet*	this work
JFG43	*spoIIB-FLAG-erm; spoIID298*	this work
JFG93	*spoIIB-his::pJSA1his-cm; spoIIGB::erm*	this work
JFG49	*divIB::spc; spoIIP::tet; amyE::P_{IID}-gfp-spoIIP-cat*	this work
JFG60	*murB::pVK3::divIBcat(Pspac-BBB); spoIIP::tet; amyE::P_{IID}-gfp-spoIIP-cat*	this work
JFG62	*murB::pVK12::divIBcat(Pspac-RRB); spoIIP::tet; amyE::P_{IID}-gfp-spoIIP-cat*	this work
JFG94	*spoIIB-his::pJSA1his-cm; spoIIAC::erm*	this work
JFG95	*ftsL::pSG441-kan-Pspac-pbp; sacA::PspoIID-cre-spc; spoIIB-mCherry; amyE::cat-Pxyl-dll*	this work
JFG96	*ftsL::pSG441-kan-Pspac-pbp; sacA::PspoIID-cre-spc; spoIIB-mCherry; amyE::cat-Pxyl-FtsL*	this work
JFG123	*spoIIB::erm; ΔspoIVFAB-cat*	this work
JFG248	*amyE::spoIIB-spc*	this work
JFG251	*amyE::spoIIBtrunc-spc*	this work
JFG252	*amyE::spoIIB-spc; spoIIB::erm*	this work
JFG254	*amyE::spoIIBtrunc-spc; spoIIB::erm*	this work
JFG256	*amyE::spoIIB-spc; spoIIB::erm; ΔspoIVFAB-cat*	this work
JFG257	*amyE::spoIIB-spc; spoIIB::erm; ΔspoIVFAB-cat*	this work
JFG258	*amyE::spoIIBtrunc-spc; spoIIB::erm; ΔspoIVFAB-cat*	this work
JFG259	*amyE::spoIIBtrunc-spc; spoIIB::erm; ΔspoIVFAB-cat*	this work
JFG118	*spoIVFAB::cat; spoIIB-FLAG-erm*	this work
JFG119	*spoIVB::spc; spoIIB-FLAG-erm*	this work
DB157	*spoIIB-FLAG-erm*	this work
DB177	*spoIIPhis::pJSA1his-Cm*	this work
KP161	*spoIIGB::erm*	ref
KP176	*spoIIAC::erm*	ref
JS51	*divIB::spc; spoIIB-mCherry-kan*	this work

Table 2. Primers used in this study	
Primer name	Sequence
JGP6	GGT CTC TAG AGT CGG GGA ATA AAG AAG CG
JGP7	GGT CTC TAG AGG AGG AAG CGG AAT TGA AA
JGP8	GGT CAC GGT ACC TTA TTT TAC CGAC GGC TAA CAG
JGP22	CCG CCG GGT ACC CGT CTT TTT ACC GGT TT
JGP23	GGT CAC GGT ACC CGT TAT TTT ACG ACG GCT AAC AG
JGP39	CCC GGA TAT CTT ATT TTA CGA CGG CTA ACA GCT CCT GCT GA
JGP40	CCC GGA TAT CGT ATC CCG CAG CAG AGC TTG TGA CAG
JFG56	GGG GAG ATC TTA CCG AAG AAA GGC CCA C
JGP57	GGG GAG ATC TAT CAA GTC AAA AGC CTC C

Figures

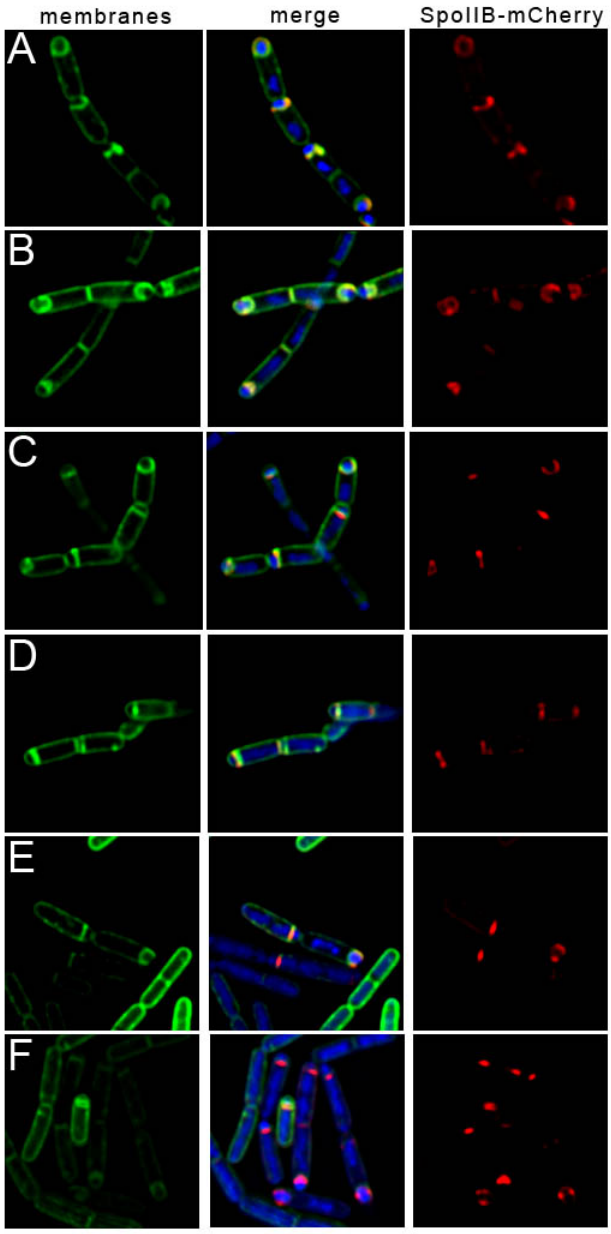

Figure 1. SpoIIB-mCherry localization in division mutant backgrounds. All images taken at T2.5 at 30°C. Membranes were stained with Mitotracker Green. SpoIIB-mCherry localizes to the division septum (and leading edges where applicable in all mutant backgrounds. (A) SpoIIB-mCherry in CCC (wild type DivIC) JFG33. (B) SpoIIB-mCherry in RRC (domain swap DivIC), JFG32. (C) SpoIIB-mCherry in BBB (wild type DivIB), JFG30. (D) SpoIIB-mCherry in RRB (domain swap DivIB), JFG31. (E) SpoIIB-mCherry in LLL (wild type FtsL), JFG96. (F) SpoIIB-mCherry in dLL (domain swap FtsL), JFG95.

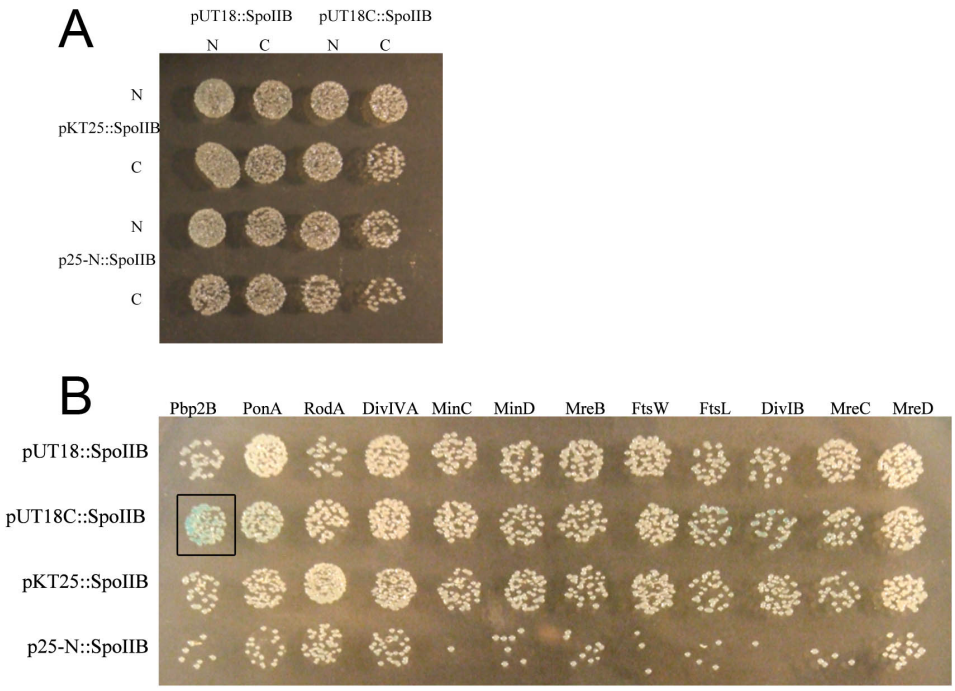

Figure 2. Bacterial two-hybrid screen results.

(A) SpoIIB C-terminal and N-terminal constructs do not show self interaction in bacterial two-hybrid assays. (B) SpoIIB full length constructs show one potential interaction with PBP2b. Spot of interest is boxed.

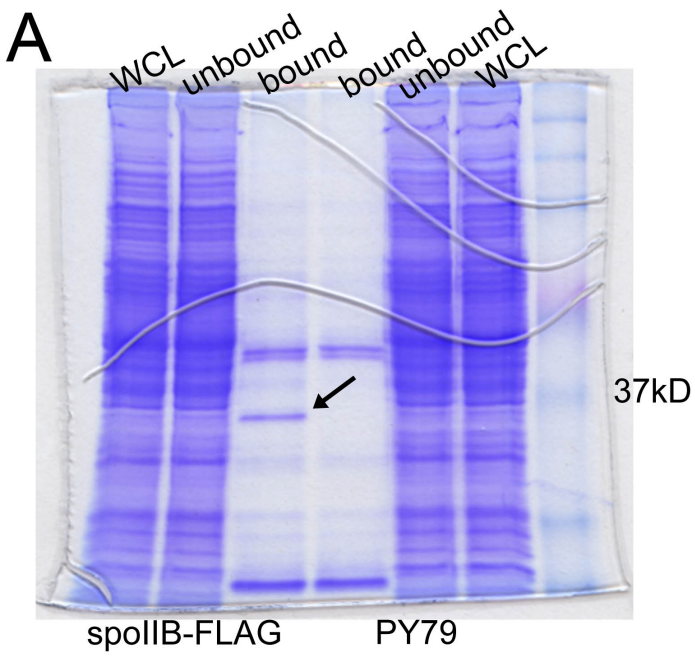

Figure 3. SDS-PAGE gel of co-immunopurified SpoIIB.

Two identical gels were run, one was transferred to a membrane, reversibly ponceau stained, and the band of interest was cut out and sent for protein sequencing at the UCSD core facility. The second gel is pictured here and stained with Coomassie blue. The band indicated with the arrow corresponds to the protein product that was sequenced.

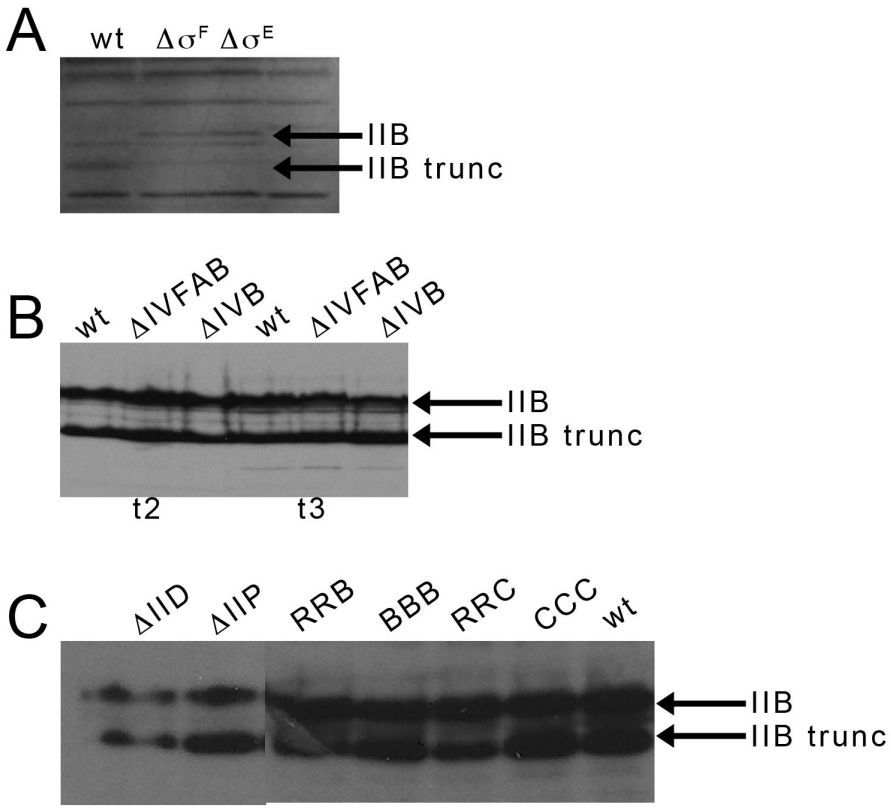

Figure 4. Western blots showing SpoIIB cleavage in mutant backgrounds.

(A) Antibodies against SpoIIB showing lack of cleavage in σ^F and σ^E mutant backgrounds. Samples from T2.5. (B) Antibodies against FLAG. All strains contain SpoIIB-FLAG and the mutation indicated above the lane. SpoIIB-FLAG is cleaved in the absence of known proteases SpoIVFB and SpoIVB. (C) Antibodies against FLAG. SpoIIB-FLAG is cleaved in the absence of peptidoglycan hydrolases SpoIID and SpoIIP and is not dependent on the cytoplasmic domain of DivIB or DivIC.

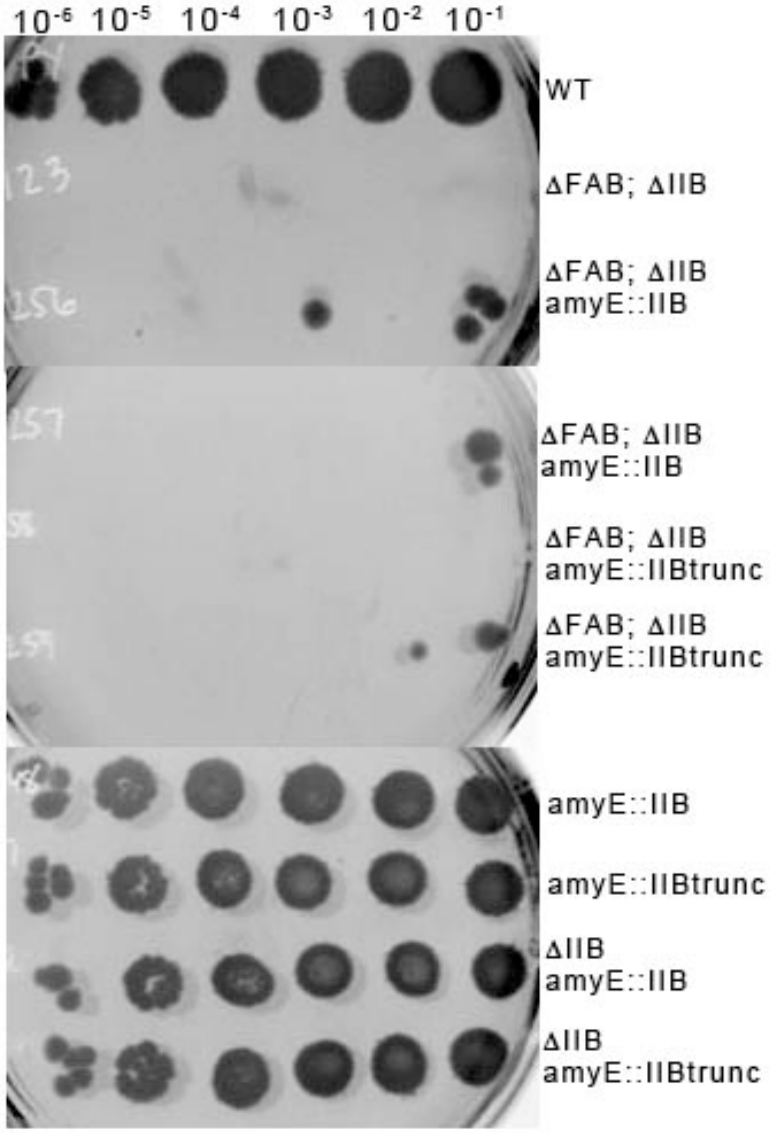

Figure 5. Spore titers of SpoIIB and SpoIIBtrunc strains.

Strains harboring either *amyE::spoIIB* or *amyE::spoIIBtrunc* were sporulated, heated to 80°C for 20 minutes, diluted and spotted on plates to assay the ability of strains of strains to produce heat-resistant spores. The dilution is indicated above, and the strain is on the right. Image contrast was inverted for easier viewing.

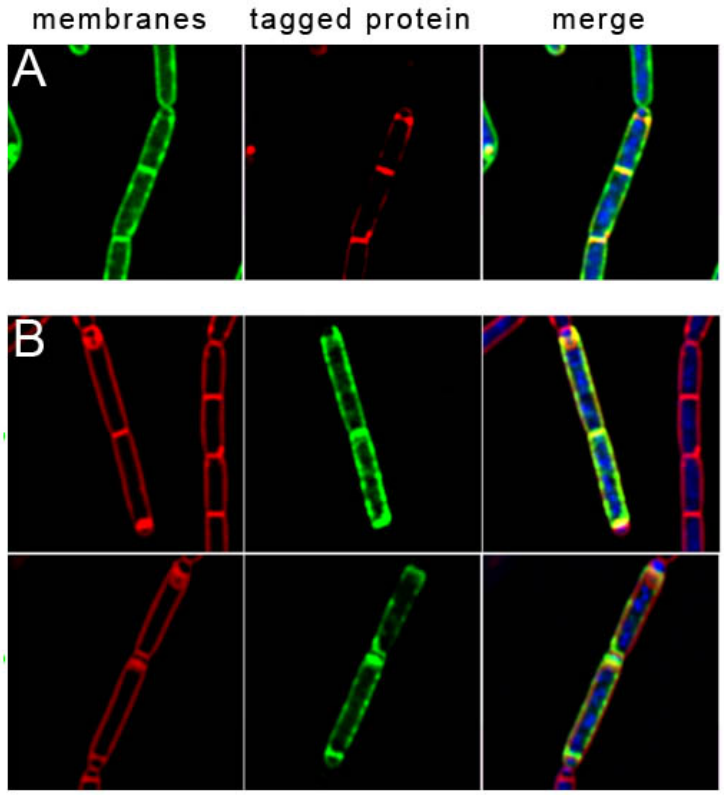

Figure 6. Localization of SpoIIB and SpoIIP in various *divIB* mutants.

(A) SpoIIB-mCherry localizes to the leading edges in a *divIB* mutant. Membranes stained with Mitotracker Green, images taken at T3. (B) GFP-SpoIIP does not localize in a *divIB* mutant, despite SpoIIB localization at T3 (upper) or T4 (lower). Membranes stained with FM4-64.

References

Abanes-De Mello, A., Y. L. Sun, S. Aung & K. Pogliano, (2002) A cytoskeleton-like role for the bacterial cell wall during engulfment of the *Bacillus subtilis* forespore. *Genes Dev* **16**: 3253-3264.

Alaedini, A. & R. A. Day, (1999) Identification of two penicillin-binding multienzyme complexes in Haemophilus influenzae. *Biochem Biophys Res Commun* **264**: 191-195.

Andre, G., S. Kulakauskas, M. P. Chapot-Chartier, B. Navet, M. Deghorain, E. Bernard, P. Hols & Y. F. Dufrene, (2010) Imaging the nanoscale organization of peptidoglycan in living Lactococcus lactis cells. *Nat Commun* **1**: 1-8.

Atrih, A., G. Bacher, G. Allmaier, M. P. Williamson & S. J. Foster, (1999) Analysis of peptidoglycan structure from vegetative cells of Bacillus subtilis 168 and role of PBP 5 in peptidoglycan maturation. *J Bacteriol* **181**: 3956-3966.

Atrih, A., P. Zollner, G. Allmaier & S. J. Foster, (1996) Structural analysis of Bacillus subtilis 168 endospore peptidoglycan and its role during differentiation. *J Bacteriol* **178**: 6173-6183.

Atrih, A., P. Zollner, G. Allmaier, M. P. Williamson & S. J. Foster, (1998) Peptidoglycan structural dynamics during germination of Bacillus subtilis 168 endospores. *J Bacteriol* **180**: 4603-4612.

Aung, S., J. Shum, A. Abanes-De Mello, D. H. Broder, J. Fredlund-Gutierrez, S. Chiba & K. Pogliano, (2007) Dual localization pathways for the engulfment proteins during *Bacillus subtilis* sporulation. *Mol Microbiol* **65**: 1534-1546.

Becker, E. C. & K. Pogliano, (2007) Cell-specific SpoIIIE assembly and DNA translocation polarity are dictated by chromosome orientation. *Mol Microbiol* **66**: 1066-1079.

Bernhardt, T. G. & P. A. de Boer, (2004) Screening for synthetic lethal mutants in Escherichia coli and identification of EnvC (YibP) as a periplasmic septal ring factor with murein hydrolase activity. *Mol Microbiol* **52**: 1255-1269.

Blackman, S. A., T. J. Smith & S. J. Foster, (1998) The role of autolysins during vegetative growth of Bacillus subtilis 168. *Microbiology* **144 (Pt 1)**: 73-82.

Blaylock, B., X. Jiang, A. Rubio, C. P. Moran, Jr. & K. Pogliano, (2004) Zipper-like interaction between proteins in adjacent daughter cells mediates protein localization. *Genes Dev* **18**: 2916-2928.

Boneca, I. G., Z. H. Huang, D. A. Gage & A. Tomasz, (2000) Characterization of Staphylococcus aureus cell wall glycan strands, evidence for a new beta-N-acetylglucosaminidase activity. *J Biol Chem* **275**: 9910-9918.

Bramkamp, M., L. Weston, R. A. Daniel & J. Errington, (2006) Regulated intramembrane proteolysis of FtsL protein and the control of cell division in Bacillus subtilis. *Mol Microbiol* **62**: 580-591.

Brandish, P. E., M. K. Burnham, J. T. Lonsdale, R. Southgate, M. Inukai & T. D. Bugg, (1996) Slow binding inhibition of phospho-N-acetylmuramyl-pentapeptide-translocase (Escherichia coli) by mureidomycin A. *J Biol Chem* **271**: 7609-7614.

Broder, D. H. & K. Pogliano, (2006) Forespore engulfment mediated by a ratchet-like mechanism. *Cell* **126**: 917-928.

Cabeen, M. T., G. Charbon, W. Vollmer, P. Born, N. Ausmees, D. B. Weibel & C. Jacobs-Wagner, (2009) Bacterial cell curvature through mechanical control of cell growth. *EMBO J* **28**: 1208-1219.

Camp, A. H. & R. Losick, (2008) A novel pathway of intercellular signalling in Bacillus subtilis involves a protein with similarity to a component of type III secretion channels. *Mol Microbiol* **69**: 402-417.

Camp, A. H. & R. Losick, (2009) A feeding tube model for activation of a cell-specific transcription factor during sporulation in Bacillus subtilis. *Genes Dev* **23**: 1014-1024.

Carballido-Lopez, R., (2006) Orchestrating bacterial cell morphogenesis. *Mol Microbiol* **60**: 815-819.

Carballido-Lopez, R. & J. Errington, (2003) The bacterial cytoskeleton: *in vivo* dynamics of the actin-like protein Mbl of *Bacillus subtilis*. *Dev Cell* **4**: 19-28.

Carballido-Lopez, R., A. Formstone, Y. Li, S. D. Ehrlich, P. Noirot & J. Errington, (2006) Actin homolog MreBH governs cell morphogenesis by localization of the cell wall hydrolase LytE. *Dev Cell* **11**: 399-409.

Chambers, H. F., (2003) Solving staphylococcal resistance to beta-lactams. *Trends Microbiol* **11**: 145-148.

Chastanet, A. & R. Losick, (2007) Engulfment during sporulation in Bacillus subtilis is governed by a multi-protein complex containing tandemly acting autolysins. *Mol Microbiol* **64**: 139-152.

Chen, L., H. Men, S. Ha, X. Y. Ye, L. Brunner, Y. Hu & S. Walker, (2002) Intrinsic lipid preferences and kinetic mechanism of Escherichia coli MurG. *Biochemistry* **41**: 6824-6833.

Chiba, S., K. Coleman & K. Pogliano, (2007) Impact of membrane fusion and proteolysis on SpoIIQ dynamics and interaction with SpoIIIAH. *J Biol Chem* **282**: 2576-2586.

Chopra, I., C. Storey, T. J. Falla & J. H. Pearce, (1998) Antibiotics, peptidoglycan synthesis and genomics: the chlamydial anomaly revisited. *Microbiology* **144 (Pt 10)**: 2673-2678.

Daniel, R. A., S. Drake, C. E. Buchanan, R. Scholle & J. Errington, (1994) The Bacillus subtilis spoVD gene encodes a mother-cell-specific penicillin-binding protein required for spore morphogenesis. *J Mol Biol* **235**: 209-220.

Daniel, R. A. & J. Errington, (2003) Control of cell morphogenesis in bacteria: two distinct ways to make a rod-shaped cell. *Cell* **113**: 767-776.

de Kruijff, B., V. van Dam & E. Breukink, (2008) Lipid II: a central component in bacterial cell wall synthesis and a target for antibiotics. *Prostaglandins Leukot Essent Fatty Acids* **79**: 117-121.

Demchick, P. & A. L. Koch, (1996) The permeability of the wall fabric of Escherichia coli and Bacillus subtilis. *J Bacteriol* **178**: 768-773.

den Blaauwen, T., M. A. de Pedro, M. Nguyen-Disteche & J. A. Ayala, (2008) Morphogenesis of rod-shaped sacculi. *FEMS Microbiol Rev* **32**: 321-344.

Denome, S. A., P. K. Elf, T. A. Henderson, D. E. Nelson & K. D. Young, (1999) Escherichia coli mutants lacking all possible combinations of eight penicillin binding proteins: viability, characteristics, and implications for peptidoglycan synthesis. *J Bacteriol* **181**: 3981-3993.

Dmitriev, B., F. Toukach & S. Ehlers, (2005) Towards a comprehensive view of the bacterial cell wall. *Trends Microbiol* **13**: 569-574.

Dmitriev, B. A., S. Ehlers & E. T. Rietschel, (1999) Layered murein revisited: a fundamentally new concept of bacterial cell wall structure, biogenesis and function. *Med Microbiol Immunol* **187**: 173-181.

Dmitriev, B. A., F. V. Toukach, K. J. Schaper, O. Holst, E. T. Rietschel & S. Ehlers, (2003) Tertiary structure of bacterial murein: the scaffold model. *J Bacteriol* **185**: 3458-3468.

Doan, T., K. A. Marquis & D. Z. Rudner, (2005) Subcellular localization of a sporulation membrane protein is achieved through a network of interactions along and across the septum. *Mol Microbiol* **55**: 1767-1781.

Dramsi, S., S. Magnet, S. Davison & M. Arthur, (2008) Covalent attachment of proteins to peptidoglycan. *FEMS Microbiol Rev* **32**: 307-320.

Driks, A. & R. Losick, (1991) Compartmentalized expression of a gene under the control of sporulation transcription factor sigma E in Bacillus subtilis. *Proc Natl Acad Sci U S A* **88**: 9934-9938.

Driks, A., S. Roels, B. Beall, C. P. Moran, Jr. & R. Losick, (1994) Subcellular localization of proteins involved in the assembly of the spore coat of Bacillus subtilis. *Genes Dev* **8**: 234-244.

Dubnau, D. & R. Davidoff-Abelson, (1971) Fate of transforming DNA following uptake by competent Bacillus subtilis. I. Formation and properties of the donor-recipient complex. *J Mol Biol* **56**: 209-221.

Eichenberger, P., P. Fawcett & R. Losick, (2001) A three-protein inhibitor of polar septation during sporulation in Bacillus subtilis. *Mol Microbiol* **42**: 1147-1162.

Eichenberger, P., S. T. Jensen, E. M. Conlon, C. van Ooij, J. Silvaggi, J. E. Gonzalez-Pastor, M. Fujita, S. Ben-Yehuda, P. Stragier, J. S. Liu & R. Losick, (2003) The sigmaE regulon and the identification of additional sporulation genes in Bacillus subtilis. *J Mol Biol* **327**: 945-972.

Errington, J., (2003) Regulation of endospore formation in Bacillus subtilis. *Nat Rev Microbiol* **1**: 117-126.

Errington, J., R. A. Daniel & D. J. Scheffers, (2003) Cytokinesis in bacteria. *Microbiol Mol Biol Rev* **67**: 52-65.

Fay, A. & J. Dworkin, (2009) Bacillus subtilis homologs of MviN (MurJ), the putative Escherichia coli lipid II flippase, are not essential for growth. *J Bacteriol* **191**: 6020-6028.

Fay, A., P. Meyer & J. Dworkin, (2009) Interactions between late acting proteins required for peptidoglycan synthesis during sporulation. *submitted*.

Fay, A., P. Meyer & J. Dworkin, (2010) Interactions between late-acting proteins required for peptidoglycan synthesis during sporulation. *J Mol Biol* **399**: 547-561.

Figge, R. M., A. V. Divakaruni & J. W. Gober, (2004) MreB, the cell shape-determining bacterial actin homologue, co-ordinates cell wall morphogenesis in Caulobacter crescentus. *Mol Microbiol* **51**: 1321-1332.

Firtel, M., G. Henderson & I. Sokolov, (2004) Nanosurgery: observation of peptidoglycan strands in Lactobacillus helveticus cell walls. *Ultramicroscopy* **101**: 105-109.

Fleming, T. C., J. Y. Shin, S. H. Lee, E. Becker, K. C. Huang, C. Bustamante & K. Pogliano, (2010) Dynamic SpoIIIE assembly mediates septal membrane fission during Bacillus subtilis sporulation. *Genes Dev* **24**: 1160-1172.

Francius, G., O. Domenech, M. P. Mingeot-Leclercq & Y. F. Dufrene, (2008) Direct observation of Staphylococcus aureus cell wall digestion by lysostaphin. *J Bacteriol* **190**: 7904-7909.

Frandsen, N. & P. Stragier, (1995) Identification and characterization of the Bacillus subtilis spoIIP locus. *J Bacteriol* **177**: 716-722.

Fukushima, T., A. Afkham, S. Kurosawa, T. Tanabe, H. Yamamoto & J. Sekiguchi, (2006) A new D,L-endopeptidase gene product, YojL (renamed CwlS), plays a role in cell separation with LytE and LytF in Bacillus subtilis. *J Bacteriol* **188**: 5541-5550.

Gan, L., S. Chen & G. J. Jensen, (2008) Molecular organization of Gram-negative peptidoglycan. *Proc Natl Acad Sci U S A* **105**: 18953-18957.

Ghosh, A. S. & K. D. Young, (2003) Sequences near the active site in chimeric penicillin binding proteins 5 and 6 affect uniform morphology of Escherichia coli. *J Bacteriol* **185**: 2178-2186.

Ghuysen, J. M. & C. Goffin, (1999) Lack of cell wall peptidoglycan versus penicillin sensitivity: new insights into the chlamydial anomaly. *Antimicrob Agents Chemother* **43**: 2339-2344.

Gilmore, M. E., D. Bandyopadhyay, A. M. Dean, S. D. Linnstaedt & D. L. Popham, (2004) Production of muramic delta-lactam in Bacillus subtilis spore peptidoglycan. *J Bacteriol* **186**: 80-89.

Glauner, B. & J. V. Holtje, (1990) Growth pattern of the murein sacculus of Escherichia coli. *J Biol Chem* **265**: 18988-18996.

Gray, M. W., D. Sankoff & R. J. Cedergren, (1984) On the evolutionary descent of organisms and organelles: a global phylogeny based on a highly conserved structural core in small subunit ribosomal RNA. *Nucleic Acids Res* **12**: 5837-5852.

Guerout-Fleury, A. M., N. Frandsen & P. Stragier, (1996) Plasmids for ectopic integration in Bacillus subtilis. *Gene* **180**: 57-61.

Gutierrez, J., R. Smith & K. Pogliano, (2010) SpoIID-mediated peptidoglycan degradation is required throughout engulfment during Bacillus subtilis sporulation. *J Bacteriol* **192**: 3174-3186.

Ha, S., D. Walker, Y. Shi & S. Walker, (2000) The 1.9 A crystal structure of Escherichia coli MurG, a membrane-associated glycosyltransferase involved in peptidoglycan biosynthesis. *Protein Sci* **9**: 1045-1052.

Hara, H., S. Narita, D. Karibian, J. T. Park, Y. Yamamoto & Y. Nishimura, (2002) Identification and characterization of the Escherichia coli envC gene encoding a periplasmic coiled-coil protein with putative peptidase activity. *FEMS Microbiol Lett* **212**: 229-236.

Hashimoto, H., (2003) Plastid division: its origins and evolution. *Int Rev Cytol* **222**: 63-98.

Hayhurst, E. J., L. Kailas, J. K. Hobbs & S. J. Foster, (2008) Cell wall peptidoglycan architecture in Bacillus subtilis. *Proc Natl Acad Sci U S A* **105**: 14603-14608.

Heidrich, C., M. F. Templin, A. Ursinus, M. Merdanovic, J. Berger, H. Schwarz, M. A. de Pedro & J. V. Holtje, (2001) Involvement of N-acetylmuramyl-L-alanine amidases in cell separation and antibiotic-induced autolysis of Escherichia coli. *Mol Microbiol* **41**: 167-178.

Hett, E. C., M. C. Chao & E. J. Rubin, (2010) Interaction and modulation of two antagonistic cell wall enzymes of mycobacteria. *PLoS Pathog* **6**: e1001020.

Hilbert, D. W. & P. J. Piggot, (2004) Compartmentalization of gene expression during Bacillus subtilis spore formation. *Microbiol Mol Biol Rev* **68**: 234-262.

Holtje, J. V., (1996) A hypothetical holoenzyme involved in the replication of the murein sacculus of Escherichia coli. *Microbiology* **142 (Pt 8)**: 1911-1918.

Holtje, J. V., (1998) Growth of the stress-bearing and shape-maintaining murein sacculus of Escherichia coli. *Microbiol Mol Biol Rev* **62**: 181-203.

Horsburgh, G. J., A. Atrih, M. P. Williamson & S. J. Foster, (2003) LytG of Bacillus subtilis is a novel peptidoglycan hydrolase: the major active glucosaminidase. *Biochemistry* **42**: 257-264.

Ishino, F., W. Park, S. Tomioka, S. Tamaki, I. Takase, K. Kunugita, H. Matsuzawa, S. Asoh, T. Ohta, B. G. Spratt & et al., (1986) Peptidoglycan synthetic activities in membranes of Escherichia coli caused by overproduction of penicillin-binding protein 2 and rodA protein. *J Biol Chem* **261**: 7024-7031.

Jiang, X., A. Rubio, S. Chiba & K. Pogliano, (2005) Engulfment-regulated proteolysis of SpoIIQ: evidence that dual checkpoints control σ^K activity. *Mol Microbiol* **58**: 102-115.

Jones, L. J., R. Carballido-Lopez & J. Errington, (2001) Control of cell shape in bacteria: helical, actin-like filaments in Bacillus subtilis. *Cell* **104**: 913-922.

Karimova, G., J. Pidoux, A. Ullmann & D. Ladant, (1998) A bacterial two-hybrid system based on a reconstituted signal transduction pathway. *Proc Natl Acad Sci U S A* **95**: 5752-5756.

Kawai, Y., K. Asai & J. Errington, (2009) Partial functional redundancy of MreB isoforms, MreB, Mbl and MreBH, in cell morphogenesis of Bacillus subtilis. *Mol Microbiol* **73**: 719-731.

Koch, A. L., (1990) Additional arguments for the key role of "smart" autolysins in the enlargement of the wall of gram-negative bacteria. *Res Microbiol* **141**: 529-541.

Koch, A. L., (1998a) Orientation of the peptidoglycan chains in the sacculus of Escherichia coli. *Res Microbiol* **149**: 689-701.

Koch, A. L., (1998b) The three-for-one model for gram-negative wall growth: a problem and a possible solution. *FEMS Microbiol Lett* **162**: 127-134.

Koch, A. L., (2000) Length distribution of the peptidoglycan chains in the sacculus of Escherichia coli. *J Theor Biol* **204**: 533-541.

Koch, A. L. & S. Woeste, (1992) Elasticity of the sacculus of Escherichia coli. *J Bacteriol* **174**: 4811-4819.

Kuntzel, H., M. Heidrich & B. Piechulla, (1981) Phylogenetic tree derived from bacterial, cytosol and organelle 5S rRNA sequences. *Nucleic Acids Res* **9**: 1451-1461.

Kuroda, A., M. H. Rashid & J. Sekiguchi, (1992) Molecular cloning and sequencing of the upstream region of the major Bacillus subtilis autolysin

gene: a modifier protein exhibiting sequence homology to the major autolysin and the spoIID product. *J Gen Microbiol* **138 (Pt 6)**: 1067-1076.

Labischinski, H., G. Barnickel, H. Bradaczek & P. Giesbrecht, (1979) On the secondary and tertiary structure of murein. Low and medium-angle X-ray evidence against chitin-based conformations of bacterial peptidoglycan. *Eur J Biochem* **95**: 147-155.

Leduc, M., C. Frehel, E. Siegel & J. Van Heijenoort, (1989) Multilayered distribution of peptidoglycan in the periplasmic space of Escherichia coli. *J Gen Microbiol* **135**: 1243-1254.

Legaree, B. A. & A. J. Clarke, (2008) Interaction of penicillin-binding protein 2 with soluble lytic transglycosylase B1 in Pseudomonas aeruginosa. *J Bacteriol* **190**: 6922-6926.

Lemon, K. P. & A. D. Grossman, (1998) Localization of bacterial DNA polymerase: evidence for a factory model of replication. *Science* **282**: 1516-1519.

Leps, B., H. Labischinski & H. Bradaczek, (1987) Conformational behavior of the polysaccharide backbone of murein. *Biopolymers* **26**: 1391-1406.

Levin, P. A., N. Fan, E. Ricca, A. Driks, R. Losick & S. Cutting, (1993) An unusually small gene required for sporulation by Bacillus subtilis. *Mol Microbiol* **9**: 761-771.

Liu, N. J., R. J. Dutton & K. Pogliano, (2006) Evidence that the SpoIIIE DNA translocase participates in membrane fusion during cytokinesis and engulfment. *Mol Microbiol* **59**: 1097-1113.

Londono-Vallejo, J. A., C. Frehel & P. Stragier, (1997) SpoIIQ, a forespore-expressed gene required for engulfment in Bacillus subtilis. *Mol Microbiol* **24**: 29-39.

Lopez-Diaz, I., S. Clarke & J. Mandelstam, (1986) spoIID operon of Bacillus subtilis: cloning and sequence. *J Gen Microbiol* **132 (Pt 2)**: 341-354.

Margolis, P. S., A. Driks & R. Losick, (1993) Sporulation gene spoIIB from Bacillus subtilis. *J Bacteriol* **175**: 528-540.

Marquis, R. E., (1968) Salt-induced contraction of bacterial cell walls. *J Bacteriol* **95**: 775-781.

Marraffini, L. A., A. C. Dedent & O. Schneewind, (2006) Sortases and the art of anchoring proteins to the envelopes of gram-positive bacteria. *Microbiol Mol Biol Rev* **70**: 192-221.

Matias, V. R., A. Al-Amoudi, J. Dubochet & T. J. Beveridge, (2003) Cryo-transmission electron microscopy of frozen-hydrated sections of Escherichia coli and Pseudomonas aeruginosa. *J Bacteriol* **185**: 6112-6118.

Matias, V. R. & T. J. Beveridge, (2005) Cryo-electron microscopy reveals native polymeric cell wall structure in Bacillus subtilis 168 and the existence of a periplasmic space. *Mol Microbiol* **56**: 240-251.

Matias, V. R. & T. J. Beveridge, (2006) Native cell wall organization shown by cryo-electron microscopy confirms the existence of a periplasmic space in Staphylococcus aureus. *J Bacteriol* **188**: 1011-1021.

Matias, V. R. & T. J. Beveridge, (2007) Cryo-electron microscopy of cell division in Staphylococcus aureus reveals a mid-zone between nascent cross walls. *Mol Microbiol* **64**: 195-206.

McPherson, D. C., A. Driks & D. L. Popham, (2001) Two class A high-molecular-weight penicillin-binding proteins of Bacillus subtilis play redundant roles in sporulation. *J Bacteriol* **183**: 6046-6053.

Meador-Parton, J. & D. L. Popham, (2000) Structural analysis of Bacillus subtilis spore peptidoglycan during sporulation. *J Bacteriol* **182**: 4491-4499.

Meisner, J., X. Wang, M. Serrano, A. O. Henriques & C. P. Moran, Jr., (2008) A channel connecting the mother cell and forespore during bacterial endospore formation. *Proc Natl Acad Sci U S A* **105**: 15100-15105.

Mengin-Lecreulx, D., L. Texier, M. Rousseau & J. van Heijenoort, (1991) The murG gene of Escherichia coli codes for the UDP-N-acetylglucosamine: N-acetylmuramyl-(pentapeptide) pyrophosphoryl-undecaprenol N-acetylglucosamine transferase involved in the membrane steps of peptidoglycan synthesis. *J Bacteriol* **173**: 4625-4636.

Mengin-Lecreulx, D. & J. van Heijenoort, (1985) Effect of growth conditions on peptidoglycan content and cytoplasmic steps of its biosynthesis in Escherichia coli. *J Bacteriol* **163**: 208-212.

Meroueh, S. O., K. Z. Bencze, D. Hesek, M. Lee, J. F. Fisher, T. L. Stemmler & S. Mobashery, (2006) Three-dimensional structure of the bacterial cell wall peptidoglycan. *Proc Natl Acad Sci U S A* **103**: 4404-4409.

Meyer, P., J. Gutierrez, K. Pogliano & J. Dworkin, (2010) Cell wall synthesis is necessary for membrane dynamics during sporulation of Bacillus subtilis. *Mol Microbiol* **76**: 956-970.

Middleton, R. & A. Hofmeister, (2004) New shuttle vectors for ectopic insertion of genes into Bacillus subtilis. *Plasmid* **51**: 238-245.

Morlot, C., T. Uehara, K. A. Marquis, T. G. Bernhardt & D. Z. Rudner, (2010) A highly coordinated cell wall degradation machine governs spore morphogenesis in Bacillus subtilis. *Genes Dev* **24**: 411-422.

Murray, T., D. L. Popham & P. Setlow, (1998) Bacillus subtilis cells lacking penicillin-binding protein 1 require increased levels of divalent cations for growth. *J Bacteriol* **180**: 4555-4563.

Nelson, D. E. & K. D. Young, (2001) Contributions of PBP 5 and DD-carboxypeptidase penicillin binding proteins to maintenance of cell shape in Escherichia coli. *J Bacteriol* **183**: 3055-3064.

Ohnishi, R., S. Ishikawa & J. Sekiguchi, (1999) Peptidoglycan hydrolase LytF plays a role in cell separation with CwlF during vegetative growth of Bacillus subtilis. *J Bacteriol* **181**: 3178-3184.

Ou, L. T. & R. E. Marquis, (1970) Electromechanical interactions in cell walls of gram-positive cocci. *J Bacteriol* **101**: 92-101.

Piggot, P. J. & D. W. Hilbert, (2004) Sporulation of Bacillus subtilis. *Curr Opin Microbiol* **7**: 579-586.

Popham, D. L., M. E. Gilmore & P. Setlow, (1999) Roles of low-molecular-weight penicillin-binding proteins in Bacillus subtilis spore peptidoglycan synthesis and spore properties. *J Bacteriol* **181**: 126-132.

Popham, D. L., J. Helin, C. E. Costello & P. Setlow, (1996) Analysis of the peptidoglycan structure of Bacillus subtilis endospores. *J Bacteriol* **178**: 6451-6458.

Popham, D. L. & P. Setlow, (1996) Phenotypes of Bacillus subtilis mutants lacking multiple class A high-molecular-weight penicillin-binding proteins. *J Bacteriol* **178**: 2079-2085.

Popham, D. L. & K. D. Young, (2003) Role of penicillin-binding proteins in bacterial cell morphogenesis. *Curr Opin Microbiol* **6**: 594-599.

Prajapati, R. S., T. Ogura & S. M. Cutting, (2000) Structural and functional studies on an FtsH inhibitor from Bacillus subtilis. *Biochim Biophys Acta* **1475**: 353-359.

Prats, R. & M. A. de Pedro, (1989) Normal growth and division of Escherichia coli with a reduced amount of murein. *J Bacteriol* **171**: 3740-3745.

Priyadarshini, R., M. A. de Pedro & K. D. Young, (2007) Role of peptidoglycan amidases in the development and morphology of the division septum in Escherichia coli. *J Bacteriol* **189**: 5334-5347.

Priyadarshini, R., D. L. Popham & K. D. Young, (2006) Daughter cell separation by penicillin-binding proteins and peptidoglycan amidases in Escherichia coli. *J Bacteriol* **188**: 5345-5355.

Ramamurthi, K. S., K. R. Clapham & R. Losick, (2006) Peptide anchoring spore coat assembly to the outer forespore membrane in Bacillus subtilis. *Mol Microbiol* **62**: 1547-1557.

Ramamurthi, K. S., S. Lecuyer, H. A. Stone & R. Losick, (2009) Geometric cue for protein localization in a bacterium. *Science* **323**: 1354-1357.

Real, G., A. Fay, A. Eldar, S. M. Pinto, A. O. Henriques & J. Dworkin, (2008) Determinants for the subcellular localization and function of a nonessential SEDS protein. *J Bacteriol* **190**: 363-376.

Rogers, H. J., (1980) *Microbial cell walls and membranes*. Chapman and Hall, London; New York.

Rubio, A. & K. Pogliano, (2004) Septal localization of forespore membrane proteins during engulfment in *Bacillus subtilis*. *EMBO J.* **23**: 1636-1646.

Sauvage, E., F. Kerff, M. Terrak, J. A. Ayala & P. Charlier, (2008) The penicillin-binding proteins: structure and role in peptidoglycan biosynthesis. *FEMS Microbiol Rev* **32**: 234-258.

Schaeffer, P., J. Millet & J. Aubert, (1965) Catabolite repression of bacterial sporulation. *Proc. Natl. Acad. Sci. USA* **54**: 704-711.

Schleifer, K. H. & O. Kandler, (1972) Peptidoglycan types of bacterial cell walls and their taxonomic implications. *Bacteriol Rev* **36**: 407-477.

Sekiguchi, J., K. Akeo, H. Yamamoto, F. K. Khasanov, J. C. Alonso & A. Kuroda, (1995) Nucleotide sequence and regulation of a new putative cell wall hydrolase gene, cwlD, which affects germination in Bacillus subtilis. *J Bacteriol* **177**: 5582-5589.

Seltmann, G. a. H., Otto, (2002) *The bacterial cell wall*. Springer, Berlin; New York.

Shaner, N. C., R. E. Campbell, P. A. Steinbach, B. N. Giepmans, A. E. Palmer & R. Y. Tsien, (2004) Improved monomeric red, orange and yellow fluorescent proteins derived from Discosoma sp. red fluorescent protein. *Nat Biotechnol* **22**: 1567-1572.

Sharp, M. D. & K. Pogliano, (1999) An *in vivo* membrane fusion assay implicates SpoIIIE in the final stages of engulfment during *Bacillus subtilis* sporulation. *Proc Natl Acad Sci U S A* **96**: 14553-14558.

Sharp, M. D. & K. Pogliano, (2002) Role of cell-specific SpoIIIE assembly in polarity of DNA transfer. *Science* **295**: 137-139.

Smith, K., M. E. Bayer & P. Youngman, (1993) Physical and functional characterization of the Bacillus subtilis spoIIM gene. *J Bacteriol* **175**: 3607-3617.

Smith, T. J., S. A. Blackman & S. J. Foster, (2000) Autolysins of Bacillus subtilis: multiple enzymes with multiple functions. *Microbiology* **146 (Pt 2)**: 249-262.

Soufo, H. J. & P. L. Graumann, (2003) Actin-like proteins MreB and Mbl from Bacillus subtilis are required for bipolar positioning of replication origins. *Curr Biol* **13**: 1916-1920.

Stachyra, T., C. Dini, P. Ferrari, A. Bouhss, J. van Heijenoort, D. Mengin-Lecreulx, D. Blanot, J. Biton & D. Le Beller, (2004) Fluorescence detection-based functional assay for high-throughput screening for MraY. *Antimicrob Agents Chemother* **48**: 897-902.

Sterlini, J. M. & J. Mandelstam, (1969) Commitment to sporulation in Bacillus subtilis and its relationship to development of actinomycin resistance. *Biochem J* **113**: 29-37.

Sun, Y. L., M. D. Sharp & K. Pogliano, (2000a) A dispensable role for forespore-specific gene expression in engulfment of the forespore during sporulation of Bacillus subtilis. *J Bacteriol* **182**: 2919-2927.

Sun, Y. L., M. D. Sharp & K. Pogliano, (2000b) A dispensable role for forespore-specific gene expression in engulfment of the forespore during sporulation of *Bacillus subtilis*. *J Bacteriol* **182**: 2919-2927.

Takano, H. & K. Takechi, (2010) Plastid peptidoglycan. *Biochim Biophys Acta* **1800**: 144-151.

Theriot, J. A., (2000) The polymerization motor. *Traffic* **1**: 19-28.

Thompson, L. S., P. L. Beech, G. Real, A. O. Henriques & E. J. Harry, (2006) Requirement for the cell division protein DivIB in polar cell division and engulfment during sporulation in Bacillus subtilis. *J Bacteriol* **188**: 7677-7685.

Tipper, D. J. & P. E. Linnett, (1976) Distribution of peptidoglycan synthetase activities between sporangia and forespores in sporulating cells of Bacillus sphaericus. *J Bacteriol* **126**: 213-221.

Todd, J. A., A. N. Roberts, K. Johnstone, P. J. Piggot, G. Winter & D. J. Ellar, (1986) Reduced heat resistance of mutant spores after cloning and mutagenesis of the Bacillus subtilis gene encoding penicillin-binding protein 5. *J Bacteriol* **167**: 257-264.

Uehara, T. & J. T. Park, (2008) Growth of Escherichia coli: significance of peptidoglycan degradation during elongation and septation. *J Bacteriol* **190**: 3914-3922.

Uehara, T., K. R. Parzych, T. Dinh & T. G. Bernhardt, (2010) Daughter cell separation is controlled by cytokinetic ring-activated cell wall hydrolysis. *EMBO J* **29**: 1412-1422.

Vadillo-Rodriguez, V., S. R. Schooling & J. R. Dutcher, (2009) In situ characterization of differences in the viscoelastic response of individual gram-negative and gram-positive bacterial cells. *J Bacteriol* **191**: 5518-5525.

van Dam, V., R. Sijbrandi, M. Kol, E. Swiezewska, B. de Kruijff & E. Breukink, (2007) Transmembrane transport of peptidoglycan precursors across model and bacterial membranes. *Mol Microbiol* **64**: 1105-1114.

van den Ent, F., L. A. Amos & J. Lowe, (2001) Prokaryotic origin of the actin cytoskeleton. *Nature* **413**: 39-44.

van Ooij, C. & R. Losick, (2003) Subcellular localization of a small sporulation protein in Bacillus subtilis. *J Bacteriol* **185**: 1391-1398.

Varma, A. & K. D. Young, (2004) FtsZ collaborates with penicillin binding proteins to generate bacterial cell shape in Escherichia coli. *J Bacteriol* **186**: 6768-6774.

Vasudevan, P., A. Weaver, E. D. Reichert, S. D. Linnstaedt & D. L. Popham, (2007) Spore cortex formation in Bacillus subtilis is regulated by accumulation of peptidoglycan precursors under the control of sigma K. *Mol Microbiol* **65**: 1582-1594.

Verwer, R. W., N. Nanninga, W. Keck & U. Schwarz, (1978) Arrangement of glycan chains in the sacculus of Escherichia coli. *J Bacteriol* **136**: 723-729.

Vollmer, W., D. Blanot & M. A. de Pedro, (2008) Peptidoglycan structure and architecture. *FEMS Microbiol Rev* **32**: 149-167.

Vollmer, W. & J. V. Holtje, (2004) The architecture of the murein (peptidoglycan) in gram-negative bacteria: vertical scaffold or horizontal layer(s)? *J Bacteriol* **186**: 5978-5987.

Vollmer, W., M. von Rechenberg & J. V. Holtje, (1999) Demonstration of molecular interactions between the murein polymerase PBP1B, the lytic transglycosylase MltA, and the scaffolding protein MipA of Escherichia coli. *J Biol Chem* **274**: 6726-6734.

Wang, S., H. Arellano-Santoyo, P. A. Combs & J. W. Shaevitz, (2010) Actin-like cytoskeleton filaments contribute to cell mechanics in bacteria. *Proc Natl Acad Sci U S A* **107**: 9182-9185.

Weidel, W. & H. Pelzer, (1964) Bagshaped Macromolecules--a New Outlook on Bacterial Cell Walls. *Adv Enzymol Relat Areas Mol Biol* **26**: 193-232.

Wientjes, F. B. & N. Nanninga, (1989) Rate and topography of peptidoglycan synthesis during cell division in Escherichia coli: concept of a leading edge. *J Bacteriol* **171**: 3412-3419.

Wu, Y. X., D. C. Masison, E. Eisenberg & L. E. Greene, (2006) Application of photobleaching for measuring diffusion of prion proteins in cytosol of yeast cells. *Methods* **39**: 43-49.

Yao, X., M. Jericho, D. Pink & T. Beveridge, (1999) Thickness and elasticity of gram-negative murein sacculi measured by atomic force microscopy. *J Bacteriol* **181**: 6865-6875.

Young, K. D., (2003) Bacterial shape. *Mol Microbiol* **49**: 571-580.

Youngman, P., J. B. Perkins & R. Losick, (1984) A novel method for the rapid cloning in Escherichia coli of Bacillus subtilis chromosomal DNA adjacent to Tn917 insertions. *Mol Gen Genet* **195**: 424-433.

Yung, P. T., H. S. Shafaat, S. A. Connon & A. Ponce, (2007) Quantification of viable endospores from a Greenland ice core. *FEMS Microbiol Ecol* **59**: 300-306.

Zuber, B., M. Haenni, T. Ribeiro, K. Minnig, F. Lopes, P. Moreillon & J. Dubochet, (2006) Granular layer in the periplasmic space of gram-positive

bacteria and fine structures of Enterococcus gallinarum and Streptococcus gordonii septa revealed by cryo-electron microscopy of vitreous sections. *J Bacteriol* **188**: 6652-6660.